AD-A202 940

DTIC

JAN 1 7 1989

H

TWO-FINGERED GRASP OF
CYLINDRICAL OBJECTS IN PLANAR MOTION

THESIS

Paul Vincent Whalen
Captain, USAF

AFIT/GAE/AA/88D-39

DEPARTMENT OF THE AIR FORCE

AIR UNIVERSITY

AIR FORCE INSTITUTE OF TECHNOLOGY

Wright-Patterson Air Force Base, Ohio

89   1 17 023

AFIT/GAE/AA/88D-39

TWO-FINGERED GRASP OF
CYLINDRICAL OBJECTS IN PLANAR MOTION

THESIS

Paul Vincent Whalen
Captain, USAF

AFIT/GAE/AA/88D-39

DTIC
SELECTED
JAN 1 7 1989
H

AFIT/GAE/AA/88D-39

TWO-FINGERED GRASP OF
CYLINDRICAL OBJECTS IN PLANAR MOTION

THESIS

Presented to the Faculty of the School of Engineering

of the Air Force Institute of Technology

Air University

In Partial Fulfillment of the

Requirements for the Degree of

Master of Science in Aeronautical Engineering

Paul Vincent Whalen, B.S.M.E.

Captain, USAF

December, 1988

Acknowledgments

Almost all significant accomplishments in one's life require the assistance and support of many people. This thesis was no exception. Probably the greatest assistance came from the patient and thoughtful help of my faculty advisor, Dr. Curtis H. Spenny. He provided the insight that only a professor can give along with the motivation and thoughtfulness that only a friend can offer. His interest and excitement threw coal to the fire of my own curiosity. I also want to thank LtCol Ron Bagley and Capt Michael Leahy for their assistance as members of my thesis committee. They both responded with enthusiasm whenever I called on their support.

I wish to acknowledge the continuous support of my parents and family whose faith in my abilities often exceeds my own. Among the most faithful was my Grandmother ████████ Whalen; in her memory I dedicate this thesis. My deepest gratitude goes to my lovely wife ███████ There were many times when I could not be there when she needed me because I was busy with school. In some ways this degree may have been more of a challenge for her than for me. Through it all, however, her understanding and concern made our first year-and-a-half of marriage the best time of my life.

Finally, I would like to thank God for giving me the perseverance and strength to make up for the many times I lacked intelligence.

Paul Vincent Whalen

i

Table of Contents

List of Figures

List of Symbols

$r \equiv$ Radius of the cylindrical object.

$m \equiv$ Mass of the cylindrical object.

$a \equiv$ The distance between the base joints of the two fingers.

$d \equiv$ The distance between the two points of contact between the fingertips and the object.

$h \equiv$ The y_p-coordinate of the center of the object.

$S \equiv$ A parameter which specifies whether the knuckles of the two-link fingers are 'in' or 'out'. 'In' is specified by $+1$ and 'out' is specified by -1.

$\vec{g} \equiv$ Gravity acceleration vector.

$\vec{a} \equiv$ Centrifugal acceleration vector.

$\hat{i}_p \equiv$ Palm coordinate system unit vector along the x-axis.

$\hat{j}_p \equiv$ Palm coordinate system unit vector along the y-axis.

$\hat{k}_p \equiv$ Palm coordinate system unit vector along the z-axis.

$\hat{i}_o \equiv$ Object coordinate system unit vector along the x-axis.

$\hat{j}_o \equiv$ Object coordinate system unit vector along the y-axis.

$\hat{k}_o \equiv$ Object coordinate system unit vector along the z-axis.

$\hat{u}_{in} \equiv$ Local contact coordinate system inward-pointing unit normal vector at contact i.

$\hat{u}_{it} \equiv$ Local contact coordinate system unit tangent vector at contact i which is oriented positive such that
$$\hat{u}_{in} \times \hat{u}_{it} = \hat{u}_{iz}.$$

$\hat{u}_{iz} \equiv$ Local contact coordinate system unit vector parallel to $\hat{k}$.

$\vec{F}_{applied} \equiv$ Resultant of all the external forces on the object due to contact with something other than the gripper.

$\vec{F}_{ext} \equiv$ Resultant external force vector of the environment on the object.

$\vec{M} \equiv$ A pure moment vector.

$\vec{C}_i \equiv$ Total contact force vector of finger i on the object.

$C_n \equiv$ Total normal force magnitude which is common to both finger contacts with the object.

C_t ≡ Total tangential force magnitude which is common to both finger contacts with the object.

C_{1n} ≡ Total normal force magnitude at the contact of finger 1 with the object.

C_{1t} ≡ Total tangential force magnitude at the contact of finger 1 with the object.

C_{2n} ≡ Total normal force magnitude at the contact of finger 2 with the object.

C_{2t} ≡ Total tangential force magnitude at the contact of finger 2 with the object.

C_n' ≡ Dimensionless parameter equal to C_n/F_{ext}.

C_{1n}' ≡ Dimensionless parameter equal to C_{1n}/F_{ext}.

C_{2n}' ≡ Dimensionless parameter equal to C_{2n}/F_{ext}.

θ ≡ Grasp angle defined as half of the angle formed by the two radial lines drawn from the center of the object to the two contact points.

α ≡ Angle of the external force vector measured positive counterclockwise from the positive y-axis.

β ≡ Friction angle common to both contact points and defined as $\arctan(C_t/C_n)$.

β_1 ≡ Friction angle at contact point 1 defined as $\arctan(C_{1t}/C_{1n})$.

β_2 ≡ Friction angle at contact point 2 defined as $\arctan(C_{2t}/C_{2n})$.

$\vec{C}_{ih}$ ≡ Internal grasp force vector (homogeneous solution) component of $\vec{C}_i$.

C_{inh} ≡ The normal component of $\vec{C}_{ih}$.

C_{ith} ≡ The tangential component of $\vec{C}_{ih}$.

C_{ixh} ≡ The component of $\vec{C}_{ih}$ in the x-direction.

C_{iyh} ≡ The component of $\vec{C}_{ih}$ in the y-direction.

λ ≡ The arbitrary magnitude of the internal grasp force.

λ' ≡ Dimensionless parameter equal to λ/F_{ext}.

$\vec{C}_{ip}$ ≡ Particular solution component of $\vec{C}_i$.

C_{inp} ≡ The normal component of $\vec{C}_{ip}$.

C_{itp} ≡ The tangential component of $\vec{C}_{ip}$.

C_{ixp} ≡ The component of $\vec{C}_{ip}$ in the x-direction.

C_{iyp} ≡ The component of $\vec{C}_{ip}$ in the y-direction.

$\mathcal{J} \equiv$ The global Jacobian matrix for the entire hand which relates the individual finger joint angle spaces to their local contact coordinate frame spaces.

$J_i \equiv$ The Jacobian matrix for the ith finger which relates the ith finger joint angle space to the local contact coordinate frame space of the ith contact.

$j_{ijk} \equiv$ The element of J_i which occupies the jth row and the kth column position of the matrix.

$J_i' \equiv$ The Jacobian matrix for the ith finger which incorporates the contact constraint information.

$B_i \equiv$ The contact constraint matrix which defines the wrench basis of ot contact type.

$l_{ij} \equiv$ The length of the jth link of the ith finger.

$\phi_i \equiv$ The angle of the ith joint of the hand.

$\phi_{ij} \equiv$ The sum of ϕ_i and ϕ_j.

$\phi_{ijk} \equiv$ The sum of ϕ_i, ϕ_j, and ϕ_k.

$P_{ix} \equiv$ The x-coordinate of the contact between the tip of the ith finger and the object.

$P_{iy} \equiv$ The y-coordinate of the contact between the tip of the ith finger and the object.

$P_{iz} \equiv$ The z-coordinate of the contact between the tip of the ith finger and the object.

$\gamma_{ix} \equiv$ The orientation angle about the x-axis of the centerline of the last link on the ith finger.

$\gamma_{iy} \equiv$ The orientation angle about the y-axis of the centerline of the last link on the ith finger.

$\gamma_{iz} \equiv$ The orientation angle about the z-axis of the centerline of the last link on the ith finger.

$V_{ix} \equiv$ The translational velocity of the tip of the ith finger in the x-direction.

$V_{iy} \equiv$ The translational velocity of the tip of the ith finger in the y-direction.

$V_{iz} \equiv$ The translational velocity of the tip of the ith finger in the z-direction.

$\omega_{ix} \equiv$ The rotational velocity of the tip of the ith finger about the x-axis.

$\omega_{iy} \equiv$ The rotational velocity of the tip of the ith finger about the y-axis.

$\omega_{iz} \equiv$ The rotational velocity of the tip of the ith finger about the z-axis.

$\vec{V}_i \equiv$ The twist velocity of the tip of the ith finger in the palm x/y/z coordinate frame.

$\vec{\dot{\Phi}}_i \equiv$ The vector of joint velocities for the ith finger.

$\psi \equiv$ The angle measured counterclockwise between the positive x_p-axis and the positive x_o-axis.

$\mathcal{S} \equiv$ The coordinates of a screw.

$\mathcal{P} \equiv$ The pitch of a screw.

$\mathcal{T} \equiv$ The coordinates of a twist.

$\mathcal{P}_t \equiv$ The pitch of a twist.

$\mathcal{W} \equiv$ The coordinates of a wrench.

$\mathcal{P}_w \equiv$ The pitch of a wrench.

$\mathbf{W} \equiv$ The grasp matrix.

$\mathcal{F}_{ext} \equiv$ A wrench of external forces on the object.

$F_{ext_{x_o}} \equiv$ the magnitude of the external force on the object in the x-direction of the object coordinate frame.

$F_{ext_{y_o}} \equiv$ the magnitude of the external force on the object in the y-direction of the object coordinate frame.

$F_{ext_{z_o}} \equiv$ the magnitude of the external force on the object in the z-direction of the object coordinate frame.

$\mathcal{N} \equiv$ A matrix whose columns are a set of orthonormal basis vectors which span the null space of $\mathbf{W}$.

$\mathbf{W}_R^+ \equiv$ The right generalized (Moore-Penrose) inverse of $\mathbf{W}$.

$\vec{\tau} \equiv$ The vector of the total solution of finger joint torques.

$\vec{\tau}_p \equiv$ The vector of the particular solution of finger joint torques.

$\vec{\tau}_h \equiv$ The vector of the homogeneous solution of finger joint torques.

$\mu_s \equiv$ Static coefficient of friction.

$C_{n_{max}} \equiv$ The maximum normal force which can be applied to the object surface without crushing it.

$C'_{n_{max}} \equiv$ The maximum allowable normalized normal force which is defined in Eq (4.15).

$\tau_{max} \equiv$ The maximum finger joint torque which is derived from the joint actuator limits.

τ'_{max} ≡ The maximum allowable normalized finger joint torque which is defined in Eq (??).

F^{nom}_{ext} ≡ The nominal magnitude of the external load wrench on the object.

F^* ≡ The maximum tolerable value of F_{ext} for which an equilibrium grasp can be maintained without changing the grasp geometry or λ'.

M'_{nom} ≡ The nominal magnitude of the external load moment on the object.

M^* ≡ A dimensionless parameter relating the difference between the varied external load moment and M'_{nom}.

AFIT/GAE/AA/88D-39

Abstract

One goal of this thesis is to develop analytic expressions which model the equilibrium requirements of a grasp by two robotic fingers on a nominally-loaded cylindrical object confined to planar motion. Another goal is to derive analytic expressions which can be used to evaluate the ability of a grasp to tolerate changes in the external load magnitude, direction, and moment without loss of equilibrium. The gripper fingers are each assumed to be two-link serial mechanisms with revolute joints. The contact of each finger on the object is taken as a point contact with friction. The resulting analytic expressions are based on the static equilibrium requirements and include consideration of constraints on: Coulomb friction forces, unisense normal forces, object crush limits, and finger joint torque limits. Plotting the expressions yields new graphical insight into the consequences of employing various fingertip spacings and 'squeeze' force levels when grasping cylindrical objects in planar motion. In addition, the analytic equations indicate the range of variation in external load configuration which can be tolerated by a selected grasp without violating any of the aforementioned grasp constraints. Variations in the magnitude, direction, and moment of the external load configuration are considered. The derived analytic expressions can be used as the foundation for developing simplified grasping algorithms under the stated conditions.

TWO-FINGERED GRASP OF
CYLINDRICAL OBJECTS IN PLANAR MOTION

I. INTRODUCTION

Robotic grasping is an area of research which has received increased research attention in recent years. Despite this attention, the current state-of-the-art industrial gripper is little more than a parallel-jaw gripper or a specialty gripper which employs suction, magnetism, or adhesives to secure an object. Such grippers are usually limited in the types and sizes of materials and objects they can handle. They also lack the ability to manipulate an object within the hand after it has been grasped. The successful future of robotics will depend on the ability of robots to be diverse in the scope of tasks they are able to perform without human intervention or a high-degree of structure, i.e. fixturing, in the working environment.

1.1 MOTIVATION AND GOAL

Methods of analyzing multifingered hands grasping three-dimensional objects in spatial motion exist in literature. However, the optimal strategy for selecting the grasping forces for overconstrained grasps is still undeveloped. The purpose of this thesis is to identify criteria for selecting the optimal grasp and to develop analytic equations which can be used to evaluate the quality of two-fingered grasps of objects which can be modeled as circular cylinders in planar motion.

1.2 ASSUMPTIONS AND LIMITATIONS

The scope of this thesis is limited to the analysis of objects which can be modeled as circular cylinders constrained to planar motion. The center of mass is assumed to coincide with the geometric centroid of the object for the nominal external load analysis. The analysis for external load variations includes non-zero external load moments that can be used to model an object whose center of mass does not coincide with its geometric

centroid. Limiting the analysis to circular cylinders does not exclude such objects as square, hexagonal, or octagonal objects which are grasped such that the contact points are at the centers of the facets. However, instead of being able to choose the grasp at any angle from a continuous set of values, one is left with discrete choices corresponding to the angles which result in the surface normals passing through the center of the object.

Only one point is assumed to contact the cylinder at each of the two fingertips regardless of the finger orientation relative to the cylinder. For a point contact, the fingertips must have a radius equal to zero. No other contact between the finger links and the object is allowed.

This thesis does not address the dynamics of impacting the object during the 'capture' phase of grasping an object, nor does it deal with manipulation of the object once it has been grasped. Consequently, it is a static analysis of the forces present due to hand/object contact and due to forces and moments applied to the object by something external to the hand. Viscous damping in the finger joints are neglected when computing the finger joint torques. In addition, the finger links are approximated as massless links, thereby eliminating concern for the influence of gravity on the fingers.

To facilitate the inverse kinematic solution so that the techniques developed in this thesis could be demonstrated, a nominal hand structure was assumed. The nominal structure is specified as a two-fingered gripper with two links per finger. The fingers are assumed to be serially actuated mechanisms with rigid links. The finger links are all assumed to have equal lengths of unity and the distance between the base joints of the two fingers, a, is also unity. The inverse kinematic solution makes no attempt to account for interferences between the object and the fingers or between the fingers themselves.

1.3 CONTRIBUTIONS

The analytic expressions derived in this thesis can be used to provide a new graphical insight into the consequences of using various fingertip configurations and internal grasp force levels when grasping cylindrical objects in planar motion. In addition, the basic expressions have been extended to forms which can be used to evaluate the ability of

a candidate grasp configuration to tolerate variations in the magnitude, direction, and moment of the external load on the object. The analytic equations derived within this thesis can serve as the basis for developing a simplified grasping algorithm for the class of grasping tasks within the scope of the assumptions and limitations set forth above.

The following is a list of the specific contributions set forth by this thesis.

- Derived the analytic expressions which model the grasp of a cylindrical object with two, two-link robotic fingers when:

  - The object is subjected to a nominal external load.

  - The external load on the object has a variation in magnitude, direction, or moment from the nominal load configuration.

- Identified a systematic method of selecting the fingertip spacing and internal grasp force for grasping a cylindrical object with two, two-link robotic fingers when the object is subjected to a nominal external load.

- Identified trends in the equilibrium requirements for friction forces, normal forces, and finger joint torques as functions of:

  - the fingertip spacing around the perimeter of the object

  - the internal grasp force level

  - variations in the magnitude, direction, and moment of the external load on the object.

- Identified a systematic method of evaluating the ability of a candidate grasp configuration to tolerate variations in the magnitude, direction, and moment of the external load on the object.

- Extended the analysis done by Kumar and Waldron [KW87] to include internal grasping forces acting through points other than the center of the cylinder.

1.4 THESIS OVERVIEW

Chapter II is a brief review of the pertinent literary works in the area of grasping theory. The remainder of this thesis is structured to start with established concepts and methods and then apply them towards the goal in a step-by-step fashion. Consequently, Chapter III is intended to take the reader from ground level using analysis tools which have been published in literature. In Chapter III, methods of determining the contact forces, global hand Jacobian matrix, finger joint torques, and inverse kinematics are applied to analyze the prescribed hand and object geometries.

Chapter IV furthers the analysis by applying the results of Chapter III to generate analytic inequality expressions which model the equilibrium grasp requirements for the grasp of an object subjected to a nominal external load in terms of three types of grasp constraints. The analytic inequality expressions are plotted as functions of the grasp angle to characterize various grasp configurations.

Chapter V examines the effects of load variations or load measurement errors on a candidate grasp configuration which may have been selected via the nominal external load analysis in Chapter IV. Changes in the nominal external load magnitude and direction, as well as variations in the external load moment are considered.

Chapter VI presents a summary of the results obtained from the analyses performed in Chapters IV and V, the conclusions, and recommendations for future research. Finally, Appendix A contains a review of screw theory for readers who are unfamiliar with it and Appendix B presents geometric derivations for several of the relations developed in Chapter IV that made use of screw theory.

II. LITERATURE REVIEW

The historical measuring-stick for evaluating the versatility and performance of robotic grippers has been the human hand. Although the versatility of the human hand promises to remain unequaled by robotic grippers for many years to come, several research grippers have been built which have kinematic abilities that are nearly identical to that of the human hand [JIKJ86] [NHF84] [CS84].

The quest to understand the human hand began in the medical community which sought to improve prosthetic devices for amputees. Early research attempted to classify all of the possible human grasps into a small set which could be emulated with mechanical hardware. In 1919 Schlesinger defined 6 basic grasps which were later summarized in 1955 by Taylor and Scharz [CW86: 1534]. Their classification was based on the possible geometric configurations of the human hand. The six grasps they identified were: cylindrical, tip, hook, palmar, spherical, and lateral grasps. These grasp categories were useful for describing the ranges of motion for the individual fingers and the shapes that the hand could assume but they lacked information about the suitability of a grasp for a specific task. With that in mind, Napier identified two major categories in 1955 which were the first task-oriented categories identified. Napier's two categories were *power* grasps and *precision* grasps. Power grasps were characterized by grasps with a high degree of stability and a low degree of mobility between the object and the hand. Precision grasps, on the other hand, were characterized by a high degree of mobility and a low degree of stability.

Napier's work was later furthered by Cutkosky and Wright [CW86] who subdivided Napier's two categories based on the types of grasps used by a machinist in a machine shop. The additional criteria for their categorization were object size, object shape, and the details of the task to be accomplished. The result of their classification was a hierarchical tree of 16 grasps. Their tree depicted trends in object-directed versus task-directed requirements, increasing-power versus increasing-dexterity requirements, and object size limitations.

Iberall [Ibe87] describes human prehension in terms of three types of *oppositions* and relates them to the postures of standard prehensile classifications. His three oppositions

are pad, palm, and side opposition. These terms describe the parts of the hand used to apply opposing forces around the object to constrain it. Pad opposition involves the fingertip pads, palm opposition involves the palm and the fingers, and side opposition involves the sides of two adjacent fingers or the thumb pad and the side of the index finger. He simplifies the categorization by introducing the concept of a virtual finger which is one or more digits operating in harmony as one appendage.

Becker et. al. [BTG86] discussed a mathematical model relating the displacement of tendons in the hand to the joint angles of the fingers and presented a finger design. Their finger used shape memory alloy (SMA) material in the form of a coil spring as joint actuators. In this way, the spring actuators simulated the properties of both tendons and muscles within the hand. Others have used SMA materials in the form of simple wires as joint actuators [NHF84]. In wire form, the SMA actuator only simulates the characteristics of human tendons and typically they must be complemented by coil springs.

In 1980 Ohwovoriole [Ohw80] extended basic screw theory for application to assembly processes. Screw theory has existed for over a century but has only recently has it been applied to grasping theory. Ohwovoriole's extensions to screw theory included defining repelling, reciprocal, and contrary screw pairs which, when they represent constraining wrenches, can be used to characterize the conditions of a contact. In this context, a repelling screw pair characterizes loss of contact between two bodies, a reciprocal screw pair maintains a contact, and a contrary screw pair would require that the two bodies penetrate each other. Ohwovoriole applies extended screw theory to examine the force and motion requirements of mating a cylindrical peg in a hole.

In 1982 Mason's dissertation [Mas82] explored grasping and pushing operations in reasonable detail. He develops a method of dealing with the uncertainty in the position and orientation of the object to be grasped without sensory feedback or adaptive motion of the manipulator. His treatment of pushing operations is cast in the form of the analogy between pushing an object and partially constraining it with a grasp. He terms these 'kinematic identities'. He demonstrates a method of automatic planning of grasping with uncertainty in the initial orientation of the object. Application to assembly processes was emphasized.

Also in 1982, Salisbury's dissertation [Sal82] presented a systematic and generalized method of analyzing the grasp of an arbitrary object by a multifingered hand. His analysis was based on simple linear algebra relationships and assumed that the characteristics of the object (size, shape, mass) and the forces on the object are known. He also assumed that the hand consists of an open-loop kinematic chain of rigid links and that there is only one contact allowed per finger which occurs at the most distal tip of each finger. Salisbury investigated grasping forces, methods of manipulating objects, determining hand workspaces, and issues in hand programming. He classified the contact between two rigid bodies as one of three types: point, line, or planar. The number and types of degrees of freedom for each of these types of contacts, both with and without friction, are given.

In 1986, two papers by Kerr and Roth presented extensions of Salisbury's work which consisted of well-defined methods of analyzing multifingered hands grasping 3-dimensional objects in spatial motion. Both of those papers are distinctly similar to sections of Kerr's doctoral dissertation. In their first paper [KR86a], Kerr and Roth discuss a linear programming method of determining the internal grasp force magnitude. The internal grasp force is an indication of how hard one is 'squeezing' the object. Their formulation includes consideration of friction and joint torque limit constraints. They also formulate a set of differential equations which describe the motion of the finger joints required to impart a desired motion on the object. Their formulation assumes the motion between the object and the fingertips is pure rolling motion with no slipping. In addition to motion analysis, they show how to develop the boundary for the total hand workspace of a simple set of fingers. The hand workspace is the range of possible manipulations with a given hand.

In their second paper [KR86b], Kerr and Roth closely examined the global hand Jacobian matrix to reveal the special configurations of general dexterous hands. The global hand Jacobian matrix relates the finger joint torques to the externally applied forces on the object. It also relates the finger joint velocities to the velocity of the object. By examining the global hand Jacobian matrix one can determine if a grasp is overconstrained, underconstrained, or singular. The global hand Jacobian matrix can also reveal the possible velocity directions that the hand may give the object and whether there are too few or too many finger joints for controlling all of the possible velocity components.

Waldron [KW87] addresses the problem of solving for the force system acting on a six-legged vehicle traversing the ground. The high degree of static-indeterminacy is similar to the problem of grasping an object with a multi-fingered dexterous hand. The basic premise to his solution is that one should maintain a zero force interaction between the feet that are in contact with the ground. Zero force interaction means that the leg actuators should not expend excess energy 'fighting' one another or causing excessive stress in the legs (or fingers for a dexterous hand.) Zero force interaction is equivalent to solving for the contact force system corresponding to an internal grasp force magnitude of zero using the linear algebra techniques given by Salisbury. Since the interaction forces are the indeterminate forces, enforcing zero force interaction allows a determinate solution to be computed for the modified system.

In 1985, Abel, Holzmann, and McCarthy [AHM85] analyzed the planar grasp of an arbitrary object by two opposing articulated fingers. They examined the equilibrium equations for point contacts with Coulomb friction and presented the set of all possible equilibrium grasps in the form of graphical curves in friction angle space.

Also in 1985, Holzmann and McCarthy [HM85] analyzed a three-fingered grasp of an arbitrary object to determine if some set of given normal contact forces could satisfy static equilibrium under the sole constraint of a Coulomb friction model for the tangential contact forces. They modeled the contact types as point contacts with friction. Using screw theory, their analysis is applicable to general spatial motion. However, the solution results in six nonlinear equations which must be solved iteratively.

Fearing [Fea86] analyzes the conditions of grasping a two-dimensional polygon with two fingers. He presents a simple method of stably grasping the polygon which depends on limited slip between the object and the fingers. The grasp attained by this passive adaptation is not claimed to be optimal but is shown to be feasible.

Trinkle et. al. [TAP87] developed an off-line system that plans and simulates the grasping of convex polygons by a gripper consisting of a palm and two single-link fingers. The system assumes that the dynamic effects of the capture of the object are negligible and the contact between the fingers and the object are frictionless. In addition, the exact

2-4

physical properties of the object and the support from which the object is taken, are known.

Tomovic et. al. [TBK87] advocate that in order to synthesize grasp strategies for multifingered robotic hands, one should use an expert system whose knowledge base is derived from study of grasping by the human hand. They present an entire hierarchy of control and specify the basic elements required in the knowledge base. In developing the expert system they break the grasping task into two phases: target approach and grasp execution. The target approach phase includes target identification, approach trajectory selection and preshaping of the hand. The grasp execution phase begins when the hand touches the object and it includes adapting the hand shape and grasp forces to secure the object. The autonomy required in the grasp execution phase is termed *reflex control*.

III. SUPPORTING THEOkY AND DERIVATIONS

The purpose of this chapter is to present the theoretical foundation for subsequent chapters. The theory is taken from published literature and applied, with some explanation, to the specific problem of this thesis to yield intermediate results. Those intermediate results are then the springboard for the further derivations and developments in subsequent chapters.

3.1 THE NUTS AND BOLTS OF SCREW THEORY

This review of screw theory is only intended to highlight the facets of screw theory which are to be used within this thesis. It is by no means a complete presentation. Refer to Hunt [Hun78] or Ball [Bal00] for more thorough treatments of screw theory and Ohwovoriole [Ohw80] or Salisbury [Sal82] for discussions of robotic applications. Much of the following review information was taken from Ohwovoriole.

3.1.1 SCREWS AND SCREW COORDINATES.
Ball [Bal00] defined a screw as being a straight line in space called the screw axis, and an associated scalar value called the pitch. The pitch is the ratio of the magnitudes of two vector quantities which act along the screw axis. The two vector quantities are usually a linear component and an angular component, such as a linear velocity along an axis and an angular velocity about an axis. If the two vectors are in the same direction then the pitch is considered to be positive; otherwise it is negative.

Screw coordinates can consist of any set of six quantities, five of which are independent. Four of the independent quantities specify the screw axis while the other one specifies the pitch. If one chooses to define a screw, S, by the coordinates

$$S = (s_1, s_2, s_3, s_4, s_5, s_6) \tag{3.1}$$

then s_1, s_2, and s_3 are proportional to the direction cosines of the screw axis and s_4, s_5, and s_6 are related to the moment of the screw axis about the origin of the coordinate

system. The pitch, $\mathcal{P}$, of the screw defined in Eq (3.1) is given by

$$\mathcal{P} = \frac{s_1 s_4 + s_2 s_5 + s_3 s_6}{\left(s_1^2 + s_2^2 + s_3^2\right)^{1/2}} \tag{3.2}$$

when it has been normalized by the screw magnitude $\left(s_1^2 + s_2^2 + s_3^2\right)^{1/2}$. However, if the pitch given in Eq (3.2) is infinite then the magnitude of the screw is given by $\left(s_4^2 + s_5^2 + s_6^2\right)^{1/2}$.

3.1.2 TWISTS AND TWIST COORDINATES.

Even the most general spatial displacement of a rigid body can be described by a rotation about a unique axis and a simultaneous translation along that same axis which is called the twist axis. When a displacement is represented in this fashion, it is known as a twist. For more detail on how to form a twist representation for a given displacement see Appendix A.

The angular displacement is called the twist amplitude and the ratio of the translation to the amplitude is called the twist pitch, $\mathcal{P}_t$. A twist can be completely specified by six independent quantities; four to specify the twist axis, one to specify the amplitude, and one to specify the pitch. Any six independent quantities which are used to specify a twist can be regarded as twist coordinates. If one defines a twist, $\mathcal{T}$, by the twist coordinates

$$\mathcal{T} = (t_1, t_2, t_3, t_4, t_5, t_6) \tag{3.3}$$

then (t_1, t_2, t_3) are the components of the angular velocity of the body and (t_4, t_5, t_6) are the components of the velocity of a point fixed on the body and lying at the origin of the coordinate system. The twist pitch, $\mathcal{P}_t$, is given by

$$\mathcal{P}_t = \frac{t_1 t_4 + t_2 t_5 + t_3 t_6}{\left(t_1^2 + t_2^2 + t_3^2\right)^{1/2}} \tag{3.4}$$

A twist with zero-pitch is a pure rotation about the twist axis while a twist with an infinite pitch is a pure translation parallel to the twist axis. The pitch is positive for a right-handed twist and negative for a left-handed twist.

The amplitude of the twist is given by

$$\left(t_1^2 + t_2^2 + t_3^2\right)^{1/2} \tag{3.5}$$

unless it has an infinite-pitch, in which case the amplitude is

$$\left(t_4^2 + t_5^2 + t_6^2\right)^{1/2} \tag{3.6}$$

It is important to note that a twist can represent several types of displacements. When a twist represents an infinitesimally small displacement (i.e. it has an infinitesimal amplitude) it can be called an <u>infinitesimal twist</u>. This is in contrast with a <u>finite twist</u> which has a finite amplitude and must be manipulated differently (see Section 3.1.4). A third type of twist is one which represents a differential displacement over a differential length of time. Such a twist is called an <u>instantaneous twist velocity</u>. The components of an instantaneous twist velocity represent the instantaneous linear and angular rates of a body in motion.

3.1.3 WRENCHES AND WRENCH COORDINATES. Any system of forces and moments can be resolved into a single force vector along a unique line and a single moment vector along that same unique line which is called the <u>wrench axis</u>. When a force system is expressed in this fashion, it is called a <u>wrench</u>. For more detail on forming a wrench representation for a force system see Hunt [Hun78: 47] or Appendix A.

A wrench is regarded as the most general 'force' because it contains both translational *forces* and *rotational moments*. The ratio of the moment to the translational force magnitude is called the <u>wrench pitch</u>. A wrench can be specified by six independent parameters; four to specify the wrench axis, one to specify the pitch, and one to specify the magnitude. Any six independent quantities which are used to represent a wrench can be regarded as the wrench coordinates. If one represents a wrench, $\mathcal{W}$, with the six independent wrench coordinates

$$\mathcal{W} = (w_1, w_2, w_3, w_4, w_5, w_6) \tag{3.7}$$

then (w_1, w_2, w_3) are the components of the net force exerted on the body and (w_4, w_5, w_6) are the components of the net moment resolved at the origin of the coordinate system. The wrench pitch, $\mathcal{P}_w$, is given by

$$\mathcal{P}_w = \frac{w_1 w_4 + w_2 w_5 + w_3 w_6}{\left(w_1^2 + w_2^2 + w_3^2\right)^{1/2}} \tag{3.8}$$

A zero-pitch wrench is a pure translational force along the wrench axis while an infinite-pitch wrench is a pure moment about the axis.

The magnitude of a wrench is called its <u>intensity</u> and it is given by

$$\left(w_1^2 + w_2^2 + w_3^2\right)^{1/2} \qquad (3.9)$$

unless it has an infinite-pitch in which case the intensity is

$$\left(w_4^2 + w_5^2 + w_6^2\right)^{1/2} \qquad (3.10)$$

3.1.4 MANIPULATING TWISTS AND WRENCHES. If twists are of infinitesimal amplitude then they can be mathematically treated the same as any other vectors. This is not true for finite twists, however, because, in general, the resultant of two finite twists depends on the order in which the twists were performed. Wrenches and instantaneous twist velocities, on the other hand, always obey the rules of vector algebra with the one precaution that they must be written in the same coordinate system. The same precaution is true for infinitesimal twists. For example, if one rigid body is moving with a twist velocity of $(\alpha_1, \alpha_2, \alpha_3, \alpha_4, \alpha_5, \alpha_6)$ and another rigid body is moving with a twist velocity of $(\beta_1, \beta_2, \beta_3, \beta_4, \beta_5, \beta_6)$ then the two-body system is moving with a twist velocity of

$$[(\alpha_1 + \beta_1), (\alpha_2 + \beta_2), (\alpha_3 + \beta_3), (\alpha_4 + \beta_4), (\alpha_5 + \beta_5), (\alpha_6 + \beta_6)]$$

3.2 EXTERNAL LOAD CONFIGURATIONS

The external wrench on the object can be categorized as either *symmetric* or *asymmetric* depending on the direction of the zero pitch component of the wrench and whether or not there is an infinite pitch component.

3.2.1 SYMMETRIC LOAD CONFIGURATION. Figure 3.1 shows the configuration of the finger contact forces and the external force on the object for the symmetric case. The origin of the coordinate system is taken at the center of the cylindrical object and the positive y-axis is directed upward through the centroid of the two finger contact points, point A, which is located at the midpoint of the line connecting the two contact points.

There are two angles which are formed by the two radial lines drawn from the center of the cylinder to the two contact points. One angle is greater than or equal to 180 degrees

3-4
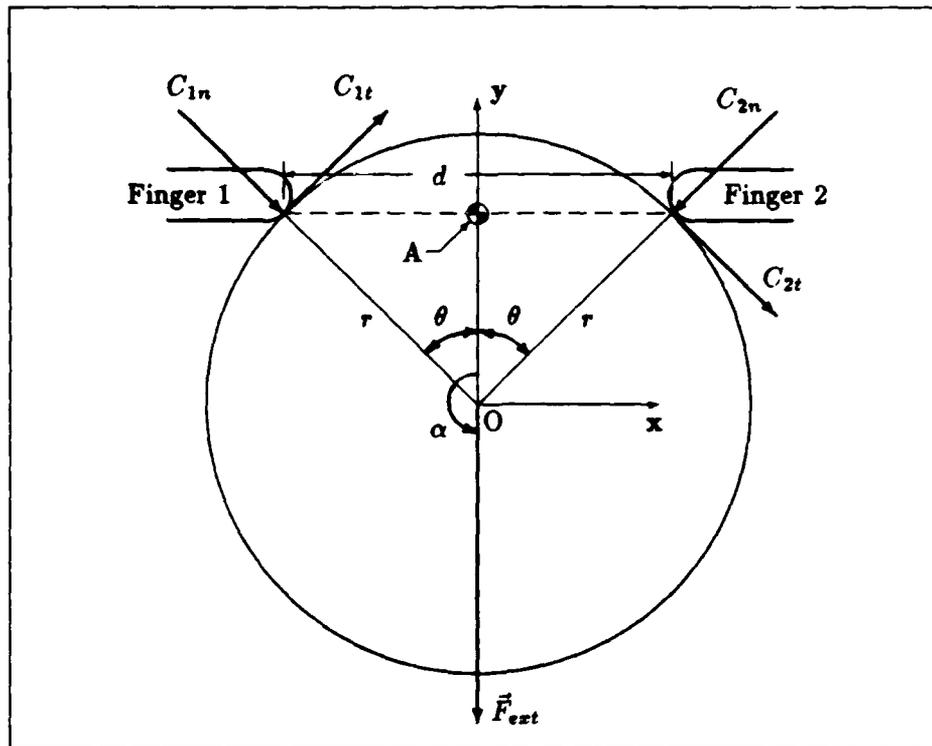
Figure 3.1. Force configuration and coordinate system for symmetric load

while the other is less than or equal to 180 degrees. One may choose to define the grasp
angle, θ, as one-half of either the smaller or the larger of the two angles. Probably the most
practical method of computing the grasp angle is to measure the straight-line distance, d,
between the two fingertips and compute θ from

$$\theta = \arcsin\left(\frac{d}{2r}\right) \qquad (3.11)$$

Using this method, requires one to choose the smaller of the two aforementioned angles as
the grasp angle.

The angle from the positive y-axis counterclockwise to $\vec{F}_{ext}$ is defined as the load
angle, α. For the symmetric load case, α is limited to being equal to either zero degrees
or 180 degrees so that $\vec{F}_{ext}$ must lie along the y-axis.

For a symmetric load configuration, any given fingertip spacing on the object can be
categorized as one of three grasp types: palming, pinching, or cradling. A *palming grasp*
is characterized by the centroid of the fingertip contacts being displaced from the center

3-5
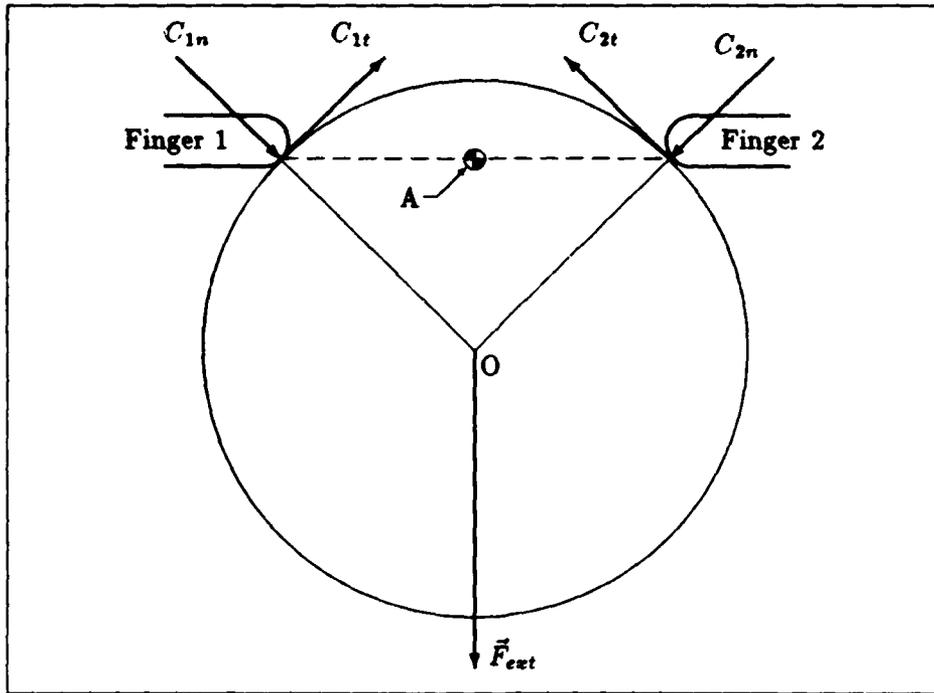
Figure 3.2.   Fingertip and $\vec{F}_{ext}$ configuration for a palming grasp on a
symmetrically loaded object

of the object and $\vec{F}_{ext}$ being directed from the object center and away from the contact
point centroid as shown in Figure 3.2.

A *pinching grasp* is one in which the centroid of the fingertip contacts is coincident
with the center of the object as shown in Figure 3.3. A *cradling grasp* has its fingertip
contact centroid not coincident with the object center and $\vec{F}_{ext}$ is directed from the CG
and through the contact point centroid as shown in Figure 3.4.

Considering symmetry, it is apparent that one can cover the full range of possible
configurations in either of two ways. First, by letting $\alpha = 180$ degrees and considering
$\theta \in (0° : 180°)$ one can transition smoothly from palming through pinching and into
cradling as θ increases. The second option is to consider only $\theta \in (0° : 90°)$ and let $\alpha = 0$
degrees for palming grips and $\alpha = 180$ degrees for cradling grips. To enhance the graphical
presentation of the data, the first option will be used.

3.2.2   ASYMMETRIC LOAD CONFIGURATION.   An asymmetric load can be caused
by either one of two conditions. The first condition is that the resultant external wrench
has zero pitch but it is not directed normal to the line connecting the contact points. This
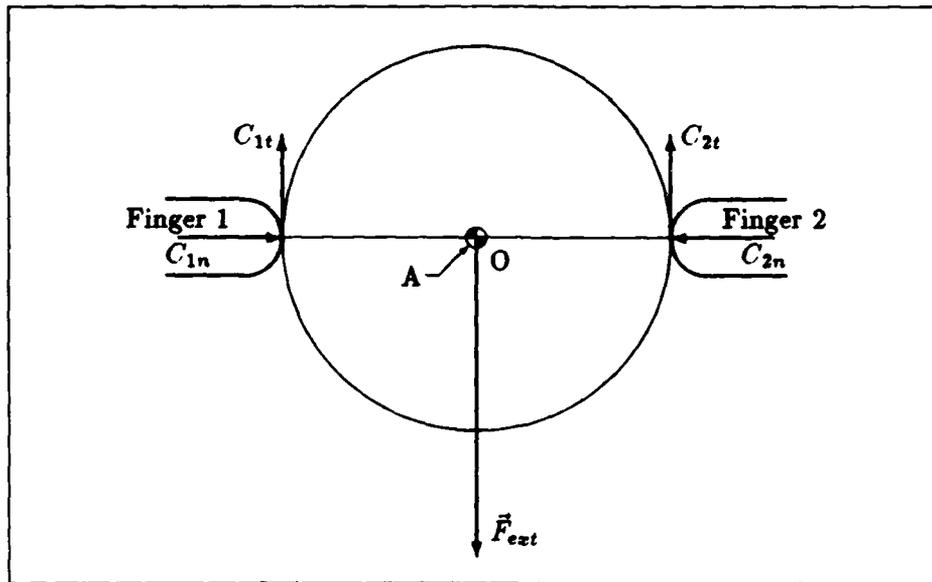
Figure 3.3. Fingertip and $\vec{F}_{ext}$ configuration for a pinching grasp on a symmetrically loaded object
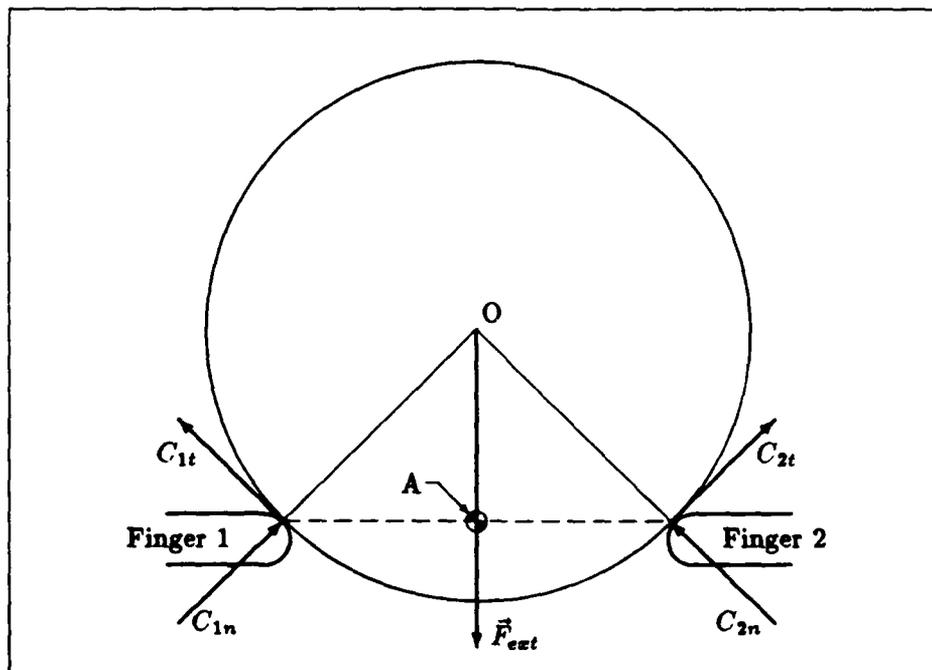
Figure 3.4. Fingertip and $\vec{F}_{ext}$ configuration for a cradling grasp on a symmetrically loaded object

3-7

corresponds to having $\alpha \neq 180°$ in Figure 3.1. The second condition is that the resultant external wrench has a non-zero-pitch, consequently it induces a moment on the object about the object center.

To study the full range of possible grasps of an asymmetrically loaded object, α will be allowed to range from 0 to 360 degrees while θ will be considered from 0 to 180 degrees.

A symmetric load configuration can be considered as a degenerate form of an asymmetric load configuration in which $\alpha = 180°$ and $M_{ext} = 0$. Therefore, the resulting equations from the asymmetric configuration analysis must reduce to those of the symmetric configuration when α is assigned the values of 180 degrees and M_{ext} is taken as zero. The classification of grasps into palming, pinching, and cradling that was discussed in Section 3.2.1 does not apply to asymmetric load configurations.

3.3   FORM AND FORCE CLOSURE

A grasp is said to have <u>form closure</u> when it is able to completely constrain the object under the influence of <u>any</u> external force magnitude and/or direction as long as the fingertip positions are held fixed [Lak78: 1].

Consider a rectangular block resting on a frictionless table. If the block is restricted to remain in contact with the table top, it can only slide across the table or spin about a vertical axis. Consequently, it is constrained to planar motion. One could obtain a form closure 'grasp' of the object by driving four nails into the table such that they just touched each side of the block. With a nail on each side, the block can no longer translate or rotate; it is completely constrained. One doesn't have to apply a certain contact force to the object to maintain equilibrium when form closure exists, one has only to maintain the positions of the contacts. Reuleaux [SR83: 38] showed that at least four point contacts without friction are required to obtain form closure on an object in planar motion. Indeed, if any one of the nails are removed, the object is no longer completely constrained. Because of its symmetry, a circular cylinder is an exception to this statement [Lak78: 4]. No matter how many nails were driven into the table around the perimeter of a cylinder, it would still be free to rotate. Therefore, form closure on a cylindrical object is not possible. Since

3-8

a form closure grasp can be thought of as the most secure grasp, this is an unfortunate result. However, all is not lost because one can obtain equilibrium without having form closure.

A grasp is said to have <u>*force closure*</u> *when the contact forces* <u>*can*</u> *be made to completely constrain the object irregardless of the magnitude and/or direction of the external load wrench* [Ngu86: 1368]. When evaluating a grasp's potential for force closure, any existing frictional forces must obey the applicable friction force model (usually a Coulomb friction model). Otherwise, there is no restriction on the magnitudes of the contact forces.

If one examines the case of a circular cylinder in planar motion, one finds that force closure can be attained by proper placement of two point contacts with friction. The proper placement of the contacts depends on the level of friction available. For a Coulomb friction model, the tangential contact force, C_t, is related to the normal contact force, C_n, by

$$C_t \le \mu_s C_n$$

where μ_s is the static coefficient of friction. The static coefficient of friction defines a friction cone at each contact according to

$$\gamma = \pm \arctan \mu_s \tag{3.12}$$

where γ is the maximum angle allowed between the surface normal and the resultant contact force vector. The friction cone depicts the allowable resultant contact force directions as an angular range about the normal to the surface at the contact point. For example, Figure 3.5 depicts the friction cones at two points of contact on the surface of a circular cylindrical object. In order for the grasp to have force closure, the line segment connecting the two contact points, as shown by the dashed line in Figure 3.5, must fall within the friction cones at both contact points [Ngu86: 1372]. Therefore, the larger the static coefficient of friction, the larger the range of proper finger placements on a cylindrical object to attain force closure. A range of angular spacings between the contact points can be specified for a force closure grasp via a knowledge of the static friction coefficient. If the acute angle subtended by the contact points is 𝚿 and the static coefficient of friction is μ_s,
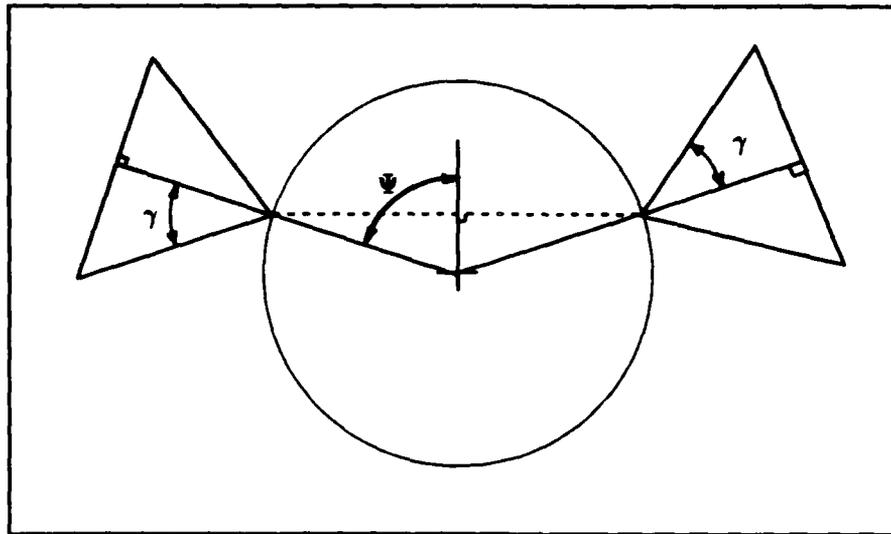
Figure 3.5.   Friction cones at two points of contact on the surface of a circular cylindrical object

then in order for force closure to exist

$$\Psi \geq 180° - 2\arctan\mu_s \tag{3.13}$$

Hence, the smaller the μ_s the closer the fingertip contacts must be to the diameter of the cylinder. On the other hand, for the limiting case when $\mu_s = \infty$, one could theoretically obtain force closure even when the fingertips contacted the object at the same point. Note, however, that although force closure is a sufficient condition for the existence of an equilibrium grasp solution, it is not a necessary condition. In other words, an equilibrium grasp may exist without the grasp having force closure.

3.4   SOLVING FOR CONTACT FORCES

An object is said to be completely constrained when its motion has zero degrees of freedom. Any grasp can be categorized as either *underconstrained, constrained, over-constrained,* or *singular* [Ker84: 34]. An underconstrained grasp occurs when there are not enough independent contact forces to allow complete constraint of the object. A constrained grasp is one in which there are just enough independent contact forces to completely constrain the object. An overconstrained grasp, on the other hand, has more contact forces than are necessary to completely constrain the object. When a grasp has

enough contact forces to completely constrain the object but they are not linearly independent, a singular grasp results.

For planar motion, a cylindrical object grasped by two point contacts with friction creates an overconstrained grasp condition. The major implication of an overconstrained grasp is that the solution is statically indeterminate. However, matrix methods have been presented which allow the solution of the overconstrained grasp problem [Ker84] [Sal82]. These methods are used here to determine the vector of contact forces for a given grasp and object load configuration.

The relationship that expresses the static equilibrium condition between the external wrench applied to the body, $\vec{\mathcal{F}}_{ext}$, and the vector of contact wrench intensities, $\vec{C}$, is given by

$$- \vec{\mathcal{F}}_{ext} = \mathbf{W}\vec{C} \tag{3.14}$$

where $\mathbf{W}$ is known as the *grasp matrix*. Each contact between a fingertip and the object exerts a system of wrenches on the object. When multiple fingertips simultaneously contact the object, the net wrench system is the union of the individual wrench systems for each contact. Therefore, for two contacts the net wrench system will be the concatenation of the wrench system at contact one with the system at contact two.

Because they are taken to be point contacts with friction, the contacts of fingertips 1 and 2 with the object cannot exert any moment on the object about the contact points. Therefore, the contact wrenches consist of zero-pitch wrenches along some arbitrary axes. If the contact wrench at fingertip one is resolved into component directions in an orthogonal coordinate system, it could be written as

$$\vec{C}_1 = C_{1n}\hat{u}_{1n} + C_{1t}\hat{u}_{1t} + C_{1z}\hat{u}_{1z} \tag{3.15}$$

where $\hat{u}_{1n}$, $\hat{u}_{1t}$, and $\hat{u}_{1z}$ are unit vectors in the normal-, tangential-, and z-directions, respectively, at contact point 1 and C_{1n}, C_{1t}, and C_{1z} are the contact wrench intensities along the respective directions. The unit vectors $\hat{u}_{1n}$, $\hat{u}_{1t}$, and $\hat{u}_{1z}$ define the local contact coordinate system at contact 1.

A similar equation can be written for the contact wrench at fingertip two expressed in a local contact coordinate system at fingertip 2 as shown in Figure 3.6. Therefore, the
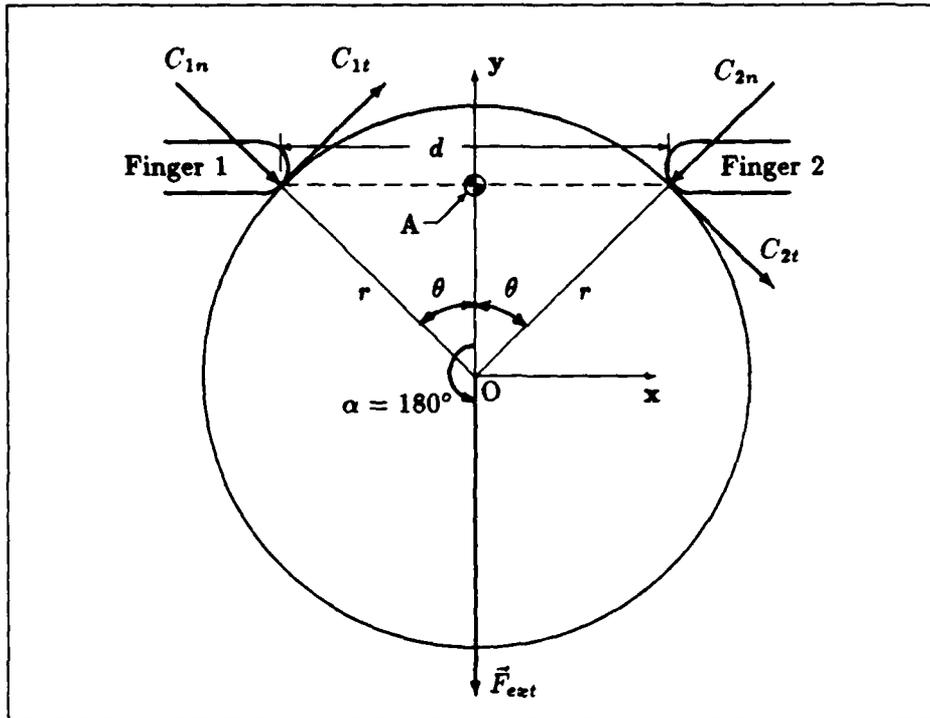
Figure 3.6. Nominal external force configuration and coordinate system for a two-fingered grasp of an object

entire vector of contact wrench intensities in the local contact coordinate space is

$$\vec{C} = \left\{ \begin{array}{cccccc} C_{1n} & C_{1t} & C_{1z} & C_{2n} & C_{2t} & C_{2z} \end{array} \right\}^T \tag{3.16}$$

For planar motion, C_{1z} and C_{2z} are not allowed. However they will be carried as place-holders and their magnitudes will be set to zero. This will allow use of the matrix methods in their fullest generality.

Under the constraint of planar motion, the applicable object coordinate system forces and moments consist of forces along x_o and y_o and moments about z_o. Therefore, $\vec{F}_{ext}$ in Eq (3.14) is given by

$$\vec{F}_{ext} = \left\{ \begin{array}{ccc} F_{ext_{x_o}} & F_{ext_{y_o}} & M_{ext_{z_o}} \end{array} \right\}^T \tag{3.17}$$

where $F_{ext_{x_o}}$ and $F_{ext_{y_o}}$ are the magnitudes of zero-pitch external wrenches on the object in the x- and y-directions of the object frame, respectively, and $M_{ext_{z_o}}$ is the magnitude of an infinite-pitch wrench (moment) on the object about the z-axis of the object frame.

3-12

Equation (3.14) is essentially a force and moment equilibrium expression with the grasp matrix transforming a set of unit wrenches from the local contact coordinate frame to the object frame. This transformation is necessary because $\vec{\mathcal{F}}_{ext}$ is expressed in the object coordinate frame and equilibrium between two wrenches is only meaningful if they are expressed in the same coordinate frame. Such a transformation of wrenches is termed a *wrench transformation* as opposed to a simple coordinate transformation.

Each column of $\mathcal{W}$ transforms a unit wrench along a local contact coordinate axis into an equivalent wrench system in the object coordinate system. For example, column one of $\mathcal{W}$ transforms a zero-pitch wrench along $\hat{u}_{1n}$ into a zero-pitch wrench with components along the x_o and y_o axes with magnitudes $\sin\theta$ and $-\cos\theta$, respectively. Column two transforms a unit zero-pitch wrench along $\hat{u}_{1t}$ into a wrench with translational components along the x_o and y_o axes having magnitudes $\cos\theta$ and $\sin\theta$, respectively, and an angular component (moment) about the $-z_o$ axis having magnitude r_o. Finally, a unit zero-pitch wrench along $\hat{u}_{1z}$ is mapped by a zero column vector in $\mathcal{W}$ because it has no components in the x-y plane or about the z_o axis. When the contact wrench at fingertip 2 is similarly transformed, the resulting $\mathcal{W}$ matrix is

$$\mathbf{W} = \begin{bmatrix} \sin\theta & \cos\theta & 0 & -\sin\theta & \cos\theta & 0 \\ -\cos\theta & \sin\theta & 0 & -\cos\theta & -\sin\theta & 0 \\ 0 & -r_o & 0 & 0 & -r_o & 0 \end{bmatrix} \tag{3.18}$$

Examining Eq (3.18) reveals that the $\mathbf{W}$ matrix is invariant with changing $\vec{\mathcal{F}}_{ext}$, therefore it will be the same for both the symmetric and asymmetric external load cases. Since the grasp is overconstrained $\mathbf{W}$ has more columns than rows and the system is statically indeterminate. To solve for $\vec{C}$ in Eq (3.14), two orthogonal vector components are introduced which make up $\vec{C}$:

$$\vec{C} = \vec{C}_p + \vec{C}_h \tag{3.19}$$

where $\vec{C}_p$ is the particular solution and $\vec{C}_h$ is the homogeneous solution. Due to the orthogonality of the homogeneous and particular solutions, they can be found independently and then summed according to Eq (3.19).

3.4.1 DETERMINING THE HOMOGENEOUS SOLUTION CONTACT FORCE

VECTOR. The homogeneous solution component of Eq (3.19) lies in the null space of $\mathbf{W}$ and can be found from

$$\vec{C}_h = \mathcal{N}\,\vec{\lambda} \tag{3.20}$$

where $\mathcal{N}$ is a matrix whose columns are a set of orthonormal basis vectors which span the null space of $\mathbf{W}$ and λ is a vector which will contain the arbitrarily selected magnitudes of the internal grasp forces.

To determine $\mathcal{N}$ such that $\mathbf{W}\mathcal{N} = 0$, $\mathbf{W}$ must first be augmented to make it a square matrix so that it can be put into the *modified Hermite normal form* [DH81: 133]. When $\mathbf{W}$ is augmented, the new matrix, $\mathbf{W}_a$ appears as

$$\mathbf{W}_a = \begin{bmatrix} \sin\theta & \cos\theta & 0 & -\sin\theta & \cos\theta & 0 \\ -\cos\theta & \sin\theta & 0 & -\cos\theta & -\sin\theta & 0 \\ 0 & -r_o & 0 & 0 & -r_o & 0 \\ 0 & 0 & 0 & 0 & 0 & 0 \\ 0 & 0 & 0 & 0 & 0 & 0 \\ 0 & 0 & 0 & 0 & 0 & 0 \end{bmatrix} \tag{3.21}$$

When the proper row operations are performed, the resulting modified Hermite normal form is

$$\mathrm{HNF}\,(\mathbf{W}_a) = \begin{bmatrix} 1 & 0 & 0 & 0 & \tan\theta & 0 \\ 0 & 1 & 0 & 0 & 1 & 0 \\ 0 & 0 & 0 & 0 & 0 & 0 \\ 0 & 0 & 0 & 1 & \tan\theta & 0 \\ 0 & 0 & 0 & 0 & 0 & 0 \\ 0 & 0 & 0 & 0 & 0 & 0 \end{bmatrix} \tag{3.22}$$

Consequently, there are three basis vectors which span the null space of $\mathbf{W}$ so $\mathcal{N}$ is given

by

$$\mathcal{N} = \text{span} \begin{bmatrix} 0 & \tan\theta & 0 \\ 0 & 1 & 0 \\ -1 & 0 & 0 \\ 0 & \tan\theta & 0 \\ 0 & -1 & 0 \\ 0 & 0 & -1 \end{bmatrix} \qquad (3.23)$$

For planar motion, the first and the third basis vectors are invalid because they are not in the x-y plane. Therefore, the second basis vector is selected to represent the null space of the grasp matrix under the restriction of planar motion. Therefore, the homogeneous solution is

$$\vec{C}_h = \left\{ \begin{array}{c} \sin\theta \\ \cos\theta \\ 0 \\ \sin\theta \\ -\cos\theta \\ 0 \end{array} \right\} \lambda \qquad (3.24)$$

where λ is the scalar magnitude of the homogeneous contact force solution.

When Eq (3.24) is examined in light of the coordinate system defined in Figure 3.6 it is apparent that the direction of the internal grasp force is parallel to the x-axis for all θ. This is true for both symmetric and asymmetric loads since the grasp matrix is invariant with changes in $\vec{\mathcal{F}}_{ext}$.

Simple geometry can confirm that if $\vec{C}_h$ always acts along the x_o-axis of the defined object coordinate system, then it always acts along the line connecting the two contact points. Thus, for a two-fingered grasp, the internal grasp force is identical to the interaction force defined by Waldron [Wal86] [KW87].

Because this planar grasp is overconstrained by one excess contact force component, the arbitrary vector of internal grasp force magnitudes, $\vec{\lambda}$, is a single element vector (scalar) which represents an independent variable in the solution of the contact force vector. In the

case of this grasp, λ corresponds exactly to the magnitude of the interaction force between the two finger contact points.

3.4.2 DETERMINING THE PARTICULAR SOLUTION CONTACT FORCE

VECTOR. The particular solution can be found from

$$\vec{C}_p = -\mathbf{W}_R^+ \mathcal{F}_{ext} \tag{3.25}$$

where $\mathbf{W}_R^+$ is the right generalized (Moore-Penrose) inverse of $\mathbf{W}$ and can be found from [BG74] to be given by

$$\mathbf{W}_R^+ = \mathbf{W}^T \left(\mathbf{W}\mathbf{W}^T \right)^{-1} \tag{3.26}$$

The first step in determining $\mathbf{W}_R^+$ is to find $\mathbf{W}\mathbf{W}^T$ which turns out to be

$$\mathbf{W}\mathbf{W}^T = \begin{bmatrix} 2 & 0 & -2r_o \cos\theta \\ 0 & 2 & 0 \\ -2r_o \cos\theta & 0 & 2r_o^2 \end{bmatrix} \tag{3.27}$$

When Eq (3.27) is inverted, the result is

$$\left(\mathbf{W}\mathbf{W}^T \right)^{-1} = \frac{1}{2\sin^2\theta} \begin{bmatrix} 1 & 0 & \cos\theta/r_o \\ 0 & \sin^2\theta & 0 \\ \cos\theta/r_o & 0 & 1/r_o^2 \end{bmatrix} \tag{3.28}$$

When this is multiplied by $\mathbf{W}^T$ the right generalized inverse is found to be

$$\mathbf{W}_R^+ = \begin{bmatrix} \frac{1}{2\sin\theta} & \frac{-\cos\theta}{2} & \frac{\cos\theta}{2r_o\sin\theta} \\ 0 & \frac{\sin\theta}{2} & \frac{-1}{2r_o} \\ 0 & 0 & 0 \\ \frac{-1}{2\sin\theta} & \frac{-\cos\theta}{2} & \frac{-\cos\theta}{2r_o\sin\theta} \\ 0 & \frac{-\sin\theta}{2} & \frac{-1}{2r_o} \\ 0 & 0 & 0 \end{bmatrix} \tag{3.29}$$

The right generalized inverse given in Eq (3.29) is valid for the particular solution of grasps with both symmetric and asymmetric loads. However, the particular solution vector, $\vec{C}_p$, will be somewhat different for the two categories of grasps because the external wrench,

3-16

$\vec{\mathcal{F}}_{ext}$, will be different. For a symmetric load configuration and no external moment as defined in the coordinate system of Figure 3.1, the external wrench applied to the body is

$$\vec{\mathcal{F}}_{ext} = \left\{ \begin{array}{ccc} 0 & -F_{ext} & 0 \end{array} \right\}^T \tag{3.30}$$

Inserting Eq (3.30) and Eq (3.29) into Eq (3.25) yields the following for the <u>symmetric</u> load configuration:

$$\vec{C}_p = \frac{F_{ext}}{2} \left\{ \begin{array}{c} -\cos\theta \\ \sin\theta \\ 0 \\ -\cos\theta \\ -\sin\theta \\ 0 \end{array} \right\} \tag{3.31}$$

One can easily see from Eq (3.31) that, for a symmetric load, $\vec{C}_p$ corresponds to having a contact force at each of the two contact points which is parallel to the y_o-axis. In addition, the magnitudes of the particular solution component of each of the two contact forces are equal so each of them equilibrates half of F_{ext}.

For an asymmetric load configuration having no external moment applied to the object as defined in the coordinate system of Figure 3.1, the external wrench applied to the body can be written as

$$\vec{\mathcal{F}}_{ext} = \left\{ \begin{array}{ccc} -F_{ext}\sin\alpha & F_{ext}\cos\alpha & 0 \end{array} \right\}^T \tag{3.32}$$

Inserting Eq (3.32) and Eq (3.29) into Eq (3.25) yields the following for the <u>asymmetric</u> load configuration:

$$\vec{C}_p = \frac{F_{ext}}{2} \left\{ \begin{array}{c} \cos\alpha\cos\theta + \frac{\sin\alpha}{\sin\theta} \\ -\sin\theta\cos\alpha \\ 0 \\ \cos\alpha\cos\theta - \frac{\sin\alpha}{\sin\theta} \\ \sin\theta\cos\alpha \\ 0 \end{array} \right\} \tag{3.33}$$

Note that Eq (3.33) is a more general form of Eq (3.31) and the two equations are equal when $\alpha = 180$ degrees. Finally, the most general expression for the particular

solution contact force vector is one where the external wrench includes an asymmetric translational load and a non-zero moment. For such a load configuration, the external wrench applied to the object can be written as

$$\vec{\mathcal{F}}_{ext} = \left\{ \begin{array}{ccc} -F_{ext}\sin\alpha & F_{ext}\cos\alpha & M_{ext} \end{array} \right\}^T \tag{3.34}$$

Solving for $\vec{C}_p$ yields

$$\vec{C}_p = \frac{1}{2r\sin\theta} \left\{ \begin{array}{c} -M_{ext}\cos\theta + F_{ext}r\sin\alpha + F_{ext}r\cos\theta\sin\theta\cos\alpha \\[1mm] M_{ext}\sin\theta - F_{ext}r\sin^2\theta\cos\alpha \\[1mm] 0 \\[1mm] M_{ext}\cos\theta - F_{ext}r\sin\alpha + F_{ext}r\cos\theta\sin\theta\cos\alpha \\[1mm] M_{ext}\sin\theta + F_{ext}r\sin^2\theta\cos\alpha \\[1mm] 0 \end{array} \right\} \tag{3.35}$$

Equation (3.35) reduces to Eq (3.33) when M_{ext} is zero and it reduces to Eq (3.31) when α is 180 degrees and M_{ext} is zero.

3.4.3   TOTAL CONTACT FORCE VECTOR SOLUTION.

The entire contact force vector can now be written in its most general form using Eqs (3.24) and (3.35) to get

$$\vec{C} = \frac{F_{ext}}{2} \left\{ \begin{array}{c} 2\lambda'\sin\theta + \cos\alpha\cos\theta + \frac{\sin\alpha}{\sin\theta} - \frac{M'\cos\theta}{r\sin\theta} \\[1mm] 2\lambda'\cos\theta - \cos\alpha\sin\theta + \frac{M'}{r} \\[1mm] 0 \\[1mm] 2\lambda'\sin\theta + \cos\alpha\cos\theta - \frac{\sin\alpha}{\sin\theta} + \frac{M'\cos\theta}{r\sin\theta} \\[1mm] -2\lambda'\cos\theta + \cos\alpha\sin\theta + \frac{M'}{r} \\[1mm] 0 \end{array} \right\} \tag{3.36}$$

where

$$\lambda' \equiv \frac{\lambda}{F_{ext}} \tag{3.37}$$

and

$$M' \equiv \frac{M_{ext}}{F_{ext}} \tag{3.38}$$

3-18

Equation (3.36) can be algebraically rearranged to give

$$\vec{C} = \frac{F_{ext}}{2r\sin\theta} \left\{ \begin{array}{c} 2r\lambda'\sin^2\theta + r\cos\alpha\sin\theta\cos\theta + r\sin\alpha - M'\cos\theta \\ 2r\lambda'\sin\theta\cos\theta - r\cos\alpha\sin^2\theta + M'\sin\theta \\ 0 \\ 2r\lambda'\sin^2\theta + r\cos\alpha\sin\theta\cos\theta - r\sin\alpha + M'\cos\theta \\ -2r\lambda'\sin\theta\cos\theta + r\cos\alpha\sin^2\theta + M'\sin\theta \\ 0 \end{array} \right\} \tag{3.39}$$

Equation (3.39) is the most general expression for the contact force vector. By substitution of $\alpha = 180$ degrees and/or $M' = 0$, it can be reduced to symmetric and asymmetric loads with no external moment.

3.5 DEVELOPMENT OF THE HAND JACOBIAN MATRIX

The first step in forming the global Jacobian matrix for the entire hand, $\mathcal{J}$, is to form the Jacobian matrices for each of the individual fingers, $\mathcal{J}_i$, as if they were manipulators. The hand Jacobian is then just the $\mathcal{J}_i$ in block diagonal form.

A hand structure must be defined before the Jacobian matrix of a gripper can be developed. For this thesis, the assumed hand structure is a two-fingered hand with planar three-link fingers. The finger links and finger joints are sequentially numbered starting with the link or joint closest to the palm as the lowest number. The length of the jth link from the base on the ith finger is denoted by l_{ij}. The angles of the finger joints are sequentially numbered starting with the angle of the base joint on finger 1 as ϕ_1 and proceeding outward to the angle of the last joint on finger 1 denoted by ϕ_3. The sequential numbering continues with the angle of the base joint on finger 2 as ϕ_4 and the angle of the last joint on finger 2 as ϕ_6. The structure of the hand and the nomenclature are depicted in Figure 3.7.

There are four coordinate frames of interest in the analysis of this two-fingered grasp. The first is termed the *palm frame* which has its origin, O_p, centered halfway between the base joints of the two fingers. Its x_p-axis is directed through the base joint pin of finger
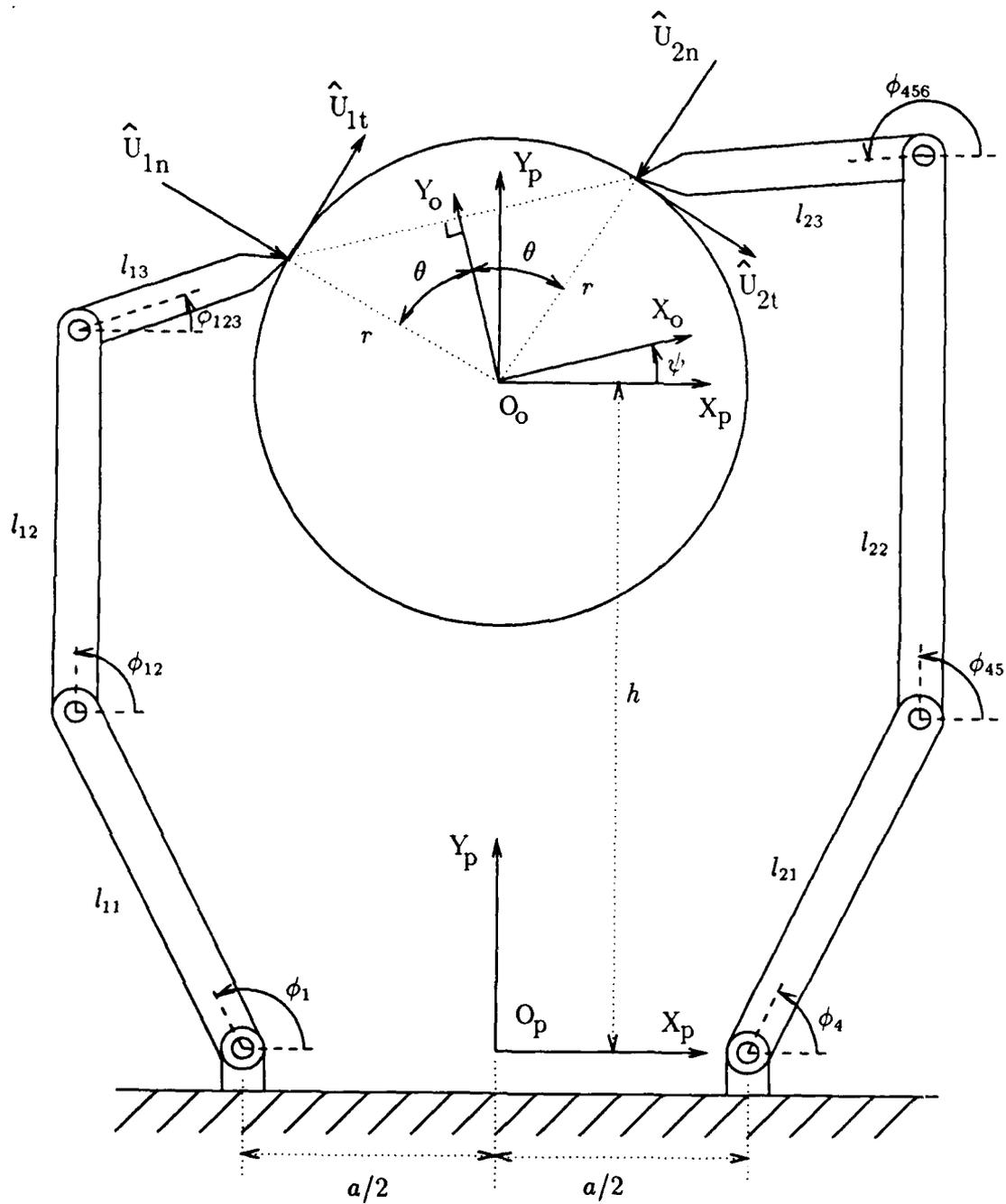
Figure 3.7. Selected hand structure and nomenclature for derivation of Jacobian matrix
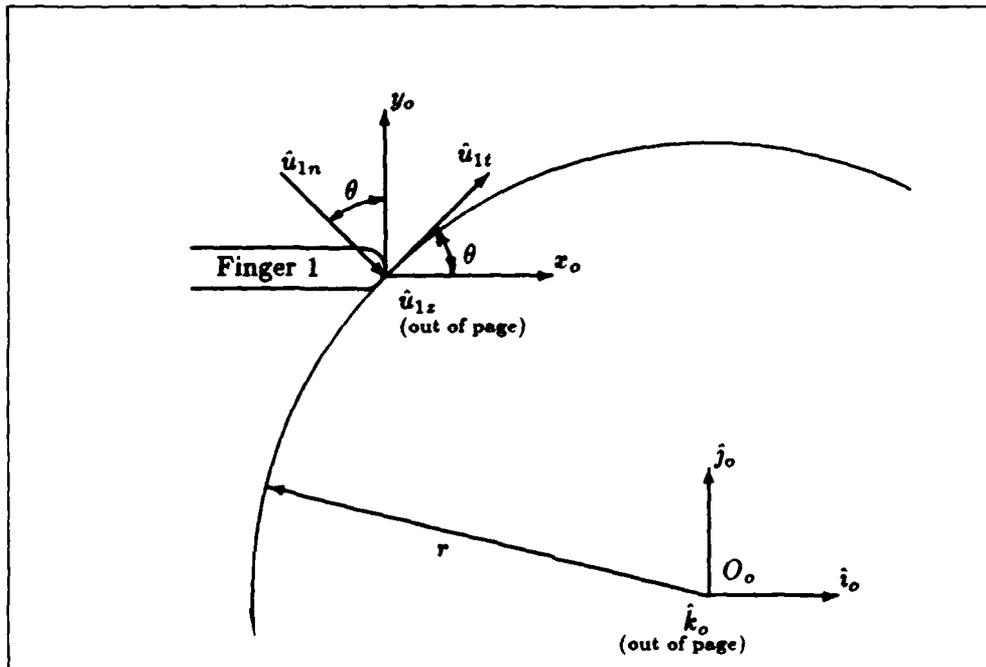
Figure 3.8. Local contact coordinate frame for contact point 1

2, its y_p-axis is directed outward from the palm, and its z_p-axis completes a right-handed coordinate system.

A second frame is the *object frame* which has it origin, O_o, at the center of the object a height h above O_p. Its x_o-axis is parallel with the line connecting the contact points of fingertips 1 and 2 and directed towards contact point 2. Its z_o-axis is aligned with the z_p-axis of the palm coordinate system and its y_o-axis completes a right-handed coordinate system. The scope of this analysis is limited to configurations with O_o on the y_p-axis of the palm coordinate frame.

The third and fourth frames of interest are the *local contact coordinate frames* which have their origins at contact points 1 and 2. They each have a normal axis, $\hat{u}_{in}$, which points inward towards the object center, a z-axis, $\hat{u}_{iz}$, which is parallel to the z-axes of the palm and object systems, and a tangential axis, $\hat{u}_{it}$, that completes the right-hand system according to $\hat{u}_{in} \times \hat{u}_{it} = \hat{u}_{iz}$. The local contact coordinate frame for contact point 1 is shown in Figure 3.8, while that of contact point 2 is shown in Figure 3.9.

The $\mathcal{J}_i$ are the first partial derivatives, with respect to the joint angles, of the finger-
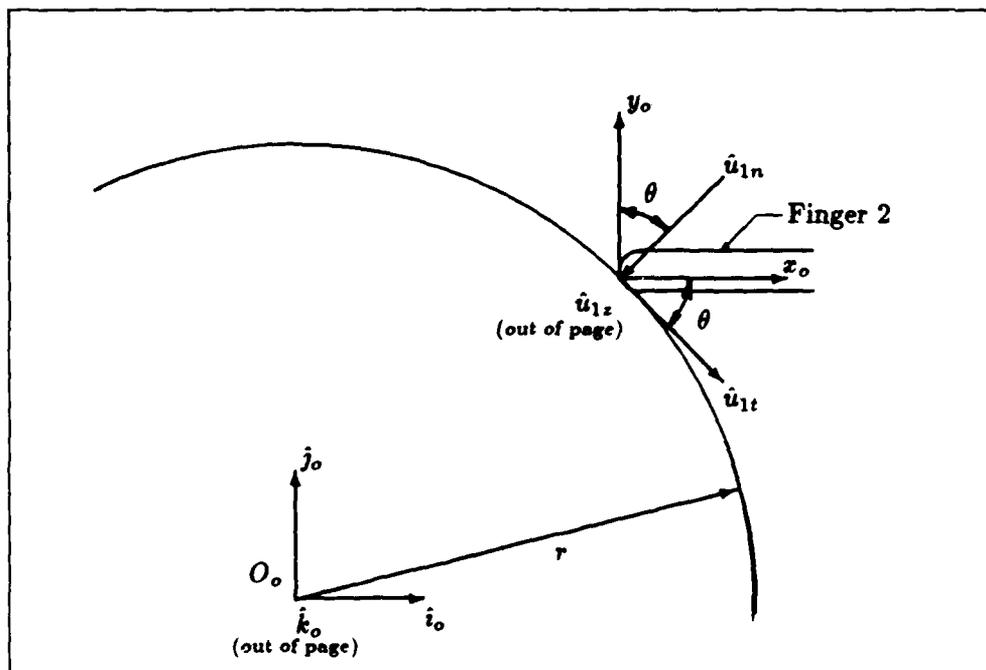
Figure 3.9. Local contact coordinate frame for contact point 2

tip positions expressed in the local contact coordinate systems. Therefore, the fingertip positions must be expressed as vectors given in the local contact coordinate frames and functions of the finger joint angles. To make the derivation more explicit the fingertip position vectors are first expressed in terms of the palm frame, then transformed into the object frame, and finally transformed into the local contact coordinate frames before the derivatives are taken. This step-by-step derivation should be more tractable than stepping right into the local contact coordinate frame, although the result may seem obvious in the end.

Begin by writing expressions for the positions of the endpoints of interest (the contact of the fingertips with the object) expressed in the palm coordinate frame as functions of the joint variables:

$$P_{1x_p} = l_{11} \cos \phi_1 + l_{12} \cos \phi_{12} + l_{13} \cos \phi_{123} - a/2 \qquad (3.40)$$

$$P_{1y_p} = l_{11} \sin \phi_1 + l_{12} \sin \phi_{12} + l_{13} \sin \phi_{123} \qquad (3.41)$$

$$P_{1z_p} = 0 \qquad (3.42)$$

where

$$\phi_{12} \equiv \phi_1 + \phi_2 \quad \text{and} \quad \phi_{123} \equiv \phi_1 + \phi_2 + \phi_3$$

The orientation of the centerline of link 3 on finger 1 can be described by

$$\gamma_{1x_p} = 0 \tag{3.43}$$

$$\gamma_{1y_p} = 0 \tag{3.44}$$

$$\gamma_{1z_p} = \phi_{123} \tag{3.45}$$

Similarly, the coordinates of the contact of fingertip 2 with the object expressed in the palm frame are

$$P_{2x_p} = l_{21} \cos \phi_4 + l_{22} \cos \phi_{45} + l_{23} \cos \phi_{456} + a/2 \tag{3.46}$$

$$P_{2y_p} = l_{21} \sin \phi_4 + l_{22} \sin \phi_{45} + l_{23} \sin \phi_{456} \tag{3.47}$$

$$P_{2z_p} = 0 \tag{3.48}$$

where

$$\phi_{45} \equiv \phi_4 + \phi_5 \quad \text{and} \quad \phi_{456} \equiv \phi_4 + \phi_5 + \phi_6$$

The orientation of the centerline of link 3 on finger 2 is given by

$$\gamma_{2x_p} = 0 \tag{3.49}$$

$$\gamma_{2y_p} = 0 \tag{3.50}$$

$$\gamma_{2z_p} = \phi_{456} \tag{3.51}$$

Now transform Eqs (3.40) through (3.51) from the palm frame to the object frame. The transformations between those frames are

$$P_{ix_o} = P_{ix_p} \cos \psi + (P_{iy_p} - h) \sin \psi \tag{3.52}$$

$$P_{iy_o} = -P_{ix_p} \sin \psi + (P_{iy_p} - h) \cos \psi \tag{3.53}$$

$$P_{iz_o} = P_{iz_p} \tag{3.54}$$

$$\gamma_{ix_o} = \gamma_{ix_p} \tag{3.55}$$

$$\gamma_{iy_o} = \gamma_{iy_p} \tag{3.56}$$

$$\gamma_{iz_o} = \gamma_{iz_p} - \psi \tag{3.57}$$

Applying Eqs (3.52) through (3.57) to the finger 1 position equations yields

$$P_{1x_o} = (l_{11} \cos \phi_1 + l_{12} \cos \phi_{12} + l_{13} \cos \phi_{123} - a/2) \cos \psi +$$

$$(l_{11} \sin \phi_1 + l_{12} \sin \phi_{12} + l_{13} \sin \phi_{123} - h) \sin \psi \qquad (3.58)$$

$$P_{1y_o} = -(l_{11} \cos \phi_1 + l_{12} \cos \phi_{12} + l_{13} \cos \phi_{123} - a/2) \sin \psi +$$

$$(l_{11} \sin \phi_1 + l_{12} \sin \phi_{12} + l_{13} \sin \phi_{123} - h) \cos \psi \qquad (3.59)$$

$$P_{1z_o} = 0 \qquad (3.60)$$

$$\gamma_{1x_o} = 0 \qquad (3.61)$$

$$\gamma_{1y_o} = 0 \qquad (3.62)$$

$$\gamma_{1z_o} = \phi_{123} - \psi \qquad (3.63)$$

Applying Eqs (3.52) through (3.57) to the finger 2 position equations yields

$$P_{2x_o} = (l_{21} \cos \phi_4 + l_{22} \cos \phi_{45} + l_{23} \cos \phi_{456} + a/2) \cos \psi +$$

$$(l_{21} \sin \phi_4 + l_{22} \sin \phi_{45} + l_{23} \sin \phi_{456} - h) \sin \psi \qquad (3.64)$$

$$P_{2y_o} = -(l_{21} \cos \phi_4 + l_{22} \cos \phi_{45} + l_{23} \cos \phi_{456} + a/2) \sin \psi +$$

$$(l_{21} \sin \phi_4 + l_{22} \sin \phi_{45} + l_{23} \sin \phi_{456} - h) \cos \psi \qquad (3.65)$$

$$P_{2z_o} = 0 \qquad (3.66)$$

$$\gamma_{2x_o} = 0 \qquad (3.67)$$

$$\gamma_{2y_o} = 0 \qquad (3.68)$$

$$\gamma_{2z_o} = \phi_{456} - \psi \qquad (3.69)$$

Equations (3.58) through (3.69) must now be transformed from the object coordinate frame to the local contact coordinate frames. This transformation will be different for each of the two fingers. The transformations for finger 1 are

$$P_{1n} = P_{1x_o} \sin \theta - P_{1y_o} \cos \theta + r \qquad (3.70)$$

$$P_{1t} = P_{1x_o} \cos \theta + P_{1y_o} \sin \theta \qquad (3.71)$$

$$P_{1z} = P_{1z_o} \qquad (3.72)$$

$$\gamma_{1n} = 0 \qquad (3.73)$$

$$\gamma_{1t} = 0 \tag{3.74}$$

$$\gamma_{1z} = \gamma_{1z_o} - \theta \tag{3.75}$$

Applying Eqs (3.70) through (3.75) to transform the position Eqs (3.58) through (3.63) from the object frame to the contact 1 coordinate frame results in

$$P_{1n} = (l_{11}\cos\phi_1 + l_{12}\cos\phi_{12} + l_{13}\cos\phi_{123} - a/2)\sin(\theta + \psi) -$$
$$(l_{11}\sin\phi_1 + l_{12}\sin\phi_{12} + l_{13}\sin\phi_{123} - h)\cos(\theta + \psi) + r \tag{3.76}$$

$$P_{1t} = (l_{11}\cos\phi_1 + l_{12}\cos\varphi_{12} + l_{13}\cos\phi_{123} - a/2)\cos(\theta + \psi) +$$
$$(l_{11}\sin\phi_1 + l_{12}\sin\phi_{12} + l_{13}\sin\phi_{123} - h)\sin(\theta + \psi) \tag{3.77}$$

$$P_{1z} = 0 \tag{3.78}$$

$$\gamma_{1n} = 0 \tag{3.79}$$

$$\gamma_{1t} = 0 \tag{3.80}$$

$$\gamma_{1z} = \phi_{123} - (\theta + \psi) \tag{3.81}$$

Transforming Eqs (3.64) to (3.69) from the object frame to the contact 2 coordinate frame requires the following equations:

$$P_{2n} = -P_{2x_o}\sin\theta - P_{2y_o}\cos\theta + r \tag{3.82}$$

$$P_{2t} = P_{2x_o}\cos\theta - P_{2y_o}\sin\theta \tag{3.83}$$

$$P_{2z} = P_{2z_o} \tag{3.84}$$

$$\gamma_{2n} = 0 \tag{3.85}$$

$$\gamma_{2t} = 0 \tag{3.86}$$

$$\gamma_{2z} = \gamma_{2z_o} + \theta \tag{3.87}$$

Applying these transformations to Eqs (3.64) through (3.69) yields

$$P_{2n} = -(l_{21}\cos\phi_4 + l_{22}\cos\phi_{45} + l_{23}\cos\phi_{456} + a/2)\sin(\theta - \psi) -$$
$$(l_{21}\sin\phi_4 + l_{22}\sin\phi_{45} + l_{23}\sin\phi_{456} - h)\cos(\theta - \psi) + r \tag{3.88}$$

$$P_{2t} = (l_{21}\cos\phi_4 + l_{22}\cos\phi_{45} + l_{23}\cos\phi_{456} + a/2)\cos(\theta - \psi) -$$
$$(l_{21}\sin\phi_4 + l_{22}\sin\phi_{45} + l_{23}\sin\phi_{456} - h)\sin(\theta - \psi) \tag{3.89}$$

3-25

$$P_{2z} = 0 \tag{3.90}$$

$$\gamma_{2n} = 0 \tag{3.91}$$

$$\gamma_{2t} = 0 \tag{3.92}$$

$$\gamma_{2z} = \phi_{456} - (\theta - \psi) \tag{3.93}$$

With the position information now in the local contact coordinate frames, the derivatives of Eqs (3.76) through (3.81) can be taken to get the following velocity relations for finger 1:

$$
\begin{aligned}
V_{1n} = & \left[-\left(l_{11} \sin \phi_1 + l_{12} \sin \phi_{12} + l_{13} \sin \phi_{123} \right) \dot{\phi}_1 - \right. \\
& \left. \left(l_{12} \sin \phi_{12} + l_{13} \sin \phi_{123} \right) \dot{\phi}_2 - \left(l_{13} \sin \phi_{123} \right) \dot{\phi}_3 \right] \sin(\theta + \psi) - \\
& \left[\left(l_{11} \cos \phi_1 + l_{12} \cos \phi_{12} + l_{13} \cos \phi_{123} \right) \dot{\phi}_1 + \right. \\
& \left. \left(l_{12} \cos \phi_{12} + l_{13} \cos \phi_{123} \right) \dot{\phi}_2 + \left(l_{13} \cos \phi_{123} \right) \dot{\phi}_3 \right] \cos(\theta + \psi)
\end{aligned}
\tag{3.94}
$$

$$
\begin{aligned}
V_{1t} = & \left[-\left(l_{11} \sin \phi_1 + l_{12} \sin \phi_{12} + l_{13} \sin \phi_{123} \right) \dot{\phi}_1 - \right. \\
& \left. \left(l_{12} \sin \phi_{12} + l_{13} \sin \phi_{123} \right) \dot{\phi}_2 - \left(l_{13} \sin \phi_{123} \right) \dot{\phi}_3 \right] \cos(\theta + \psi) + \\
& \left[\left(l_{11} \cos \phi_1 + l_{12} \cos \phi_{12} + l_{13} \cos \phi_{123} \right) \dot{\phi}_1 + \right. \\
& \left. \left(l_{12} \cos \phi_{12} + l_{13} \cos \phi_{123} \right) \dot{\phi}_2 + \left(l_{13} \cos \phi_{123} \right) \dot{\phi}_3 \right] \sin(\theta + \psi)
\end{aligned}
\tag{3.95}
$$

$$V_{1.} = 0 \tag{3.96}$$

$$\omega_{1n} = 0 \tag{3.97}$$

$$\omega_{1t} = 0 \tag{3.98}$$

$$\omega_{1z} = \dot{\phi}_1 + \dot{\phi}_2 + \dot{\phi}_3 \tag{3.99}$$

Note that θ, ψ, r, h, and the l_{ij} are all considered as constants.

Likewise, the derivatives of Eqs (3.88) through (3.93) give the velocities of fingertip 2 in the contact 2 coordinate system as functions of the joint angles and their derivatives:

$$
\begin{aligned}
V_{2n} = & \left[\left(l_{21} \sin \phi_4 + l_{22} \sin \phi_{45} + l_{23} \sin \phi_{456} \right) \dot{\phi}_4 + \right. \\
& \left. \left(l_{22} \sin \phi_{45} + l_{23} \sin \phi_{456} \right) \dot{\phi}_5 + \left(l_{23} \sin \phi_{456} \right) \dot{\phi}_6 \right] \sin(\theta - \psi) - \\
& \left[\left(l_{21} \cos \phi_4 + l_{22} \cos \phi_{45} + l_{23} \cos \phi_{456} \right) \dot{\phi}_4 + \right. \\
& \left. \left(l_{22} \cos \phi_{45} + l_{23} \cos \phi_{456} \right) \dot{\phi}_5 + \left(l_{23} \cos \phi_{456} \right) \dot{\phi}_6 \right] \cos(\theta - \psi)
\end{aligned}
\tag{3.100}
$$

$$V_{2t} = \left[-\left(l_{21} \sin \phi_4 + l_{22} \sin \phi_{45} + l_{23} \sin \phi_{456} \right) \dot{\phi}_4 - \right.$$

$$\left(l_{22} \sin \phi_{45} + l_{23} \sin \phi_{456} \right) \dot{\phi}_5 - \left(l_{23} \sin \phi_{456} \right) \dot{\phi}_6 \Big] \cos \left(\theta - \psi \right) -$$

$$\left[\left(l_{21} \cos \phi_4 + l_{22} \cos \phi_{45} + l_{23} \cos \phi_{456} \right) \dot{\phi}_4 + \right.$$

$$\left(l_{22} \cos \phi_{45} + l_{23} \cos \phi_{456} \right) \dot{\phi}_5 + \left(l_{23} \cos \phi_{456} \right) \dot{\phi}_6 \Big] \sin \left(\theta - \psi \right) \tag{3.101}$$

$$V_{2z} = 0 \tag{3.102}$$

$$\omega_{2n} = 0 \tag{3.103}$$

$$\omega_{2t} = 0 \tag{3.104}$$

$$\omega_{2z} = \dot{\phi}_4 + \dot{\phi}_5 + \dot{\phi}_6 \tag{3.105}$$

Equations (3.94) through (3.99) can be put into the matrix form given by

$$\vec{V}_1 = J_1 \, \dot{\vec{\Phi}}_1 \tag{3.106}$$

where the vector $\vec{V}_1$ is the velocity of fingertip 1 in the contact 1 coordinate frame given by

$$\vec{V}_1 = \left\{ \begin{array}{cccccc} V_{1n} & V_{1t} & V_{1z} & \omega_{1n} & \omega_{1t} & \omega_{1z} \end{array} \right\}^T \tag{3.107}$$

the vector $\dot{\vec{\Phi}}_1$ is the vector of joint velocities of finger 1 given by

$$\dot{\vec{\Phi}}_1 = \left\{ \begin{array}{ccc} \dot{\phi}_1 & \dot{\phi}_2 & \dot{\phi}_3 \end{array} \right\}^T \tag{3.108}$$

and the matrix J_1 is the Jacobian matrix for finger 1 which relates the finger 1 joint velocities to the fingertip 1 velocity in the contact 1 coordinate frame. The matrix J_1 is given by

$$J_1 = \begin{bmatrix} j_{111} & j_{112} & j_{113} \\ j_{121} & j_{122} & j_{123} \\ 0 & 0 & 0 \\ 0 & 0 & 0 \\ 0 & 0 & 0 \\ 1 & 1 & 1 \end{bmatrix} \tag{3.109}$$

where

$$j_{111} = -\left(l_{11} \sin \phi_1 + l_{12} \sin \phi_{12} + l_{13} \sin \phi_{123} \right) \sin \left(\theta + \psi \right) -$$

$$(l_{11}\cos\phi_1 + l_{12}\cos\phi_{12} + l_{13}\cos\phi_{123})\cos(\theta + \psi) \tag{3.110}$$

$$j_{112} = -(l_{12}\sin\phi_{12} + l_{13}\sin\phi_{123})\sin(\theta + \psi) -$$

$$(l_{12}\cos\phi_{12} + l_{13}\cos\phi_{123})\cos(\theta + \psi) \tag{3.111}$$

$$j_{113} = -l_{13}\sin\phi_{123}\sin(\theta + \psi) - l_{13}\cos\phi_{123}\cos(\theta + \psi) \tag{3.112}$$

$$j_{121} = -(l_{11}\sin\phi_1 + l_{12}\sin\phi_{12} + l_{13}\sin\phi_{123})\cos(\theta + \psi) +$$

$$(l_{11}\cos\phi_1 + l_{12}\cos\phi_{12} + l_{13}\cos\phi_{123})\sin(\theta + \psi) \tag{3.113}$$

$$j_{122} = -(l_{12}\sin\phi_{12} + l_{13}\sin\phi_{123})\cos(\theta + \psi) +$$

$$(l_{12}\cos\phi_{12} + l_{13}\cos\phi_{123})\sin(\theta + \psi) \tag{3.114}$$

$$j_{123} = -l_{13}\sin\phi_{123}\cos(\theta + \psi) + l_{13}\cos\phi_{123}\sin(\theta + \psi) \tag{3.115}$$

Similarly, Eqs (3.100) through (3.105) can be put into the matrix form given by

$$\vec{V}_2 = J_2\,\dot{\vec{\Phi}}_2 \tag{3.116}$$

where the vector $\vec{V}_2$ is the velocity of fingertip 2 in the contact 2 coordinate frame given by

$$\vec{V}_2 = \left\{ \begin{array}{cccccc} V_{2n} & V_{2t} & V_{2z} & \omega_{2n} & \omega_{2t} & \omega_{2z} \end{array} \right\}^T \tag{3.117}$$

the vector $\dot{\vec{\Phi}}_2$ is the vector of joint velocities of finger 2 given by

$$\dot{\vec{\Phi}}_2 = \left\{ \begin{array}{ccc} \dot{\phi}_4 & \dot{\phi}_5 & \dot{\phi}_6 \end{array} \right\}^T \tag{3.118}$$

and the matrix J_2 is the Jacobian matrix for finger 2 which relates the finger 2 joint velocities to the fingertip 2 velocity in the contact 2 coordinate frame. The matrix J_2 is given by

$$J_2 = \begin{bmatrix} j_{211} & j_{212} & j_{213} \\ j_{221} & j_{222} & j_{223} \\ 0 & 0 & 0 \\ 0 & 0 & 0 \\ 0 & 0 & 0 \\ 1 & 1 & 1 \end{bmatrix} \tag{3.119}$$

3-28

where

$$j_{211} = (l_{21} \sin \phi_4 + l_{22} \sin \phi_{45} + l_{23} \sin \phi_{456}) \sin (\theta - \psi) -$$
$$(l_{21} \cos \phi_4 + l_{22} \cos \phi_{45} + l_{23} \cos \phi_{456}) \cos (\theta - \psi) \qquad (3.120)$$

$$j_{212} = (l_{22} \sin \phi_{45} + l_{23} \sin \phi_{456}) \sin (\theta - \psi) -$$
$$(l_{22} \cos \phi_{45} + l_{23} \cos \phi_{456}) \cos (\theta - \psi) \qquad (3.121)$$

$$j_{213} = l_{23} \sin \phi_{456} \sin (\theta - \psi) - l_{23} \cos \phi_{456} \cos (\theta - \psi) \qquad (3.122)$$

$$j_{221} = - (l_{21} \sin \phi_4 + l_{22} \sin \phi_{45} + l_{23} \sin \phi_{456}) \cos (\theta - \psi) -$$
$$(l_{21} \cos \phi_4 + l_{22} \cos \phi_{45} + l_{23} \cos \phi_{456}) \sin (\theta - \psi) \qquad (3.123)$$

$$j_{222} = - (l_{22} \sin \phi_{45} + l_{23} \sin \phi_{456}) \cos (\theta - \psi) -$$
$$(l_{22} \cos \phi_{45} + l_{23} \cos \phi_{456}) \sin (\theta - \psi) \qquad (3.124)$$

$$j_{223} = -l_{23} \sin \phi_{456} \cos (\theta - \psi) - l_{23} \cos \phi_{456} \sin (\theta - \psi) \qquad (3.125)$$

To get the Jacobian matrices in their final form, the contact constraint information must be incorporated. That is, information about which contact forces can be applied by the given type of finger contact. For instance, a *frictionless point contact cannot impart* any force on the object in the plane tangent to the object surface. Nor can it impart any moments about the point of contact. It is constrained to impart only a normal contact force component on the object because of the type of contact. An efficient method of incorporating this information is by defining a matrix, B_i, for each contact whose columns are the vectors in the wrench basis of the contact type [MS85: 21]. For the two point contacts with friction

$$B_1 = B_2 = \begin{bmatrix} 1 & 0 & 0 \\ 0 & 1 & 0 \\ 0 & 0 & 1 \\ 0 & 0 & 0 \\ 0 & 0 & 0 \\ 0 & 0 & 0 \end{bmatrix} \qquad (3.126)$$

The B_i matrices are then used in the relationship

$$\mathcal{J}_i = B_i^T J_i \qquad (3.127)$$

to select only the portions of the J_i which are supported by the contact type. Performing the operations in Eq (3.127) results in

$$\mathcal{J}_1 = \begin{bmatrix} j_{111} & j_{112} & j_{113} \\ j_{121} & j_{122} & j_{123} \\ 0 & 0 & 0 \end{bmatrix} \tag{3.128}$$

and

$$\mathcal{J}_2 = \begin{bmatrix} j_{211} & j_{212} & j_{213} \\ j_{221} & j_{222} & j_{223} \\ 0 & 0 & 0 \end{bmatrix} \tag{3.129}$$

where the definitions of the elements were given previously in Eqs (3.110) through (3.115) and Eqs (3.120) through (3.125).

The matrices in Eqs (3.128) and (3.129) can be used to calculate the vector of torques required to apply a given contact force vector on the object. The relationship to give such a solution is presented in the next section and requires the transposes of the J_i. Therefore, with forethought, the required transposes are found to be

$$\mathcal{J}_1^T = \begin{bmatrix} j_{111} & j_{121} & 0 \\ j_{112} & j_{122} & 0 \\ j_{113} & j_{123} & 0 \end{bmatrix} \qquad \mathcal{J}_2^T = \begin{bmatrix} j_{211} & j_{221} & 0 \\ j_{212} & j_{222} & 0 \\ j_{213} & j_{223} & 0 \end{bmatrix} \tag{3.130}$$

When the $\mathcal{J}_i^T$ are assembled into block diagonal form, the transpose of the global hand Jacobian matrix, $\mathcal{J}^T$ is formed. The resulting matrix is given by

$$\mathcal{J}^T = \begin{bmatrix} j_{111} & j_{121} & 0 & 0 & 0 & 0 \\ j_{112} & j_{122} & 0 & 0 & 0 & 0 \\ j_{113} & j_{123} & 0 & 0 & 0 & 0 \\ 0 & 0 & 0 & j_{211} & j_{221} & 0 \\ 0 & 0 & 0 & j_{212} & j_{222} & 0 \\ 0 & 0 & 0 & j_{213} & j_{223} & 0 \end{bmatrix} \tag{3.131}$$

3.6 COMPUTING TORQUES FROM CONTACT FORCES

The number of fingers in contact with the object, the number of links on each finger, and the dimensions of the hand influence the required vector of joint torques for a given

3-30

set of contact forces. Therefore, in order to determine the finger joint torques required to apply a given set of contact forces, one must first assume a hand structure. For this thesis a planar two-fingered hand with three links per finger as shown in Figure 3.7 is assumed. The lengths of the finger links will be carried through the analysis symbolically so as to maximize the generality of the results.

The relationship which relates the contact force vector, $\vec{C}$, to the vector of finger joint torques, $\vec{\tau}$, is given by Kerr [Ker84: 24] as

$$\vec{\tau} = \mathcal{J}^T \vec{C} \tag{3.132}$$

where $\mathcal{J}^T$ is the transpose of the global hand Jacobian matrix given by Eq (3.131) in Section 3.5 for the hand structure assumed above. For two point contacts with friction, the contact force vector is given by Eq (3.16) as

$$\vec{C} = \left\{ \begin{array}{cccccc} C_{1n} & C_{1t} & C_{1z} & C_{2n} & C_{2t} & C_{2z} \end{array} \right\}^T \tag{3.133}$$

For an overconstrained grasp, such as one having two point contacts with friction on an object constrained to planar motion, the contact force vector is not unique. It can be separated into two orthogonal components; one for the unique particular solution, $\vec{C}_p$, and one for the indeterminate homogeneous solution, $\vec{C}_h$. These two components are linearly related to $\vec{C}$ by Eq (3.19). The homogeneous solution component is termed the internal grasp force by Salisbury [Sal82: 41].

When Eq (3.19) is substituted into Eq (3.132), the following expression results:

$$\vec{\tau} = \mathcal{J}^T \vec{C}_p + \mathcal{J}^T \vec{C}_h \tag{3.134}$$

The linearity of Eq (3.134) allows the vector of joint torques, $\vec{\tau}$, to be separated into two orthogonal components, $\vec{\tau}_p$ and $\vec{\tau}_h$, in the same way that $\vec{C}$ was separated into $\vec{C}_p$ and $\vec{C}_h$. Therefore,

$$\vec{\tau} = \vec{\tau}_p + \vec{\tau}_h \tag{3.135}$$

where

$$\vec{\tau}_p \equiv \mathcal{J}^T \vec{C}_p \tag{3.136}$$

and

$$\vec{\tau}_h \equiv \mathcal{J}^T \vec{C}_h \tag{3.137}$$

The torque vector in Eq (3.136) is called the *particular solution torque vector* because it generates the particular contact force components. Similarly, the torque vector in Eq (3.137) is called the *internal grasp torque vector* because it is the set of finger joint torques which generate the internal grasp forces.

3.6.1 DETERMINING THE PARTICULAR SOLUTION TORQUE VECTOR. The

vector $\vec{\tau}_p$ is unique for a grasp configuration and externally applied load, $\vec{F}_{ext}$. The grasp configuration information is contained in the global hand Jacobian matrix, $\mathcal{J}$. In general, the externally applied load may be either symmetric or asymmetric depending on the value of α. The symmetry or asymmetry of the load affects the particular solution torque vector via the particular solution contact force vector, $\vec{C}_p$. Section 3.4.2 derives $\vec{C}_p$ for the cases of nominal, asymmetric with no external moment, and asymmetric with an external moment. For a nominal load the vector given in Eq (3.31) is used in Eq (3.136) while for an asymmetric load with no external moment, the vector in Eq (3.33) is used in Eq (3.136). Finally, if the load is asymmetric and has a nonzero external moment, then the vector in Eq (3.39) is substituted into Eq (3.136). As an example, the case of a nominal load will be analyzed here to illustrate the method which can also be applied to the asymmetric cases.

When Eq (3.31) is substituted into Eq (3.136), the result is

$$\vec{\tau}_p = \mathcal{J}^T \left\{ \begin{array}{c} -\cos\theta \\ \sin\theta \\ 0 \\ -\cos\theta \\ -\sin\theta \\ 0 \end{array} \right\} \frac{F_{ext}}{2} \tag{3.138}$$

where $\mathcal{J}^T$ is given in Eq (3.131).

When the operations in Eq (3.138) are carried out, it yields

$$\vec{\tau}_p = \frac{F_{ext}}{2} \left\{ \begin{array}{c} l_{11}\cos(\phi_1 - \psi) + l_{12}\cos(\phi_{12} - \psi) + l_{13}\cos(\phi_{123} - \psi) \\ l_{12}\cos(\phi_{12} - \psi) + l_{13}\cos(\phi_{123} - \psi) \\ l_{13}\cos(\phi_{123} - \psi) \\ l_{21}\cos(\phi_4 - \psi) + l_{22}\cos(\phi_{45} - \psi) + l_{23}\cos(\phi_{456} - \psi) \\ l_{22}\cos(\phi_{45} - \psi) + l_{23}\cos(\phi_{456} - \psi) \\ l_{23}\cos(\phi_{456} - \psi) \end{array} \right\} \tag{3.139}$$

The torques given in Eq (3.139) are the joint torques required to maintain equilibrium of the object with no internal grasp force present. Recall, however, that the contact forces represented by the particular solution torque vectors may not provide positive normal forces which are required to activate frictional forces. Therefore, $\vec{\tau}_p$ may not in reality be able to equilibrate the externally applied force because of the unisense constraint on the normal contact forces.

3.6.2 DETERMINING THE HOMOGENEOUS TORQUE VECTOR.

The vector $\vec{\tau}_h$ is indeterminate and depends on the arbitrary internal grasping force magnitude, λ, as well as the configuration of the hand and the object. When Eq (3.24) is substituted into Eq (3.137) the following relationship results:

$$\vec{\tau}_h = \mathcal{J}^T \left\{ \begin{array}{c} \sin\theta \\ \cos\theta \\ 0 \\ \sin\theta \\ -\cos\theta \\ 0 \end{array} \right\} \lambda \tag{3.140}$$

Now if Eq (3.131) is substituted into Eq (3.140) the result is

$$
\vec{\tau}_h = \lambda
\left\{
\begin{array}{c}
-l_{11}\sin(\phi_1 - \psi) - l_{12}\sin(\phi_{12} - \psi) - l_{13}\sin(\phi_{123} - \psi) \\[6pt]
-l_{12}\sin(\phi_{12} - \psi) - l_{13}\sin(\phi_{123} - \psi) \\[6pt]
-l_{13}\sin(\phi_{123} - \psi) \\[6pt]
l_{21}\sin(\phi_4 - \psi) + l_{22}\sin(\phi_{45} - \psi) + l_{23}\sin(\phi_{456} - \psi) \\[6pt]
l_{22}\sin(\phi_{45} - \psi) + l_{23}\sin(\phi_{456} - \psi) \\[6pt]
l_{23}\sin(\phi_{456} - \psi)
\end{array}
\right\}
\qquad (3.141)
$$

Equation (3.141) is the portion of the torque vector which creates an internal grasp force when the external load on the object is characterized as a nominal or symmetric load.

The total joint torque vector is assembled by substituting Eqs (3.139) and (3.141) into Eq (3.135). Examining Eqs (3.139) and (3.141), reveals that the torque vector is not an explicit function of the object geometry parameters (r, θ, h) but instead is a function of the hand geometry parameters $(\phi_{ij}, \psi, l_{ij}, a)$. However, through the use of inverse kinematics, the solution can be conditioned to make the torque vector a function of the object geometry parameters.

3.7 INVERSE KINEMATIC SOLUTION

In general, there are an infinite number of hand structures and finger positions which can correspond to the grasp of an object in a particular geometry. Therefore, several parameters must be specified to reduce the complexity of the problem so a unique solution will result.

For planar motion and three links per finger, the inverse kinematic solution of the fingers will be indeterminate. For simplicity the number of degrees of freedom per finger will be reduced from three to two for the remainder of this analysis. The expressions for the torque vectors in Eqs (3.139) and (3.141) can be adapted to two-link fingers by requiring that $l_{13} = l_{23} = 0$ and eliminating the third and sixth row elements. The resulting torque

expressions are

$$\vec{\mathcal{T}}_p = \frac{F_{ext}}{2} \left\{ \begin{array}{c} l_{11} \cos \zeta_1 + l_{12} \cos \zeta_{12} \\ l_{12} \cos \zeta_{12} \\ l_{21} \cos \zeta_4 + l_{22} \cos \zeta_{45} \\ l_{22} \cos \zeta_{45} \end{array} \right\} \tag{3.142}$$

and

$$\vec{\mathcal{T}}_h = \lambda \left\{ \begin{array}{c} -l_{11} \sin \zeta_1 - l_{12} \sin \zeta_{12} \\ -l_{12} \sin \zeta_{12} \\ l_{21} \sin \zeta_4 + l_{22} \sin \zeta_{45} \\ l_{22} \sin \zeta_{45} \end{array} \right\} \tag{3.143}$$

where

$$\zeta_1 = (\phi_1 - \psi) \tag{3.144}$$

$$\zeta_{12} = (\phi_{12} - \psi) \tag{3.145}$$

$$\zeta_4 = (\phi_4 - \psi) \tag{3.146}$$

$$\zeta_{45} = (\phi_{45} - \psi) \tag{3.147}$$

With the problem simplified to enable a unique inverse kinematic solution, appropriate parameters must be selected as fixed values for the object and hand geometries. Since the previous analysis was conducted using the grasp angle, θ, as a variable, it will remain as a variable for this analysis. The fixed values will then be r, h, a, l_{ij}, and ψ. The task then is to determine the inverse kinematic solutions for the finger joint angles as a function of θ when given r, h, a, l_{ij}, and ψ.

Figure 3.10 depicts the geometry and nomenclature for the planar grasp of a cylindrical object with two fingers having two-links per finger. From Figure 3.10 the positions of the contact points between the fingertips and the object can be written in the palm frame using the finger parameters:

$$P_{1x_p} = l_{11} \cos \phi_1 + l_{12} \cos \phi_{12} - \frac{a}{2} \tag{3.148}$$

$$P_{1y_p} = l_{11} \sin \phi_1 + l_{12} \sin \phi_{12} \tag{3.149}$$

$$P_{2x_p} = l_{21} \cos \phi_4 + l_{22} \cos \phi_{45} + \frac{a}{2} \tag{3.150}$$

$$P_{2y_p} = l_{21} \sin \phi_4 + l_{22} \sin \phi_{45} \tag{3.151}$$
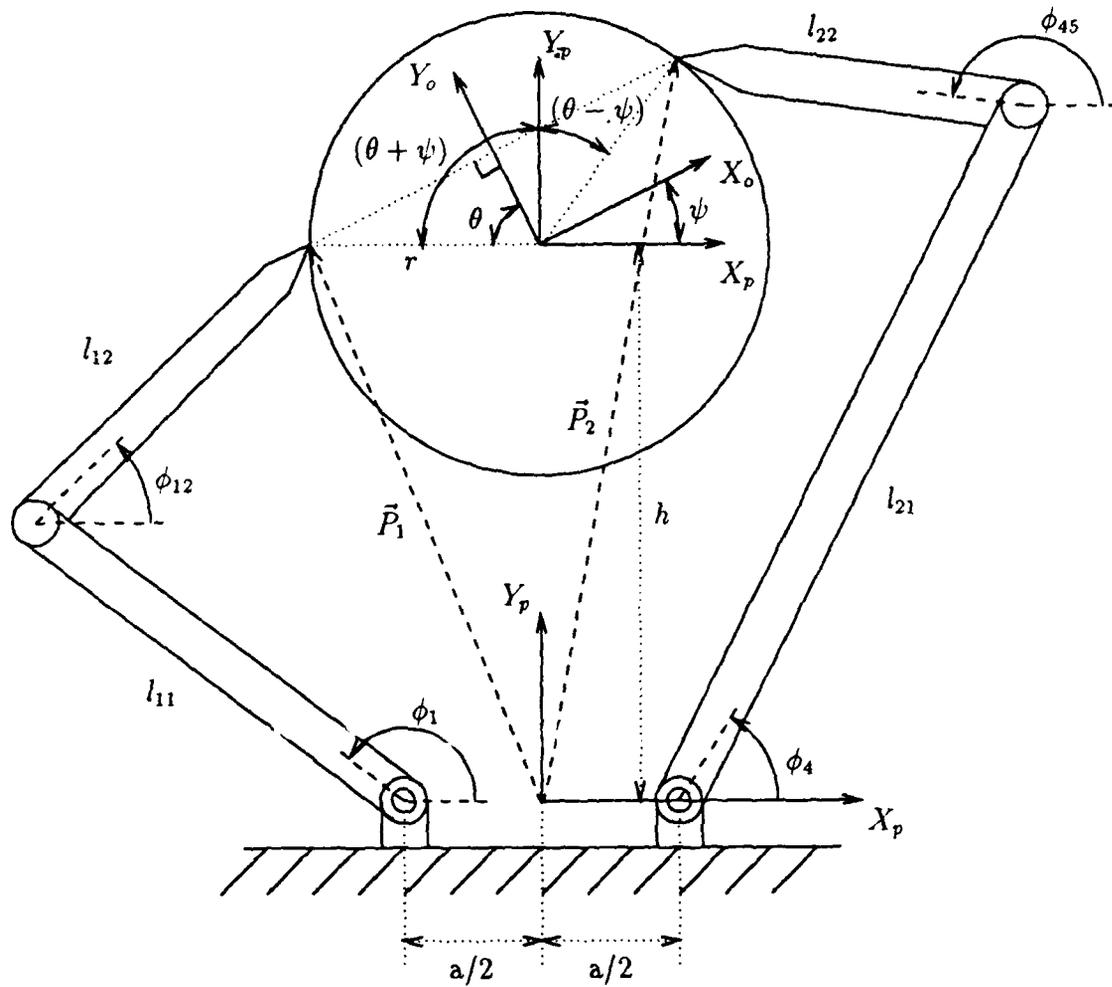
Figure 3.10. Geometry and Nomenclature for Inverse Kinematic Solution of Two Fingers with Two-Links Per Finger Grasping a Cylindrical Object

The fingertip positions can also be written is the palm frame using the object parameters:

$$P_{1x_p} \;=\; -r \sin(\theta + \psi) \tag{3.152}$$

$$P_{1y_p} \;=\; h + r \cos(\theta + \psi) \tag{3.153}$$

$$P_{2x_p} \;=\; r \sin(\theta - \psi) \tag{3.154}$$

$$P_{2y_p} \;=\; h + r \cos(\theta - \psi) \tag{3.155}$$

Equating the expressions in Eqs (3.148) through (3.151) with the corresponding expressions in Eqs (3.152) through (3.155) yields the following expressions:

$$l_{11}\cos\phi_1 + l_{12}\cos\phi_{12} - \frac{a}{2} \;=\; -r \sin(\theta + \psi) \tag{3.156}$$

$$l_{11}\sin\phi_1 + l_{12}\sin\phi_{12} \;=\; h + r \cos(\theta + \psi) \tag{3.157}$$

$$l_{21}\cos\phi_4 + l_{22}\cos\phi_{45} + \frac{a}{2} \;=\; r \sin(\theta - \psi) \tag{3.158}$$

$$l_{21}\sin\phi_4 + l_{22}\sin\phi_{45} \;=\; h + r \cos(\theta - \psi) \tag{3.159}$$

To solve these equations, begin by rearranging them so that all of the hand geometry parameters are on one side of the equality and the object geometry parameters are on the other:

$$l_{11}\cos\phi_1 + l_{12}\cos\phi_{12} \;=\; \frac{a}{2} - r \sin(\theta + \psi) \tag{3.160}$$

$$l_{11}\sin\phi_1 + l_{12}\sin\phi_{12} \;=\; h + r \cos(\theta + \psi) \tag{3.161}$$

$$l_{21}\cos\phi_4 + l_{22}\cos\phi_{45} \;=\; -\frac{a}{2} + r \sin(\theta - \psi) \tag{3.162}$$

$$l_{21}\sin\phi_4 + l_{22}\sin\phi_{45} \;=\; h + r \cos(\theta - \psi) \tag{3.163}$$

Squaring both sides of Eqs (3.160) and (3.161) and adding them together results in

$$l_{11}^2 + l_{12}^2 + 2l_{11}l_{12}\left(\cos\phi_1 \cos\phi_{12} + \sin\phi_1 \sin\phi_{12}\right)$$
$$= \left[\frac{a}{2} - r\sin(\theta + \psi)\right]^2 + [h + r\cos(\theta + \psi)]^2 \tag{3.164}$$

while squaring both sides of Eqs (3.162) and (3.163) and adding them together results in

$$l_{21}^2 + l_{22}^2 + 2l_{21}l_{22}\left(\cos\phi_4 \cos\phi_{45} + \sin\phi_4 \sin\phi_{45}\right)$$
$$= \left[\frac{-a}{2} + r\sin(\theta - \psi)\right]^2 + [h + r\cos(\theta - \psi)]^2 \tag{3.165}$$

Applying several trigonometric identities to the parenthetical expression on the left hand side of Eq (3.164) reveals that it is equal to simply $\cos\phi_2$ while that of Eq (3.165) is equal to $\cos\phi_5$. Making these substitutions into Eqs (3.164) and (3.165) yields

$$l_{11}^2 + l_{12}^2 + 2l_{11}l_{12}\cos\phi_2 \;=\; \left[\frac{a}{2} - r\sin(\theta+\psi)\right]^2 + [h + r\cos(\theta+\psi)]^2 \quad (3.166)$$

$$l_{21}^2 + l_{22}^2 + 2l_{21}l_{22}\cos\phi_5 \;=\; \left[\frac{-a}{2} + r\sin(\theta-\psi)\right]^2 + [h + r\cos(\theta-\psi)]^2 \quad (3.167)$$

Solving Eq (3.166) for ϕ_2 yields

$$\phi_2 = S\ \arccos\left\{\frac{\left[\frac{a}{2} - r\sin(\theta+\psi)\right]^2 + [h + r\cos(\theta+\psi)]^2 - l_{11}^2 - l_{12}^2}{2l_{11}l_{12}}\right\} \quad (3.168)$$

while solving Eq (3.167) for ϕ_5 yields

$$\phi_5 = -S\ \arccos\left\{\frac{\left[\frac{-a}{2} + r\sin(\theta-\psi)\right]^2 + [h + r\cos(\theta-\psi)]^2 - l_{21}^2 - l_{22}^2}{2l_{21}l_{22}}\right\} \quad (3.169)$$

where S is $+1$ for knuckle-in configuration and -1 for knuckle-out configuration.

To solve for ϕ_1 and ϕ_4 begin by using the following trigonometric identities:

$$\cos(\alpha+\beta) \;=\; \cos\alpha\cos\beta - \sin\alpha\sin\beta \quad (3.170)$$

$$\sin(\alpha+\beta) \;=\; \sin\alpha\cos\beta + \cos\alpha\sin\beta \quad (3.171)$$

When these identities are substituted into Eqs (3.160) and (3.161) and rearranged slightly, the result is

$$-l_{12}\sin\phi_2\sin\phi_1 + (l_{11} + l_{12}\cos\phi_2)\cos\phi_1 \;=\; \frac{a}{2} - r\ \sin(\theta+\psi) \quad (3.172)$$

$$(l_{11} + l_{12}\cos\phi_2)\sin\phi_1 + l_{12}\sin\phi_2\cos\phi_1 \;=\; h + r\ \cos(\theta+\psi) \quad (3.173)$$

while substituting them into Eqs (3.162) and (3.163) yields

$$-l_{22}\sin\phi_5\sin\phi_4 + (l_{21} + l_{22}\cos\phi_5)\cos\phi_4 \;=\; \frac{-a}{2} + r\ \sin(\theta-\psi) \quad (3.174)$$

$$(l_{21} + l_{22}\cos\phi_5)\sin\phi_4 + l_{22}\sin\phi_5\cos\phi_4 \;=\; h + r\ \cos(\theta-\psi) \quad (3.175)$$

To solve Eqs (3.172) and (3.173) simultaneously for $\sin\phi_1$ and $\cos\phi_1$ they can be put in the matrix form of $\mathbf{Ax} = \mathbf{b}$ and Cramer's method [Kre83: 319] can be used. The matrix form of Eqs (3.172) and (3.173) is

$$\begin{bmatrix} -l_{12}\sin\phi_2 & (l_{11} + l_{12}\cos\phi_2) \\ (l_{11} + l_{12}\cos\phi_2) & l_{12}\sin\phi_2 \end{bmatrix} \left\{\begin{array}{c} \sin\phi_1 \\ \cos\phi_1 \end{array}\right\} = \left\{\begin{array}{c} \frac{a}{2} - r\ \sin(\theta+\psi) \\ h + r\ \cos(\theta+\psi) \end{array}\right\} \quad (3.176)$$

The determinant of the coefficient matrix in Eq (3.176) is

$$\det \mathbf{A} = - \left(l_{11}^2 + l_{12}^2 + 2l_{11}l_{12}\cos\phi_2 \right) \tag{3.177}$$

To solve for $\sin\phi_1$ requires the determinant of the coefficient matrix with its first column replaced by the vector $\mathbf{b}$. That determinant is found to be

$$- \left\{ l_{11}\left[h + r\cos(\theta + \psi)\right] + l_{12}\left[h\cos\phi_2 - \frac{a}{2}\sin\phi_2 + r\cos(\theta + \psi - \phi_2)\right] \right\} \tag{3.178}$$

Dividing Eq (3.178) by Eq (3.177) gives the solution for $\sin\phi_1$ as

$$\sin\phi_1 = \frac{\left\{ l_{11}\left[h + r\cos(\theta + \psi)\right] + l_{12}\left[h\cos\phi_2 - \frac{a}{2}\sin\phi_2 + r\cos(\theta + \psi - \phi_2)\right] \right\}}{\left(l_{11}^2 + l_{12}^2 + 2l_{11}l_{12}\cos\phi_2 \right)} \tag{3.179}$$

Similarly, the solution for $\cos\phi_1$ requires the determinant of the coefficient matrix with its second column replaced by the vector $\mathbf{b}$. This determinant is found to be

$$- \left\{ l_{11}\left[\frac{a}{2} - r\sin(\theta + \psi)\right] + l_{12}\left[h\sin\phi_2 + \frac{a}{2}\cos\phi_2 - r\sin(\theta + \psi - \phi_2)\right] \right\} \tag{3.180}$$

The solution for $\cos\phi_1$ then yields

$$\cos\phi_1 = \frac{\left\{ l_{11}\left[\frac{a}{2} - r\sin(\theta + \psi)\right] + l_{12}\left[h\sin\phi_2 + \frac{a}{2}\cos\phi_2 - r\sin(\theta + \psi - \phi_2)\right] \right\}}{\left(l_{11}^2 + l_{12}^2 + 2l_{11}l_{12}\cos\phi_2 \right)} \tag{3.181}$$

To find ϕ_1 divide Eq (3.179) by Eq (3.181) to form $\tan\phi_1$ and then use the ATAN2 function which is an inverse tangent function that places ϕ_1 in the proper quadrant depending on the signs of the numerator and denominator. Although the denominators of Eqs (3.179) and (3.181) are common, it is important that they are not canceled when forming $\tan\phi_1$ because they may affect the signs of Eqs (3.179) and (3.181) and thereby affect the resulting quadrant of the solution.

Using the same solution method for determining ϕ_4 yields

$$\sin\phi_4 = \frac{\left\{ l_{21}\left[h + r\cos(\theta - \psi)\right] + l_{22}\left[h\cos\phi_5 + \frac{a}{2}\sin\phi_5 + r\cos(\theta - \psi + \phi_5)\right] \right\}}{\left(l_{21}^2 + l_{22}^2 + 2l_{21}l_{22}\cos\phi_5 \right)} \tag{3.182}$$

and

$$\cos\phi_4 = \frac{\left\{ l_{21}\left[-\frac{a}{2} + r\sin(\theta - \psi)\right] + l_{22}\left[h\sin\phi_5 - \frac{a}{2}\cos\phi_5 + r\sin(\theta - \psi + \phi_5)\right] \right\}}{\left(l_{21}^2 + l_{22}^2 + 2l_{21}l_{22}\cos\phi_5 \right)} \tag{3.183}$$

To find ϕ_4 Eq (3.182) is divided by Eq (3.183) to form $\tan\phi_4$ which is then solved for ϕ_4 using the ATAN2 function.

3.8 SUMMARY

In this chapter the underlying theory for further derivations has been presented. The basics of screw theory has been explained and used to solve for the contact forces required to equilibrate an external force system on the grasped object. The configuration of the external force system has been categorized as either symmetric or asymmetric, and a discussion of force closure and form closure was presented. In order to compute the finger joint torques of the gripper, the global hand Jacobian matrix was derived for a gripper structure consisting of two, three-link fingers having serially-actuated, revolute joints. Since the global hand Jacobian matrix is a function of the gripper configuration, the inverse kinematic solution is required. The gripper structure was redefined as having two, two-link fingers to reduce the complexity of the inverse kinematics so that a unique 'knuckle-out' configuration resulted.

The derivations of this chapter serve as the starting point for the developments un-dertaken in the following chapter.

IV. EQUILIBRIUM ANALYSIS OF
NOMINALLY-LOADED OBJECTS

The magnitude and orientation of the external load vector has a direct influence on the grasp angle, θ, and the internal grasp force, λ', required for an equilibrium grasp. The magnitude of the external load is characterized by F_{ext} while its orientation is characterized by the load angle, α. In most cases the grasp angle is not unique and may be selected from a range of allowable values. Often the range of allowable values for θ is limited by the value of λ' chosen and one or more constraints which must be simultaneously satisfied. In general, there are three types of constraints which must be considered when configuring a grasp. They are:

- Frictional force magnitude is constrained by a Coulomb friction model.

- For contacts characterized by point contacts with friction, normal contact forces cannot 'pull' on the object surface. Nor should they crush the object being grasped.

- The contact forces that can be applied by the gripper fingers are limited in magnitude by the capabilities of the actuators.

The first constraint requires that the tangential contact force magnitude be less than or equal to the product of the normal contact force and some coefficient of static friction, μ_s. Any grasp requiring a tangential force larger than this product will slip. In order to have active friction the normal contact force must be directed inward towards the object center.

This leads to the second constraint which is termed the crush limit constraint. This constraint limits the range of magnitudes of the normal components of the contact forces. Because one cannot 'pull' on a surface without the aide of some adhesive, only a positive sense normal is considered feasible. In addition, there are practical limits on the allowable magnitudes of the normal forces if one is concerned about crushing the object. This effectively limits the magnitudes to a range from zero to a maximum value which is determined by the object structure.

4-1

The final constraint concerns the physical limitations of the finger actuators. Since the hand configuration under analysis is limited to revolute joints, the actuator limits can be characterized in terms of joint motor torque limits. In general a joint motor will have a maximum torque rating, τ_{max}, which is considered here to be a symmetric rating with respect to the direction of shaft rotation.

The goal of this chapter is to present a graphical method for selecting the grasp angle and the internal force level for two-fingered grasps of cylindrical objects under a *nominal load*. A nominal load is considered to be one with the load orientation angle, α, equal to 180 degrees and the external moment on the object, M_{ext}, equal to zero. The method is based on the static equilibrium analysis of the grasping forces presented in Chapter III and will include consideration of the three types of constraints mentioned above.

In order to illustrate how the derived analytic expressions might be used to select grasp parameters, an example grasp analysis will be presented. In the process of this example, it will be necessary at times to specify limiting values for several of the contraining variables or to specify the dimensions of the gripper and its relationship to the object. Each of the constraints will require a different number of variables to be specified. The example values for the required specified variables are presented as needed in the discussion and summarized in Table 4.1 at the end of this chapter.

4.1 COULOMB FRICTION LIMIT CONSTRAINT

For a point contact with friction the Coulomb friction model relating the normal contact force component magnitude, C_n, to the tangential contact force component magnitude, C_t, is given by

$$C_t \leq \mu_s C_n \qquad (4.1)$$

where μ_s is the static friction coefficient. Equation (4.1) defines a Coulomb friction limit constraint for the allowable magnitudes of the normal and tangential contact force components. The *friction angle* of a contact, β, is defined as

$$\beta \equiv \arctan\left(\frac{C_t}{C_n}\right) \qquad (4.2)$$

It is easily shown that $\mu_s = \tan\beta$. The static friction coefficient can be used to define maximum and minimum limits on the allowable friction angle. Doing so yields

$$-\arctan\mu_s \leq \beta \leq \arctan\mu_s \tag{4.3}$$

In order to keep from slipping, the friction angle must remain within the allowable limits defined by Eq (4.3). If only positive values of μ_s are physically possible, then even for the generous case where $\mu_s = \infty$, the range of allowable β would only be from $-90°$ to $+90°$. This point will be further examined shortly.

Expressions for β as functions of the known grasp configuration variables will enable an investigate of the regions of feasibility based on the friction limit constraint. It is clear from Eq (4.2) that the friction angle may, in general, be different for each of the two fingertip contacts under consideration. Therefore, the friction angles at the contacts are individually defined as

$$\beta_1 = \arctan\left(\frac{C_{1t}}{C_{1n}}\right) \tag{4.4}$$

$$\beta_2 = \arctan\left(\frac{C_{2t}}{C_{2n}}\right) \tag{4.5}$$

Recalling the components C_{1n} and C_{1t} from the total contact force vector given in Eq (3.39), one can express the friction angle for the contact between fingertip one and the object as

$$\beta_1 = \arctan\left(\frac{2r\lambda'\sin\theta\cos\theta - r\cos\alpha\sin^2\theta + M'\sin\theta}{2r\lambda'\sin^2\theta + r\cos\alpha\sin\theta\cos\theta + r\sin\alpha - M'\cos\theta}\right) \tag{4.6}$$

Similarly, the friction angle for the contact between fingertip two and the object is

$$\beta_2 = \arctan\left(\frac{-2r\lambda'\sin\theta\cos\theta + r\cos\alpha\sin^2\theta + M'\sin\theta}{2r\lambda'\sin^2\theta + r\cos\alpha\sin\theta\cos\theta - r\sin\alpha + M'\cos\theta}\right) \tag{4.7}$$

Since the quantity $F_{eet}/(2r\sin\theta)$ is always positive, one need not be concerned about changing the quadrant of β_1 or β_2 by canceling this common factor when the ratio in Eqs (4.4) and (4.5) are formed from the components given in Eq (3.39).

Equations (4.6) and (4.7) are the most general expressions for the friction angles. Under the nominal load conditions mentioned above, Eq (4.6) reduces to

$$\beta_1 = \arctan\left(\frac{2\lambda'\cos\theta + \sin\theta}{2\lambda'\sin\theta - \cos\theta}\right) \tag{4.8}$$

4-3
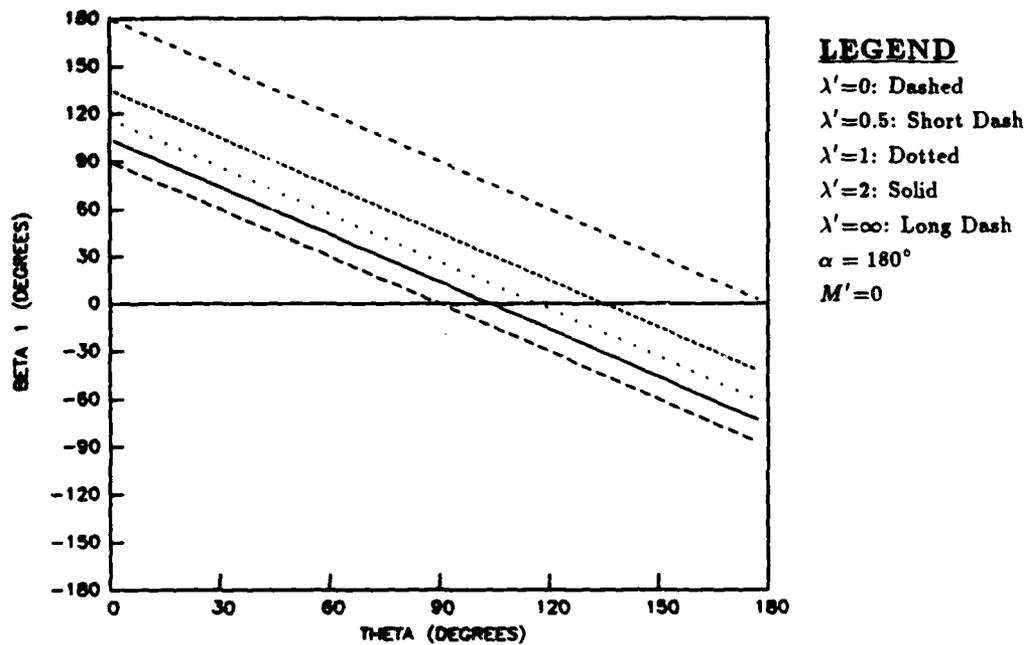
Figure 4.1. Friction angle at fingertip 1 versus grasp angle for a nominal external load on the object

while Eq (4.7) reduces to

$$\beta_2 = \arctan\left(\frac{-2\lambda'\cos\theta - \sin\theta}{2\lambda'\sin\theta - \cos\theta}\right) \tag{4.9}$$

Examining Eqs (4.8) and (4.9) reveals that, for a nominal load, $\beta_1 = -\beta_2$. As will be shown in Section 4.2 the sign difference between β_1 and β_2 is due to a difference in the signs of the tangential contact force components rather than the normal force components. If β_1 and β_2 are plotted versus the grasp angle, θ, and let the normalized magnitude of the internal grasp force, λ', remain as a parameter, one can explore the friction requirements for grasping the object at different symmetric fingertip positions and internal grasp force levels.

Figure 4.1 depicts such a plot for the contact of fingertip 1 with the object using several different values of λ' while Figure 4.2 depicts such a plot for fingertip 2. One immediately notes that there appears to be a linear relationship between β and θ for constant λ'. Examining and manipulating the expressions in Eqs (4.8) and (4.9), however, revealed no obvious linearity to the author.

4-4
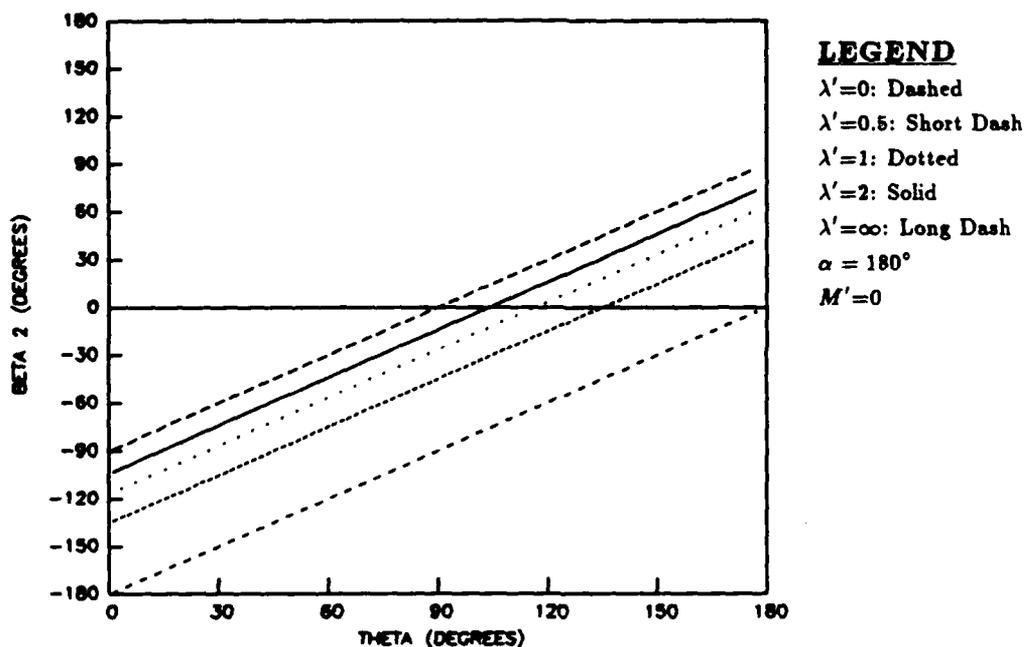
Figure 4.2. Friction angle at fingertip 2 versus grasp angle for a nominal external load on the object

If one maintains that the friction angle is measured from the positive normal unit vector, then the friction angle for a contact force vector having a negative normal component will be greater than $+90°$ or less than $-90°$, depending on the direction of the tangential component. For positive coefficients of friction, however, a negative normal contact force component is not allowable. Because only a positive-sense normal force is allowed, this constraint is called a *unisense normal force constraint*. The unisense normal force constraint represents an upper bound on β corresponding to $\mu_s = \infty$. In general, $\mu_s << \infty$ and the grasp slips due to violation of the friction limit constraint long before the unisense normal force constraint becomes a factor. The unisense normal force constraint does, however, quickly identify regions where no grasp is possible unless an adhesive is used to interface between the object and the fingertips.

Based on the unisense normal force constraint, the regions in Figures 4.1 and 4.2 which require $\beta \geq +90°$ or $\beta \leq -90°$ are excluded from consideration as feasible grasp regions. In Figure 4.1 this means that it is not feasible to grasp the object at $\theta < 90°$ if one wanted to maintain $\lambda' = 0$. Similarly, Figure 4.2 indicates that one cannot grasp the object

4-5

at $\theta < 90°$ for $\lambda' = 0$. Therefore, by simultaneously considering β_1 and β_2 it is concluded that one cannot obtain an equilibrium grasp of the object with $\theta < 90°$ if $\lambda' = 0$. However, if λ' is increased to 1 then the unisense normal force constraint relaxes somewhat to allow grasps at $\theta \in (27° \leq \theta \leq 180°)$.

Using Eq (4.3) as criteria for defining a range of allowable friction angles reveals that the regions of feasible grasps in Figures 4.1 and 4.2 are bounded above and below by straight lines at $\beta_i = \pm \arctan \mu_s$. As an example, assume $\mu_s = 1$ for the contact of the object with the material used for the finger pads. Equation (4.3) gives the corresponding limits on β as ± 45 degrees. So from Figure 4.1, if $\lambda' = 0$ one cannot achieve an equilibrium grasp for θ less than 135 degrees if $\mu_s = 1$. The same condition holds true for fingertip 2 as shown in Figure 4.2. However, if $\lambda' = 1$ and both β_1 and β_2 are considered, the range of allowable θ includes all angles given by

$$\theta \in (72° \leq \theta \leq 162°)$$

It is interesting to note in Figure 4.1 that as λ' increases, the lines of constant internal grasp force quickly approach the line running from $(\theta, \beta_1) = (0°, 90°)$ to $(\theta, \beta_1) = (180°, -90°)$ which represents $\lambda' = \infty$. Figure 4.2 shows an identical trend as one would expect since $\beta_2 = -\beta_1$.

Examining the effect on the friction angle of changing λ' for a constant θ, can yield several physical insights about the grasp. For $\mu_s = 1$ and θ in the neighborhood of 180°, as λ' increases from 0 towards ∞ the grasp is driven unstable. The object is essentially ejected from the grasp in a fashion similar to pinching a watermelon seed until it 'shoots' from one's grasp. Therefore, in this region one would want to hold the object gently so as not to lose stability.

By contrast, for $\mu_s = 1$ and θ in the neighborhood of 90°, as λ' increases the grasp goes from unstable to stable. In this region one would want to hold the object as firmly as the other constraints would allow.

Kumar and Waldron [KW87: 253] proposed a two-step suboptimal grasping strategy for a two-fingered grasp of a circular cylinder with $\theta = 90°$. Step A of the strategy corresponds to beginning the grasp at $\lambda' = 0$. Step B proposes to increase λ' until the

friction limit constraint is just met and stop. Although this might conserve actuator energy, it leaves the grasp very near the boundary of failure due to slip. Also, based on the observations mentioned just above, this strategy will only work in the immediate neighborhood of $\theta = 90°$.

4.2 CRUSH LIMIT CONSTRAINT

In order for frictional forces to be active, the normal contact forces must be directed inward towards the object center. This corresponds to positive normal forces in the coordinate system defined by Figure 3.6. Since only one sense (positive sense) of the normal force is allowable, this is termed the unisense normal force constraint. In addition, there may be a limit on the magnitude of the normal force which can be tolerated by the structure of the object. If such a limit exists it is termed the *crush limit* of the object. This section presents a simple graphical way of selecting the grasp angle and internal grasp force level based on the unisense normal and crush limit constraints.

The total contact force vector in Eq (3.39) includes generalized expressions for the normal contact force components at fingertips 1 and 2. For convenience they are repeated here:

$$C_{1n} = F_{ext} \left\{ \frac{2r\lambda' \sin^2 \theta + r \cos \alpha \sin \theta \cos \theta + r \sin \alpha - M' \cos \theta}{2r \sin \theta} \right\} \quad (4.10)$$

$$C_{2n} = F_{ext} \left\{ \frac{2r\lambda' \sin^2 \theta + r \cos \alpha \sin \theta \cos \theta - r \sin \alpha + M' \cos \theta}{2r \sin \theta} \right\} \quad (4.11)$$

It may be beneficial to define normalized normal forces as the normal force magnitudes divided by the magnitude of the external force, F_{ext}. Doing so, yields

$$C'_{1n} \equiv \frac{C_{1n}}{F_{ext}} = \left\{ \frac{2r\lambda' \sin^2 \theta + r \cos \alpha \sin \theta \cos \theta + r \sin \alpha - M' \cos \theta}{2r \sin \theta} \right\} \quad (4.12)$$

$$C'_{2n} \equiv \frac{C_{2n}}{F_{ext}} = \left\{ \frac{2r\lambda' \sin^2 \theta + r \cos \alpha \sin \theta \cos \theta - r \sin \alpha + M' \cos \theta}{2r \sin \theta} \right\} \quad (4.13)$$

The expressions in Eqs (4.12) and (4.13) are for any general external wrench on the object. If the conditions which constitute a nominal external load as defined in Section IV are substituted into Eqs (4.12) and (4.13), they reduce to

$$C'_{1n} = C'_{2n} = \frac{2\lambda' \sin \theta - \cos \theta}{2} \quad (4.14)$$

LEGEND
$\lambda'=0$: Dashed
$\lambda'=1$: Dotted
$\lambda'=2$: Solid
$\alpha = 180°$
$M'=0$
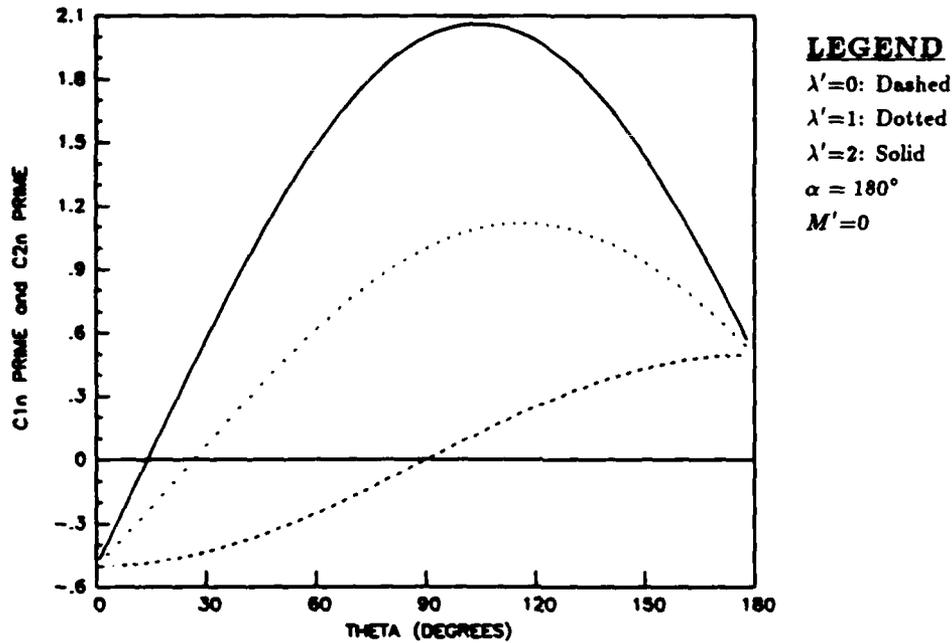
Figure 4.3. Normalized contact normal forces 1 and 2 versus grasp angle for a nominal external load on the object

The magnitudes of the normal forces at the two contacts are equal in sign and magnitude for a nominal load as one would expect from the symmetry of the grasp.

Plotting Eq (4.14) as a function of θ and parameterized by λ' will give insight into the range of θ for feasible grasps based on the crush limit constraint. Figure 4.3 depicts such a plot for three different values of λ'. For a uniform object structure, a crush limit would be characterized by a straight horizontal line on the plot in Figure 4.3 at the magnitude given by

$$C'_{n_{max}} = \frac{C_{n_{max}}}{F_{ext}} \qquad (4.15)$$

where $C_{n_{max}}$ is the maximum allowable normal force which can be tolerated by the structure of the object. In general, however, the crush limit may be a function of the angle θ. In such a case, that function would have to be evaluated over the range of θ from 0 to 180 degrees.

For a given λ', then, all values of θ corresponding to C'_n between zero and $C'_{n_{max}}$, are feasible values for the grasp angle. For example, assume that $C'_{n_{max}}$, is found to be 1.5

4-8

from a knowledge of the object structure and a measurement of F_{ext} and it is desired to grasp the object with $\lambda'=1$. Based on the crush limit constraint, the feasible grasp region in Figure 4.3 would be defined by

$$\theta \in (0^\circ \leq \theta \leq 180^\circ)$$

If $C'_{n_{max}}$ had been found to be 1, then the feasible grasp regions in Figure 4.3 would have been defined by

$$\theta \in (0^\circ \leq \theta \leq 80^\circ \ \cup \ 153^\circ \leq \theta \leq 180^\circ)$$

As λ' increases the peak value rises and the slope steepens near $\theta = 0^\circ$ and $\theta = 180^\circ$ until eventually, for $\lambda'=\infty$ the curve rises with infinite slope at $\theta = 0^\circ$ and essentially remains at ∞ until it falls with infinite slope at $\theta = 180^\circ$. For all λ', however, the endpoints of the curve are the same because the normal forces do not contribute anything to the internal grasp force when $\theta = 0^\circ$ or $\theta = 180^\circ$. As one might expect, for large λ' the band of allowable θ corresponding to positive C'_n increases unless there exists a low $C'_{n_{max}}$ in which case the band becomes smaller.

4.3 TORQUE LIMIT CONSTRAINT

The final constraint that shall be examined concerns the torque output limitations of the finger joint motors. Given that the contact force solution vector for a grasp configuration meets the constraints on friction angle, unisense normal force, and crush limit discussed previously, the torque limits must still be considered. If one bases the optimality of a grasp on minimizing the dependence on friction forces and ignores the limits on realizable torques, the 'optimal' solution to many overconstrained grasps will demand infinite torques from the finger joint actuators. In general a joint motor will have a maximum torque rating, τ_{max}, which is not dependent on the direction of shaft rotation. The torque limit constraint defined by τ_{max} may or may not be more constraining to a grasp than the previously considered constraints; however, it requires investigation.

If one were to plot the torque requirement of the ith joint, τ_i, versus the grasp angle, θ for a given λ', the band of achievable torques would be bounded above by τ_{max} and below by $-\tau_{max}$. Such a plot would not only identify the feasible grasp angles, but could

also give insight into choosing the 'optimal' grasp based on the criteria of minimizing the joint torque levels. Therefore, the goal is to obtain an expression for τ_i as a function of θ and parameterized by λ'.

As was mentioned in Section 3.6 several physical characteristics of the gripper configuration affect the vector of required joint torques for a given set of contact forces between the gripper and an object. Among these are:

- The number of fingers in contact with the object.

- The number of contacts between each finger and the object.

- The number of links in each finger of the gripper.

- The lengths of the finger links.

- The distance between the joints of the fingers connected to the palm of the gripper.

- The distance between the object and the palm of the gripper.

- The orientation of the object and external load wrench with respect to the palm of the gripper.

In order to reasonably limit the scope of this thesis, it was assumed that there are only two gripper fingers which may contact the object in at most one point each. In order to make the inverse kinematics determinate, only two-links per finger are considered to be actively controlled. If one wished to apply the analysis to a three-link finger set, one would have to lock a joint on each of the fingers and effectively reduce them to two links each. The last four items in the list above are variables in the analysis which are used in Section 3.7 to determine the joint angles of the fingers required to grasp the object in the configuration specified. The length of the jth link of the ith finger is given by l_{ij}. The distance between the joints of the two fingers connected to the palm of the gripper is given by a, while the distance between the center of the object and the palm of the gripper is given by h. Finally, the orientations of the object and external load wrench are given by α and ψ.

The procedure for generating a plot of τ_i as a function of θ is to specify enough object and hand variables to determine the inverse kinematic solutions for the joint angles as

4-10

developed in Section 3.7 and then use those joint angles to calculate the joint torques using the relationships developed in Section 3.6. From Section 3.7 the following relationships are recalled for the solutions of the joint angles:

$$\phi_2 = S \; \arccos \left\{ \frac{\left[\frac{a}{2} - r \sin\left(\theta + \psi\right)\right]^2 + \left[h + r \cos\left(\theta + \psi\right)\right]^2 - l_{11}^2 - l_{12}^2}{2l_{11}l_{12}} \right\} \qquad (4.16)$$

$$\phi_5 = -S \; \arccos \left\{ \frac{\left[\frac{-a}{2} + r \sin\left(\theta - \psi\right)\right]^2 + \left[h + r \cos\left(\theta - \psi\right)\right]^2 - l_{21}^2 - l_{22}^2}{2l_{21}l_{22}} \right\} \qquad (4.17)$$

where S is +1 for knuckle-in configuration and −1 for knuckle-out configuration. The knuckle-out configuration is preferred because it minimizes interference between the fingers and the object as well as interference between the fingers themselves. To determine ϕ_1 and ϕ_4 the tangent of each angle is formed from expressions for their sine and cosine and the ATAN2 function is used to arrive at solutions in the proper quadrants. The expressions for the sine and cosine of each angle are given below:

$$\sin\phi_1 = \frac{\left\{l_{11}\left[h + r \cos\left(\theta + \psi\right)\right] + l_{12}\left[h \cos\phi_2 - \frac{a}{2}\sin\phi_2 + r \cos\left(\theta + \psi - \phi_2\right)\right]\right\}}{l_{11}^2 + l_{12}^2 + 2l_{11}l_{12}\cos\phi_2)} \qquad (4.18)$$

$$\cos\phi_1 = \frac{\left\{l_{11}\left[\frac{a}{2} - r \sin\left(\theta + \psi\right)\right] + l_{12}\left[h \sin\phi_2 + \frac{a}{2}\cos\phi_2 - r \sin\left(\theta + \psi - \phi_2\right)\right]\right\}}{l_{11}^2 + l_{12}^2 + 2l_{11}l_{12}\cos\phi_2)} \qquad (4.19)$$

$$\sin\phi_4 = \frac{\left\{l_{21}\left[h + r \cos\left(\theta - \psi\right)\right] + l_{22}\left[h \cos\phi_5 + \frac{a}{2}\sin\phi_5 + r \cos\left(\theta - \psi + \phi_5\right)\right]\right\}}{l_{21}^2 + l_{22}^2 + 2l_{21}l_{22}\cos\phi_5)} \qquad (4.20)$$

$$\cos\phi_4 = \frac{\left\{l_{21}\left[-\frac{a}{2} + r \sin\left(\theta - \psi\right)\right] + l_{22}\left[h \sin\phi_5 - \frac{a}{2}\cos\phi_5 + r \sin\left(\theta - \psi + \phi_5\right)\right]\right\}}{l_{21}^2 + l_{22}^2 + 2l_{21}l_{22}\cos\phi_5)} \qquad (4.21)$$

Using these joint angles, the joint torques are found using relationships recalled from Section 3.6. In keeping with the previous developments, dimensionless torque parameters are defined as

$$\tau_i' \equiv \frac{\tau_i}{aF_{ext}} \qquad (4.22)$$

4-11

Applying Eq (4.22) to Eq (3.135) yields

$$\vec{\tau}\,' = \vec{\tau}_p\,' + \vec{\tau}_h\,' \tag{4.23}$$

where, for a nominal load,

$$\vec{\tau}_p\,' = \frac{1}{2a} \left\{ \begin{array}{c} l_{11}\cos\zeta_1 + l_{12}\cos\zeta_{12} \\[2mm] l_{12}\cos\zeta_{12} \\[2mm] l_{21}\cos\zeta_4 + l_{22}\cos\zeta_{45} \\[2mm] l_{22}\cos\zeta_{45} \end{array} \right\} \tag{4.24}$$

and

$$\vec{\tau}_h\,' = \frac{\lambda'}{a} \left\{ \begin{array}{c} -l_{11}\sin\zeta_1 - l_{12}\sin\zeta_{12} \\[2mm] -l_{12}\sin\zeta_{12} \\[2mm] l_{21}\sin\zeta_4 + l_{22}\sin\zeta_{45} \\[2mm] l_{22}\sin\zeta_{45} \end{array} \right\} \tag{4.25}$$

As an example let us assume a gripper with

$$a = l_{11} = l_{12} = l_{21} = l_{22} = 1$$

which is to grasp an object having a radius $r = a/2 = 0.5$ such that the center of the object is a height $h = a = 1$ above the palm and the line connecting the fingertips is parallel to the palm (i.e. $\psi = 0°$). Figures 4.4 through 4.7 depict the required torques in joints 1, 2, 4, and 5, respectively, assuming the object is subjected to a nominal load.

These plots reveal a trend in the torques of joints 1 and 4. Generally, for a constant λ' joints 1 and 4 must have higher torques as θ gets larger. As the desired λ' increases, the required torques in joints 1 and 4 also increase as one would expect. Due to the symmetry of the grasp and the definition of the coordinate system, the torque in joint 4 is equal and opposite to that of joint 1.

The plots for joints 2 and 5, however, have unexpected crossover points where the required torques are identical for all internal grasp force magnitudes. This invariance is an indication that the inverse kinematic solution of the hand at this grasp angle results in joint angles that position links 2 and 5 perpendicular to the direction of the external
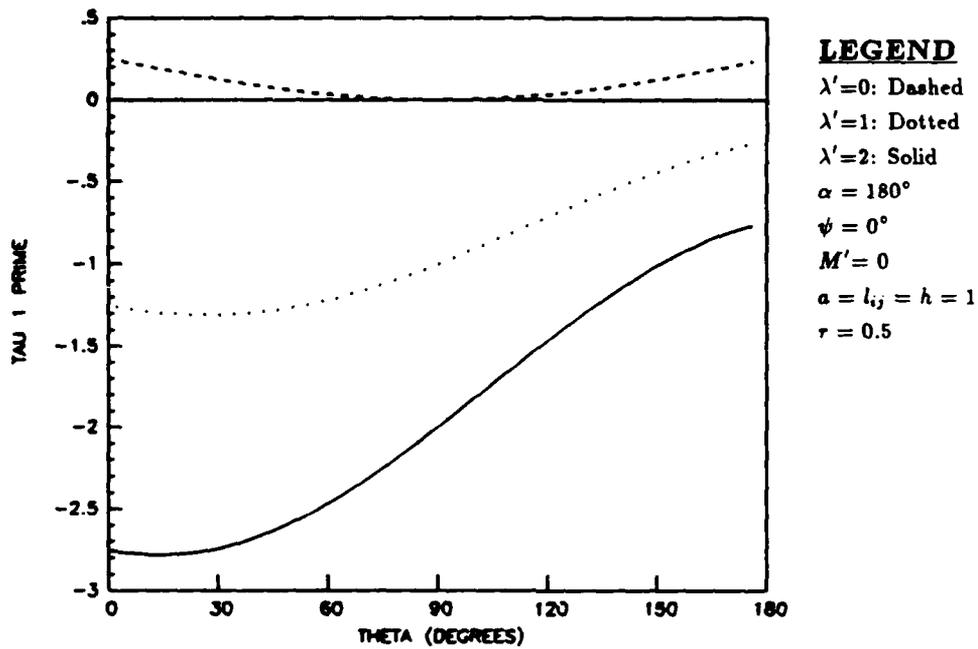
Figure 4.4. Dimensionless torque of joint 1 versus grasp angle for a nominal external load on the object
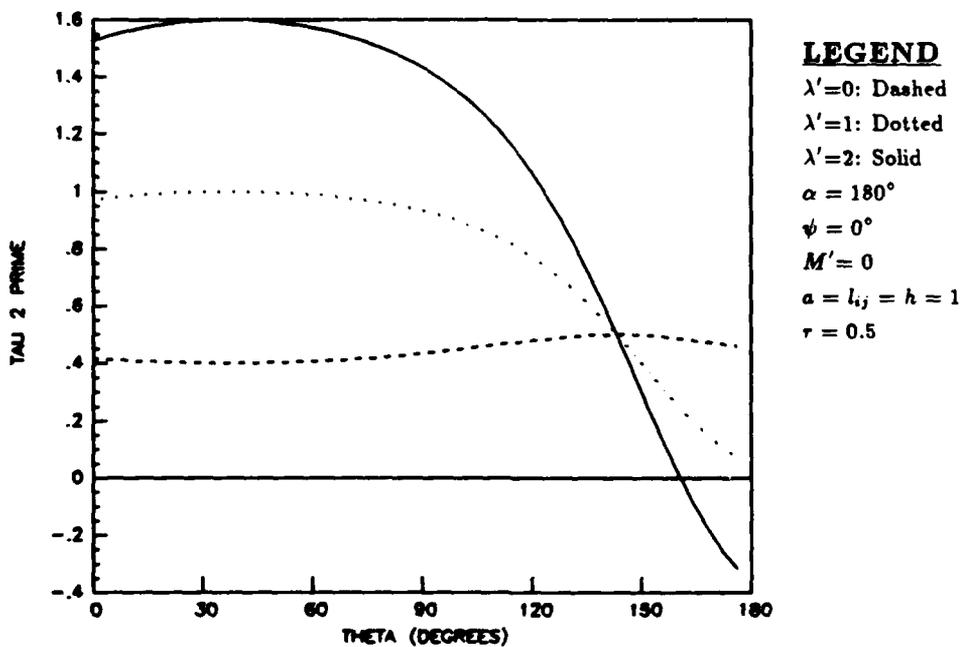
Figure 4.5. Dimensionless torque of joint 2 versus grasp angle for a nominal external load on the object

LEGEND

$\lambda'=0$: Dashed
$\lambda'=1$: Dotted
$\lambda'=2$: Solid
$\alpha = 180°$
$\psi = 0°$
$M' = 0$
$a = l_{ij} = h = 1$
$r = 0.5$
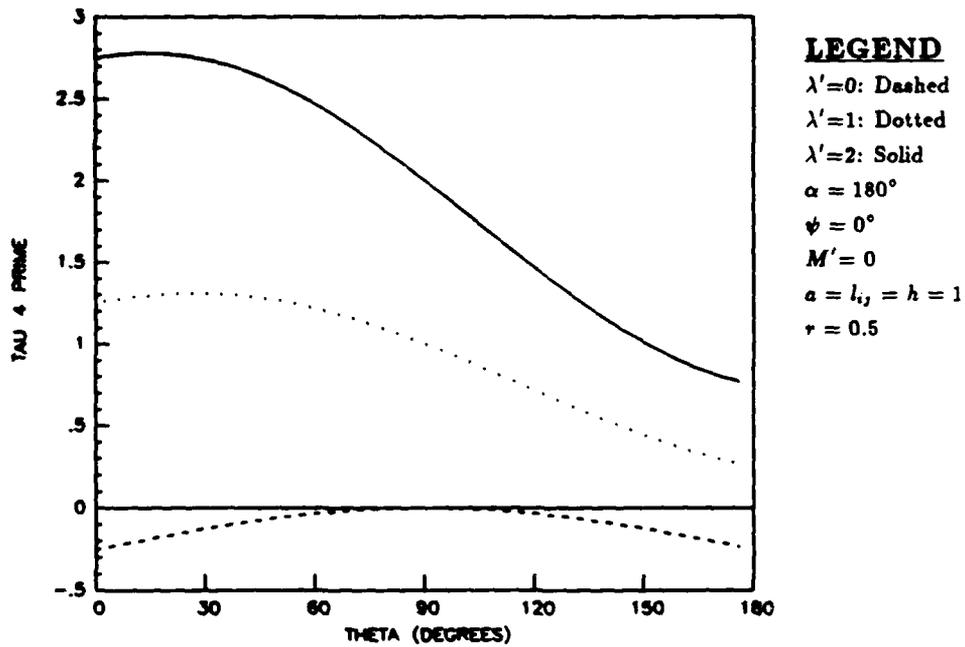
Figure 4.6.   Dimensionless torque of joint 4 versus grasp angle for a nominal external load
on the object

LEGEND

$\lambda'=0$: Dashed
$\lambda'=1$: Dotted
$\lambda'=2$: Solid
$\alpha = 180°$
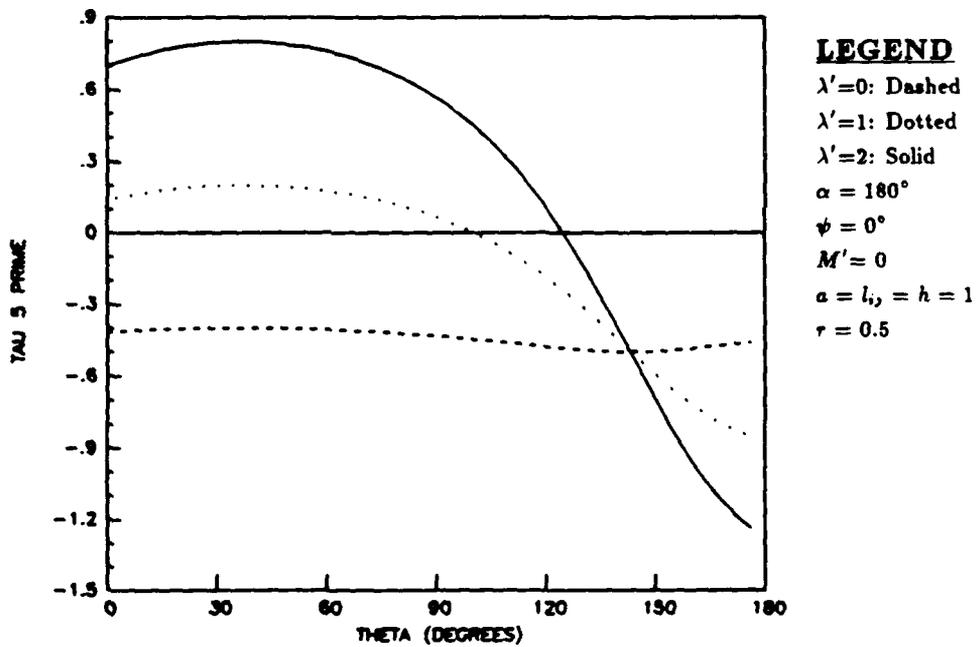$\psi = 0°$
$M' = 0$
$a = l_{ij} = h = 1$
$r = 0.5$

Figure 4.7.   Dimensionless torque of joint 5 versus grasp angle for a nominal external load
on the object

wrench. That is, in the given position, the torques applied to joints 2 and 5 can make no contribution to the internal grasp force but, instead constitute the particular solution contact force vectors. Therefore, the configuration of the gripper at this point is one with the centerlines of links 2 and 5 along the line connecting the contact points (i.e. horizontal).

One can superimpose the torque limit constraint on the plots by computing the corresponding τ'_{max} from the given τ_{max} and aF_{ext}

$$\tau'_{max} = \frac{\tau_{max}}{aF_{ext}} \qquad (4.26)$$

The feasible grasp region is identified by the range of θ which is within the band of $\pm\theta$. For a given τ_{max}, the range of allowable θ decreases with increasing λ'. This is in contrast with the trend for the crush limit constraint where increasing λ' resulted in a larger range of allowable θ.

As an example, assume that the maximum torque which can be generated by any of the joint motors results in $\tau'_{max} = 1$ and the internal grasp force is to be maintained at $\lambda' = 1$. Figures 4.4 and 4.6 indicate that, based on the torque capabilities of joints 1 and 4, the object must be grasped with $\theta \in (90° \leq \theta \leq 180°)$. Examining Figures 4.5 and 4.7 reveals that joints 2 and 5 impose no restriction on the range of allowable θ since for $\lambda'=1$ they remain below τ'_{max} for all θ.

4.4 SIMULTANEOUS CONSIDERATION OF CONSTRAINTS

In order for a grasp configuration to be physically feasible, it must simultaneously satisfy all of the constraints previously mentioned in this chapter. The intersection of the allowable grasping angle regions identified in the example of Sections 4.1 through 4.3 identifies the 'good' grasp region for $\lambda'=1$. When all of the constraints are simultaneously considered and $\lambda'=1$, the choice of θ is reduced to $\theta \in (90° \leq \theta \leq 162°)$. In order to remain as far removed from the constraint boundaries one might suggest that the midpoint of this region be selected. However, one should examine the trends in Figures 4.1 through 4.7 within this range of θ before arbitrarily selecting the midpoint. Upon examining the trends of the curves from 90° to 162° one discovers it is beneficial to tend towards 162° based on the crush limit and torque limit constraints, but it is detrimental with respect to

the friction limit constraint. With this controversy, it is not clear which way one should tend.

The next chapter presents a method of evaluating the benefits of tending towards one bound or the other. By way of illustration, however, let us arbitrarily choose to further examine the grasp at $\theta = 135°$ and $\lambda' = 1$. The trigonometric relations for $\theta = 135°$ are relatively simple so this configuration should serve well as an illustration. Figure 4.8 shows the configuration of the gripper for this example when θ is chosen to be 135 degrees.
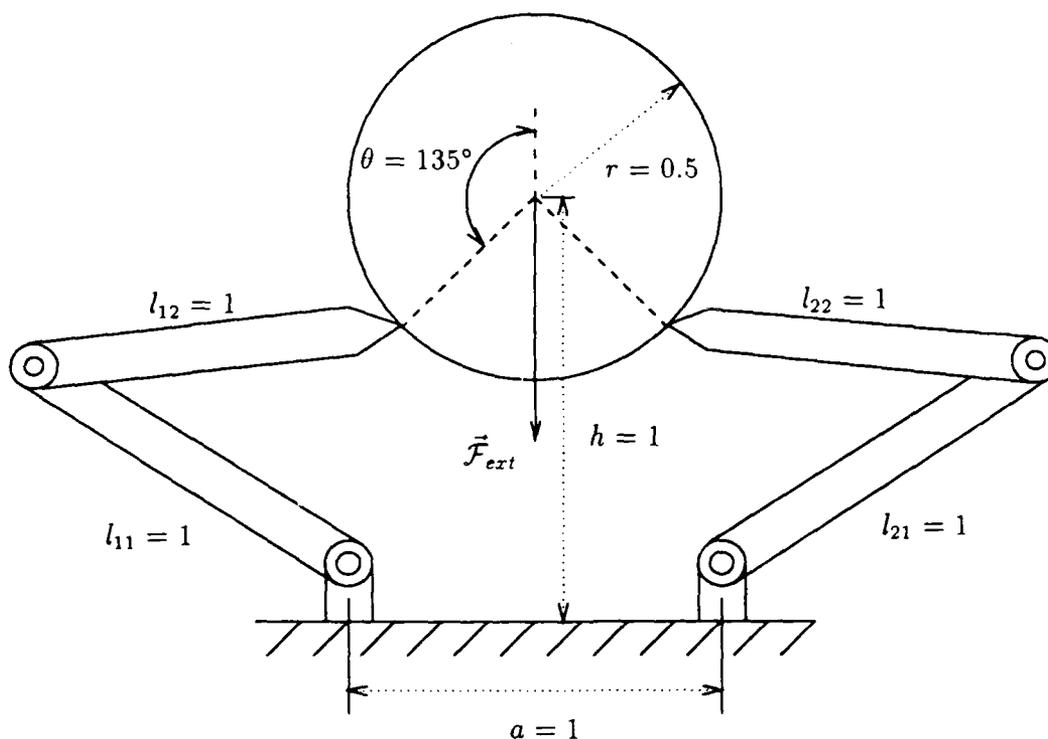

Figure 4.8. Configuration of the gripper fingers for the grasp example with $\theta = 135°$, $a = l_{ij} = h = 1$, $r = 0.5$, and $\psi = 0°$

4.5 CHAPTER SUMMARY

Analytic expressions are presented which model the equilibrium requirements of two-fingered grasps of cylindrical objects confined to planar motion. The analytic expressions

are three sets of inequality relations which correspond to three grasp constraints; friction limits, crush limits, and joint torque limits. Use of these expressions is restricted by the assumptions and limitations mentioned in Section 1.2. A nominal external load wrench was defined as a zero-pitch wrench (a pure force) acting along the y_o-axis such that $\alpha = 180°$. The inequality relations were then plotted as equalities for the conditions of the nominal external load wrench. To construct the plots for this indeterminate system, the grasp angle, θ, was arbitrarily chosen as the independent variable and the internal grasp force magnitude, λ', was chosen as a parameter. Trends in the requirements for friction angle, contact normal force, and finger joint torques for selected values of λ' as functions of θ were then examined. These plotting trends were interpreted in terms of the physical conditions of the grasp.

During the course of the examination of constraint requirements for <u>nominal load conditions</u>, the following trends were noted:

- The friction angle required to maintain an equilibrium grasp varies linearly with the grasp angle, θ, if one maintains a constant internal grasp force magnitude, λ'.

- The friction angles at fingertips 1 and 2 are equal in magnitude and opposite in sign.

- For any positive static coefficient of friction, μ_s, and any internal grasp force, there exists some θ which corresponds to an equilibrium grasp if there are no crush or joint torque limits.

- At every θ, one can vary the required friction angle through a range of 90° by varying λ' between zero and infinity.

- Increasing the internal grasp force magnitude, λ', tends to be detrimental to grasp equilibrium when θ is in the neighborhood of 180° and it enhances grasp equilibrium when θ is in the neighborhood of 90°.

- The magnitudes of the contact normal forces are less affected by increasing λ' when θ is near 0° or 180° than they are when θ is near 90°.

- When the centerlines of the finger links are aligned with the direction of the internal grasp force, their joint torques required for grasp equilibrium are independent of λ'.

4-17

Coulomb Friction Limit	$\mu_s = 1$ $\lambda' = 1$	
Crush Limit	$C'_{n_{max}} = 1.5$ $\lambda' = 1$	
Finger Joint Torque Limit	$\tau'_{max} = 1$ $\lambda' = 1$ $a = 1$ $h = 1$	$r = 0.5$ $\psi = 0°$ $l_{ij} = 1$

Table 4.1. Values of variables specified in each section for the example grasp analysis

- Depending on the configuration of the grasp, there may be regions of θ whose joint torques required for grasp equilibrium are less sensitive to changes in λ' than other regions.

An example was presented to illustrate a method of using the analytic expressions to determine feasible grasp angles and internal grasp force magnitudes. The values which were specified in each section of this chapter for the example are summarized in Table 4.1. The method includes graphical displays of data which depict trends in the equilibrium requirements as functions of the grasp angle and the internal grasp force level. One can select grasp configurations using this method and be guaranteed that it will achieve equilibrium. However, if one was interested in optimizing the grasp configuration's ability to tolerate changes in the external load wrench, one would need a further method. The additional method would be intended to evaluate the merit of a range of feasible grasp configurations with respect to the criteria mentioned. Chapter V presents such a method.

A basic premise of using the analytic expressions presented in this chapter is that one has a means of determining several factors about the object and the external load on the object. A camera system could be used to acquire the radius and location of the object if the lighting conditions were sufficient. Once the radius and position of the object are known, one must additionally determine the type of material on the object's surface, so that an estimate of the static coefficient of friction can be made, and the mass of the

object so its weight can be estimated. Probably the most difficult measurement, however, is that of the magnitude and direction of the external load on the object. If the object is known to be resting on a supporting surface, then the net external wrench is zero. If the object is being held stationary by the gripper, one can guess with fairly high confidence that the external wrench consists only of gravity. On the other hand, if the object is being held by the gripper and someone pulls on the object, then some instrumentation is needed to determine the characteristics of the wrench caused by the pulling. It is unclear to the author as to what type of instrumentation could provide this information.

V. EVALUATING THE EFFECTS OF
LOAD VARIATIONS ON A GRASP

Chapter IV presents a graphical method of selecting the grasp angle based on a nominal load. The term 'nominal' load was used to describe an external wrench on the object having zero-pitch and acting along the y_o-axis such that $\alpha = 180°$. Once a candidate grasp configuration has been chosen by the methods in Chapter IV, one would like to check the 'quality' of the grasp. For the purposes of this thesis, the 'quality' of a grasp is determined by its ability to tolerate disturbances or changes in the external load wrench. Figure 4.8 shows the configuration of the gripper fingers and the object for the conditions given by the grasp example in Chapter IV. That configuration will be further analyzed to illustrate the concepts in this chapter.

The variations in the external load wrench may be viewed in either one of two ways. If one wishes, he can view the nominal value for the external load wrench as a measured quantity and the variations as possible measurement errors. Or one can view the nominal load as currently being an accurate value and the variations as possible future configurations of the load. If the load varies quasistatically, a static equilibrium analysis can correctly evaluate the behavior of the grasp during the change. However, if inertial effects become significant, the static equilibrium analysis presented will no longer be suitable.

In this chapter, a method for evaluating the ability of a grasp to tolerate variations in the nominal load wrench is defined. The nominal load wrench can vary in three ways. The zero-pitch component of the external wrench may vary in direction or magnitude from the nominal and the infinite-pitch component may vary from its nominal zero magnitude. The first two variations are characterized by changes in α and F_{ext}, respectively, while the third variation is characterized by a nonzero M'.

5.1 CHANGES IN THE NOMINAL LOAD DIRECTION

When the direction of the external load wrench changes from the nominal condition of $\alpha = 180°$ the load is then said to be asymmetric. This asymmetry destroys the equal and

LEGEND
$\lambda'=0$: Dashed
$\lambda'=0.5$: Dash-Dot
$\lambda'=1$: Dotted
$\lambda'=2$: Solid
$\theta = 135°$
$M'=0$
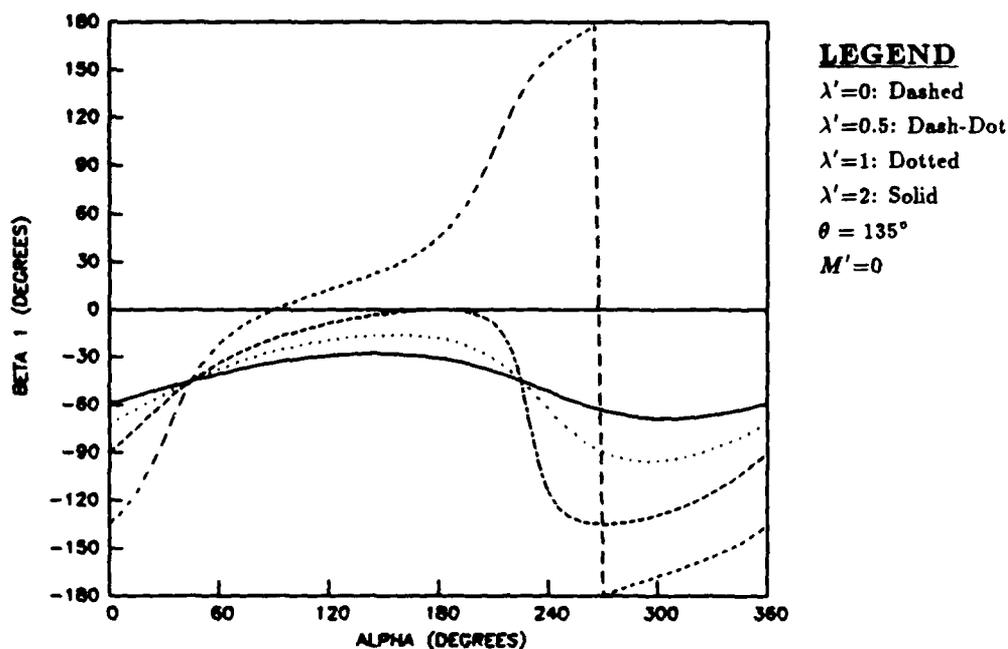
Figure 5.1.   Friction angle at fingertip 1 versus variation in α, the angle of the external load

opposite relationship between β_1 and β_2 which existed for the nominal case. In addition, C_{1n} is no longer identical to C_{2n} and the symmetry in the torques vanishes.

By examining the friction, contact normal magnitude, and finger joint torque requirements of a grasp for values of α in the neighborhood of the nominal condition, one can determine the ability of a grasp to tolerate a variation in α.

5.1.1   FRICTION LIMIT CONSTRAINT. If candidate values for θ and λ' have been chosen by the methods of Chapter IV and α is assigned as the free variable in Eqs (4.6) and (4.7), one can plot the required β_1 and β_2 for various α using those same equations to explore the effect. Doing this for the example problem given in Chapter IV, yields Figures 5.1 and 5.2.

When $\alpha = 45°$ or $\alpha = 225°$ all values of $\lambda'> 0$ share the same β_1 in Figure 5.1. These two orientations of the external load wrench correspond to $\vec{F}_{ext}$ pointing either directly away from, or directly at the point of contact between fingertip 2 and the object. In these configurations, one might think that $\vec{C}_1$ would be zero and $\vec{C}_2$ would entirely equilibrate $\vec{F}_{ext}$. However, this is not the case because of the premise that two contacts must exist
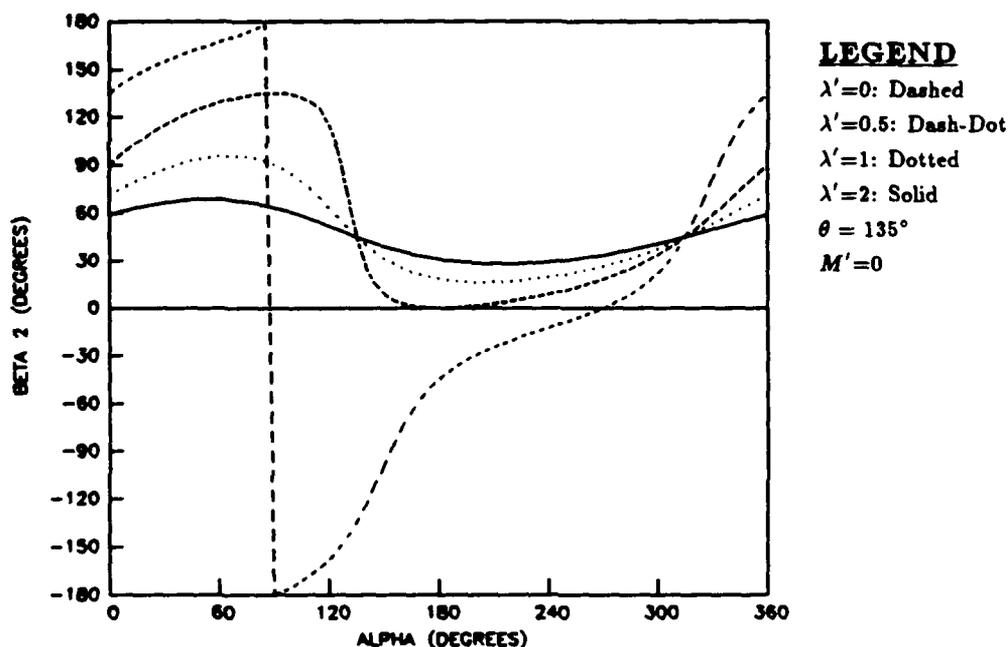
Figure 5.2.   Friction angle at fingertip 2 versus variation in α, the angle of the external load

between the hand and the object rather than one. There are, in fact, equilibrium solutions for the case of two finger contacts that require nonzero $\vec{C_1}$ and $\vec{C_2}$, neither of which are pure normal forces.

Let us examine for a moment these configurations when $\lambda' = 0$. The conditions for $\lambda' = 0$ require that there be no internal grasp force. This does not mean that the resultant contact forces, $\vec{C_1}$ and $\vec{C_2}$, do not have components along the direction of the internal grasp force (the line connecting the two contact points). Rather, it means that there is *zero force interaction* along this direction [Wal86: 215]. This implies that if $\vec{C_1}$ and $\vec{C_2}$ have components in this direction, they must be oriented in the same sense so as not to oppose each other. A vector diagram of the resulting solution for $\alpha = 45°$ is given in Figure 5.3 while that for $\alpha = 225°$ is given in Figure 5.4.   When $\alpha = 45°$ and λ' is increased, the normal and tangential components of the additional contact force must increase proportionally to act along the direction of the internal grasp force. Therefore, β_1 remains at $-45°$ for all λ'.

When $\alpha = 225°$, however, the direction of $\vec{C_1}$ will change as λ' increases. Thus, β_1
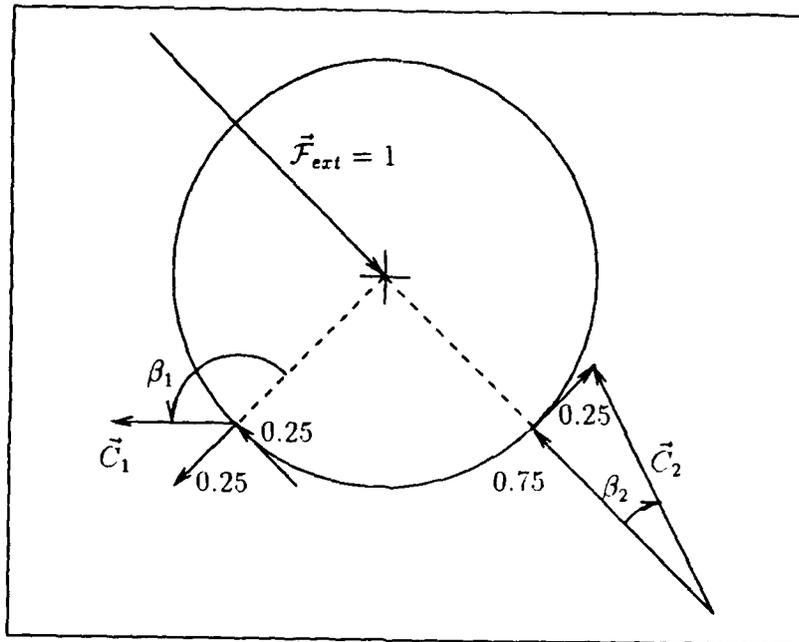
Figure 5.3. Vector diagram of the contact force vector solution when $\lambda' = 0$ and $\alpha = 45°$
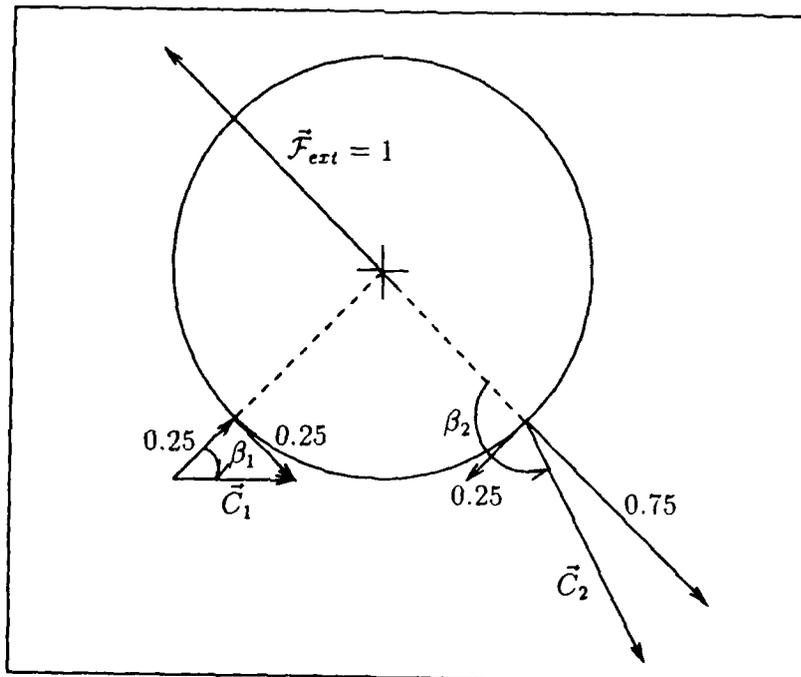
Figure 5.4. Vector diagram of the contact force vector solution when $\lambda' = 0$ and $\alpha = 225°$

starts at 135° and when λ' exceeds $((.25)^2 + (.25)^2)^{0.5} = 0.3535$, β_1 transitions abruptly to $-45°$. β_2 behaves in a similar fashion except at $\alpha = 135°$ and $\alpha = 315°$ as shown in Figure 5.2.

As λ' increases towards infinity, the internal grasp force overshadows the external load wrench and the contact force vector becomes decreasingly sensitive to changing α. As a result, when $\lambda' = \infty$, β_1 remains constant at $-45°$ while β_2 remains constant at $+45°$.

Since $\beta = \pm 45°$ is the boundary of the friction limit constraint for the example, Figures 5.1 and 5.2 indicate that this constraint will not be violated as long as $\lambda' \geq 0.3535$ and

$$\alpha \in (135° \leq \alpha \leq 225)$$

This means that, based on the friction limit constraint, the direction of the external load wrench can vary by 45 degrees to either side of the nominal configuration and the object will not slip from the grasp as long as the contact forces are adjusted accordingly. For variations beyond this range, it is impossible to maintain an equilibrium grasp. It is interesting to note that 'squeezing' the object harder does nothing to improve the range of tolerable α variation for this configuration of the grasp.

5.1.2 CRUSH LIMIT CONSTRAINT. By plotting the magnitude of the contact normal force versus α one can evaluate the effect of changing the direction of the external load wrench on the crush limit constraint. In Section IV expressions were derived for the normalized normal forces at contact points 1 and 2 as functions of r, θ, α, λ', and M'. Since $M' = 0$ for a nominal load and only the effect of varying α is to be explored, $M' = 0$ can be substituted into Eqs (4.12) and (4.13) and r can be canceled from the numerator and denominator to get the following expressions:

$$C'_{1n} = \left\{ \frac{2\lambda' \sin^2 \theta + \cos \alpha \, \sin \theta \, \cos \theta + \sin \alpha}{2 \sin \theta} \right\} \tag{5.1}$$

$$C'_{2n} = \left\{ \frac{2\lambda' \sin^2 \theta + \cos \alpha \, \sin \theta \, \cos \theta - \sin \alpha}{2 \sin \theta} \right\} \tag{5.2}$$

Since the goal is to evaluate candidate values for λ' and θ which were chosen by the method in Section IV, those chosen values can be substituted into Eqs (5.1) and (5.2)

LEGEND

$\lambda'=0$: Dashed
$\lambda'=1$: Dotted
$\lambda'=2$: Solid
$\theta = 135°$
$M'=0$
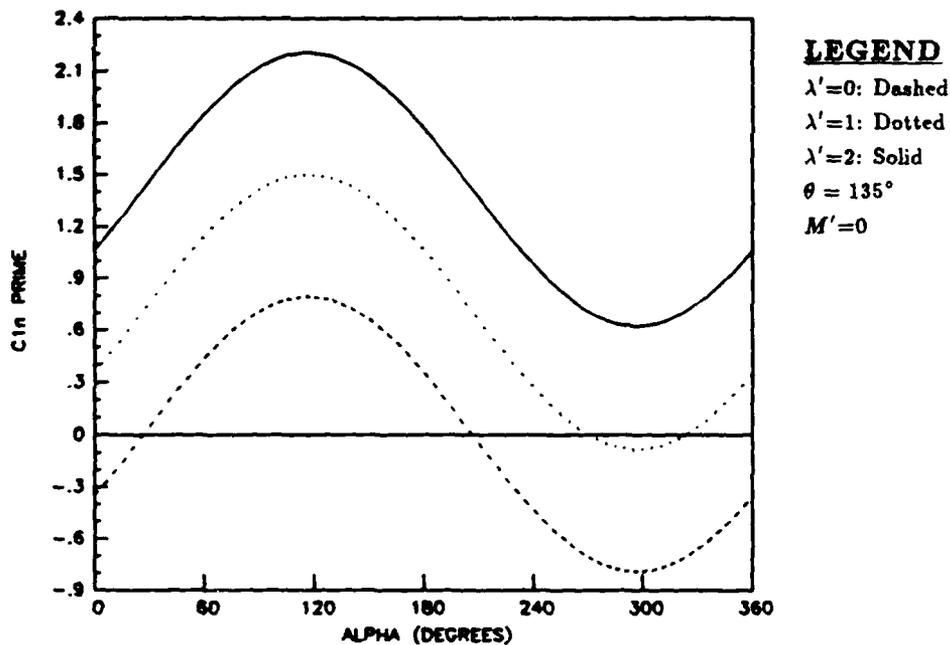
Figure 5.5. Normalized contact normal force at fingertip 1 versus variation in α, the angle of the external load

which can in turn be used to plot C'_{1n} and C'_{2n} versus α. For the nominal condition having $\alpha = 180°$, the plots of C'_{1n} and C'_{2n} versus α will be reflections of each other about $\alpha = 180°$. Figure 5.5 shows a plot of C'_{1n} versus α for the example problem using three different values of λ'.

Figure 5.6 shows a similar plot for C'_{2n} versus α. As one would expect, the required normal forces increase without bound as λ' is increased towards infinity. The plots are sinusoidal in nature owing to the cyclic nature of varying α from 0 to 360 degrees. Since the crush limit of the example is 1.5 and the candidate λ' is 1, the plots indicate that α variations cannot violate the crush limit constraint. In the regions of α near 120 degrees or 240 degrees the crush limit is approached, however, it is never exceeded for either of the contacts. The conclusion is that the equilibrium of the grasp can be maintained despite the variations in α without being concerned about crushing the object.

5.1.3 TORQUE LIMIT CONSTRAINT. In order to explore the ability of the gripper to generate the torques required to maintain grasp equilibrium when the direction

5-6
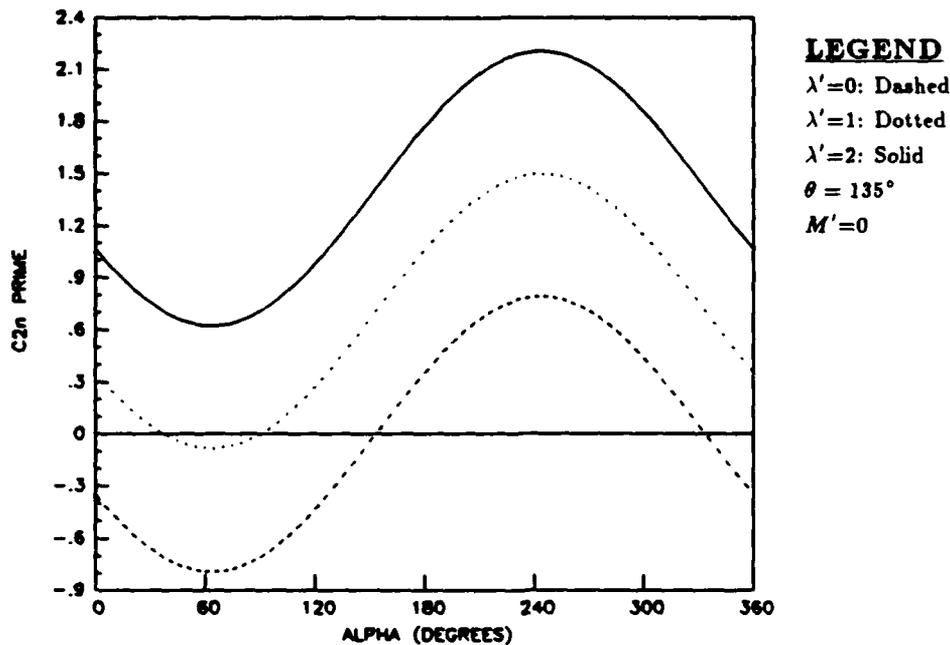
Figure 5.6. Normalized contact normal force at fingertip 2 versus variation in α, the angle of the external load

of the external load varies, it would be useful to obtain expressions for the finger joint torques as explicit functions of α. For the nominal load explicit symbolic expressions were derived for the normalized homogeneous and particular solutions of the joint torque vector and summed them using Eq (4.23) to get $\bar{\tau}'$. If α is retained as a variable, however, the complexity of the resulting expressions for $\bar{\tau}'$ becomes unmanageable. Therefore, numerical evaluation of subexpressions are used to generate the data required to plot the joint torques as functions of α.

The procedure is as follows. The same inverse kinematic equations as were presented in Eqs (4.18) through (4.22) are used to yield the two joint angles for each finger. These joint angles are then used in Eqs (3.110) through (3.115) and Eqs (3.120) through (3.125) to determine the j_{ijk} that are in turn substituted into Eq (3.131) to yield the transpose of the global hand Jacobian matrix, $\mathcal{J}^T$. One must next evaluate the contact force vector for the given grasp and load configuration. This is done by substituting the appropriate

θ, α, and λ' into the following equation:

$$\vec{C} = \frac{F_{ext}}{2\sin\theta} \left\{ \begin{array}{c} 2\lambda' \sin^2\theta + \cos\alpha \sin\theta \cos\theta + \sin\alpha \\ 2\lambda' \sin\theta \cos\theta - \cos\alpha \sin^2\theta \\ 0 \\ 2\lambda' \sin^2\theta + \cos\alpha \sin\theta \cos\theta - \sin\alpha \\ -2\lambda' \sin\theta \cos\theta + \cos\alpha \sin^2\theta \\ 0 \end{array} \right\} \tag{5.3}$$

The final step in determining the vector of joint torques is to multiply the global hand Jacobian matrix by the contact force vector via

$$\vec{\tau}' = \mathcal{J}^T \vec{C} \tag{5.4}$$

Although Eq (5.4) is presented as a matrix multiplication, one does not have to multiply all of the row elements of $\mathcal{J}^T$ by all of the column elements of $\vec{C}$ because of the numerous zero elements. By planning ahead, one can greatly reduce the computation time for the joint torque vector.

One can now use this method to produce plots of the four different finger joint torques versus α for the example problem under study. Using $\theta = 135°$, the plots given in Figures 5.7 through 5.10 were generated. These figures indicate that the joint torques vary in a sinusoidal fashion as α goes from 0 to 360 degrees. Also note that while increasing α from the nominal reduces the torques in joints 1 and 4, it increases the torques required in joints 2 and 5. When α varies below the nominal, the opposite occurs. However, none of the joint torques are driven outside of the allowable band defined in the example problem as $\tau'_{max} = \pm 1$ by any value of α. Based on the torque limit constraint one should conclude that the equilibrium of the grasp will not be destroyed by variations in the direction of the external load if we choose $\lambda' = 1$.

As a result of this investigation into the tolerance of the grasp in the example problem to variations in the direction of the external load wrench, it is concluded that the candidate values of 135° for θ and unity for λ' are good enough to maintain static equilibrium under variations in α of as much as 45 degrees away from the nominal direction. When α varies

Figure 5.7. Dimensionless torque of joint 1 versus variation in α, the angle of the external load
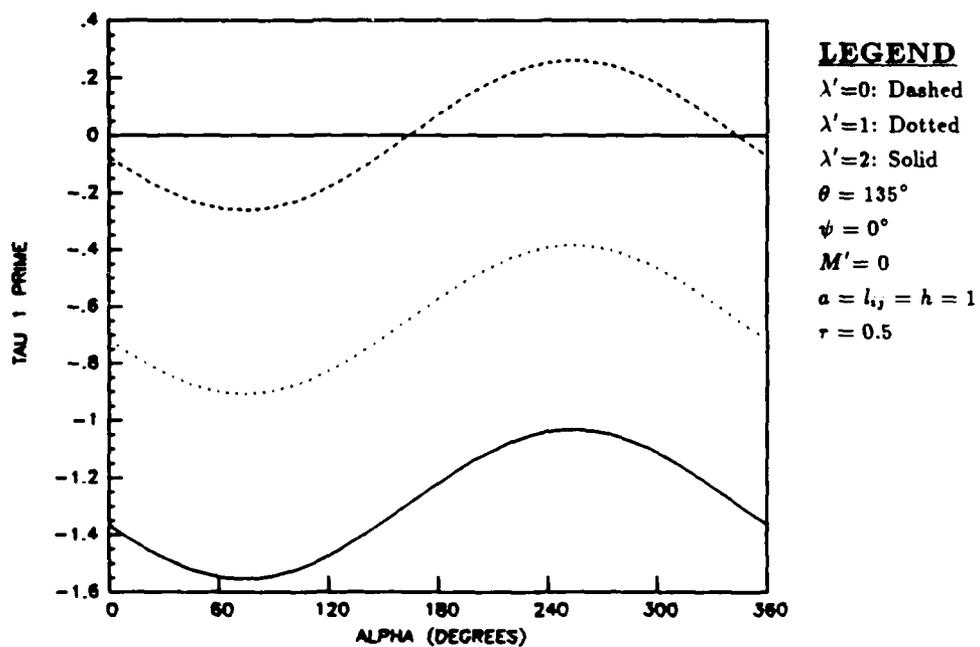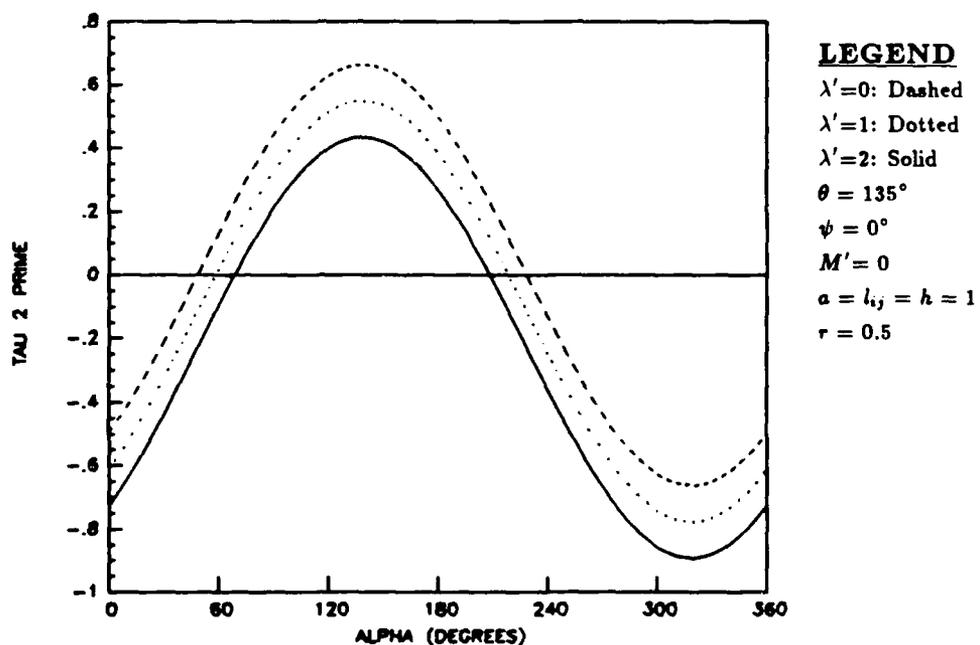

Figure 5.8. Dimensionless torque of joint 2 versus variation in α, the angle of the external load
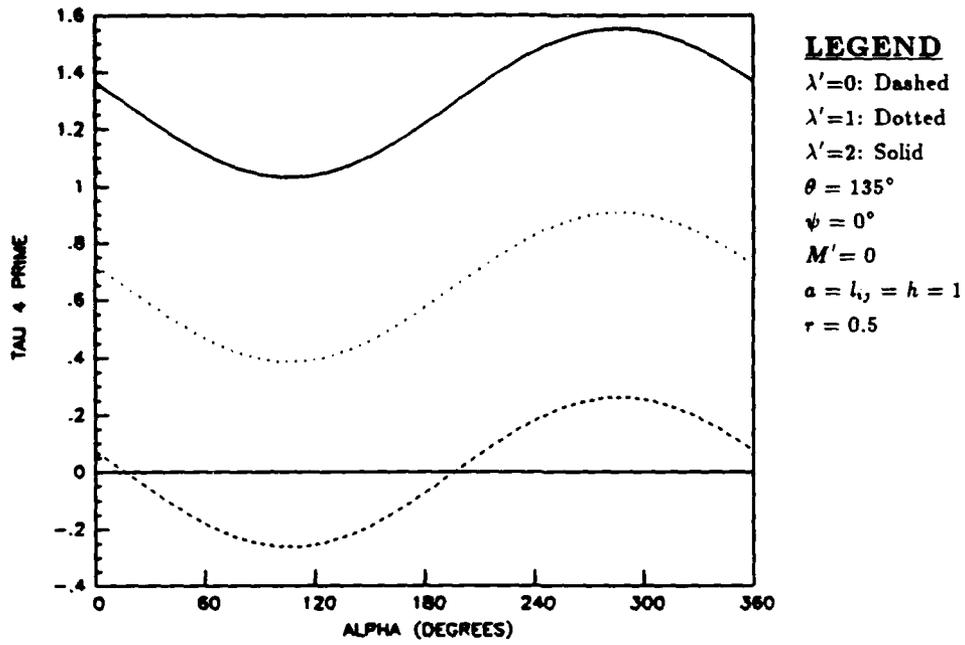
Figure 5.9. Dimensionless torque of joint 4 versus variation in α, the angle of the external load
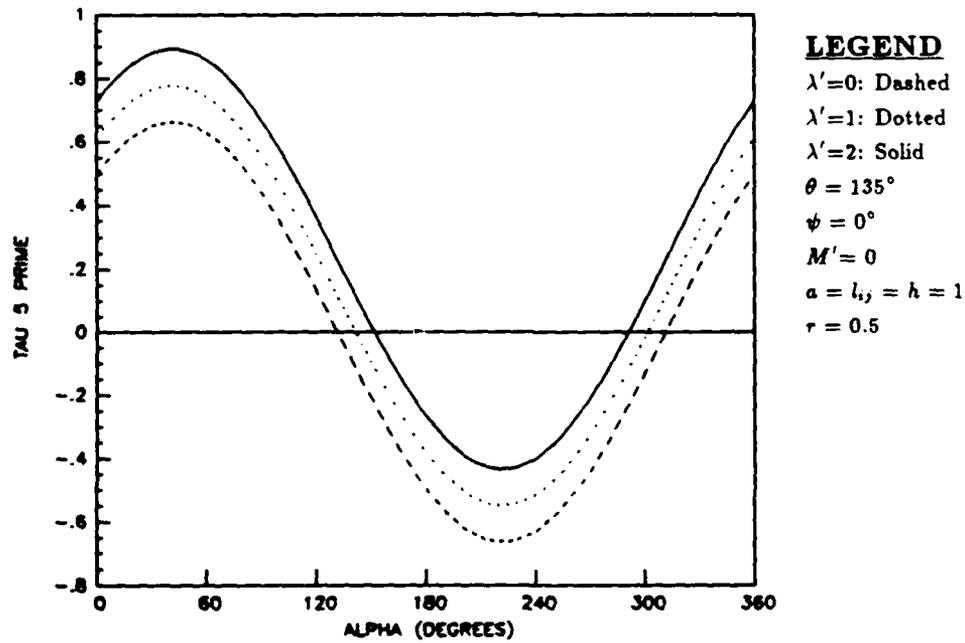

Figure 5.10. Dimensionless torque of joint 5 versus variation in α, the angle of the external load

by more than 45 degrees, the object will slip from the grasp due to a violation of the friction limit constraint.

5.2 CHANGES IN THE NOMINAL LOAD MAGNITUDE

When the magnitude of the external load wrench changes, it affects the equilibrium demands of the grasp. Having determined candidate values for the grasp angle, θ, and the internal grasp force, λ', by means of a nominal load analysis in Chapter IV, one would like to determine the range of variation in the magnitude of F_{ext} that can be tolerated by the grasp without losing equilibrium or violating any one of the other two constraints. To do this, one must examine each of the three constraints, in turn, as F_{ext} is allowed to vary in magnitude. In order to distinguish between the nominal or reference magnitude of F_{ext} and the varied magnitude of F_{ext}, the magnitude of the nominal external load wrench is denoted as F_{ext}^{nom}.

In general, the range of tolerable F_{ext} will have an upper and a lower bound when each of the constraints is examined in the presence of a variation in the external load wrench magnitude. Since only positive F_{ext} are considered, the lower bound itself is bounded by zero. The subsequent analysis will indicate that, in general, the friction limit constraint will define upper and lower bounds on F_{ext} which are finite and non-zero. The types of bounds corresponding to the crush limit constraint will be dependent on the quadrant in which θ lies, and the bounds corresponding to the torque limit constraint will be dependent on the configuration of the gripper fingers as they grasp the object.

A fundamental assumption used in determining the bounds on F_{ext} for which the grasp can maintain equilibrium is that the grasp configuration and internal grasp force magnitude will be maintained during the variation. This implies that θ, λ' [1], α, the link lengths, and the finger joint angles are to be held constant in the analysis that follows. A new parameter, F^*, is defined as

$$F^* \equiv \frac{F_{ext}}{F_{ext}^{nom}} \tag{5.5}$$

---

[1] In Chapter III λ' was defined in Eq (3.37) as the ratio of the magnitudes of the internal grasp force and F_{ext}. In this chapter, this definition is refined by defining λ' as the ratio of the magnitudes of the internal grasp force, λ, and the nominal external load wrench F_{ext}^{nom}.

The magnitude of F^* at the upper and lower bounds will reflect the ratios of the bounding values of F_{ext} to F_{ext}^{nom}. Thus, the larger the bounding F^* limits, the more 'headroom' one has for the candidate grasp configuration.

5.2.1 FRICTION LIMIT CONSTRAINT.

To consider the effect of increasing F_{ext} on the required values of β_1 and β_2, begin by recalling the expressions for the homogeneous and particular solutions to the contact force vector while the object is subjected to nominal load conditions. In Chapter III Eq (3.24) gave the homogeneous contact force vector solution as

$$
\vec{C}_h = \left\{ \begin{array}{c} \sin\theta \\ \cos\theta \\ \sin\theta \\ -\cos\theta \end{array} \right\} \lambda
\tag{5.6}
$$

and (3.31) gave the particular solution contact force vector as

$$
\vec{C}_p \approx \frac{F_{ext}}{2} \left\{ \begin{array}{c} -\cos\theta \\ \sin\theta \\ -\cos\theta \\ -\sin\theta \end{array} \right\}
\tag{5.7}
$$

where the C_{1z} and C_{2z} components have been intentionally excluded. Summing $\vec{C}_h$ and $\vec{C}_p$ to get the total contact force vector $\vec{C}$, yields

$$
\vec{C} = 0.5 \left\{ \begin{array}{c} 2\lambda\sin\theta - F_{ext}\cos\theta \\ 2\lambda\cos\theta + F_{ext}\sin\theta \\ 2\lambda\sin\theta - F_{ext}\cos\theta \\ -2\lambda\cos\theta - F_{ext}\sin\theta \end{array} \right\}
\tag{5.8}
$$

If the definition of λ' is introduced into Eq (5.8), the result is

$$
\vec{C} = \frac{F_{ext}^{nom}}{2} \left\{ \begin{array}{c} 2\lambda'\sin\theta - \frac{F_{ext}}{F_{ext}^{nom}}\cos\theta \\ 2\lambda'\cos\theta + \frac{F_{ext}}{F_{ext}^{nom}}\sin\theta \\ 2\lambda'\sin\theta - \frac{F_{ext}}{F_{ext}^{nom}}\cos\theta \\ -2\lambda'\cos\theta - \frac{F_{ext}}{F_{ext}^{nom}}\sin\theta \end{array} \right\}
\tag{5.9}
$$

5-12

Substituting the definition of F^* given by Eq (5.5) into Eq (5.8) gives

$$\vec{C} = \frac{F_{ext}^{nom}}{2} \left\{ \begin{array}{c} 2\lambda' \sin\theta - F^* \cos\theta \\ 2\lambda' \cos\theta + F^* \sin\theta \\ 2\lambda' \sin\theta - F^* \cos\theta \\ -2\lambda' \cos\theta - F^* \sin\theta \end{array} \right\} \tag{5.10}$$

The friction angles at contact points one and two are formed by substituting the appropriate expressions from Eq (5.10) into the defining equations for β_1 and β_2 given by Eqs (4.4) and (4.5) to get

$$\beta_1 = \frac{2\lambda' \cos\theta + F^* \sin\theta}{2\lambda' \sin\theta - F^* \cos\theta} \tag{5.11}$$

and

$$\beta_2 = \frac{-2\lambda' \cos\theta - F^* \sin\theta}{2\lambda' \sin\theta - F^* \cos\theta} \tag{5.12}$$

Once again, note that $\beta_1 = -\beta_2$ for the symmetric load conditions under which the external load magnitude variations are analyzed. β_1 and β_2 are plotted as functions of F^* to evaluate the range of F_{ext} which can be tolerated without loss of grasp equilibrium. Figures 5.11 and 5.12 show the plots for β_1 and β_2, respectively, for the example grasp under study. In those figures, the data has been plotted from $F^* = 0$ up to $F^* = 2$ in order to represent variations of ± 100 percent on F_{ext}.

There are several interesting features of Figures 5.11 and 5.12. Consider for a moment the data at $F^* = 0$ which corresponds to no external load on the object. For $\lambda' = 0$ and $F^* = 0$ the total contact force is zero at both fingertips so the fingertips are not in contact with the object and the friction angles are undefined. For a differentially small F^*, however, the friction angles are defined and equal to $\pm 45°$ for $\lambda' = 0$ as shown in Figures 5.11 and 5.12. These friction angles correspond to having the total contact force vectors at fingertips 1 and 2 pointing straight up along the positive y_o-axis. This is known to be the case when a symmetric load and zero internal grasp force coexist.

With the exception of $\lambda' = 0$, all λ' require $\beta_1 = -45°$ and $\beta_2 = 45°$ at $F^* = 0$. When $F^* = 0$ there is no external force on the object and, therefore, the particular solution contact force vector, $\vec{C}_p$, is identically a zero vector. Such a condition would exist when
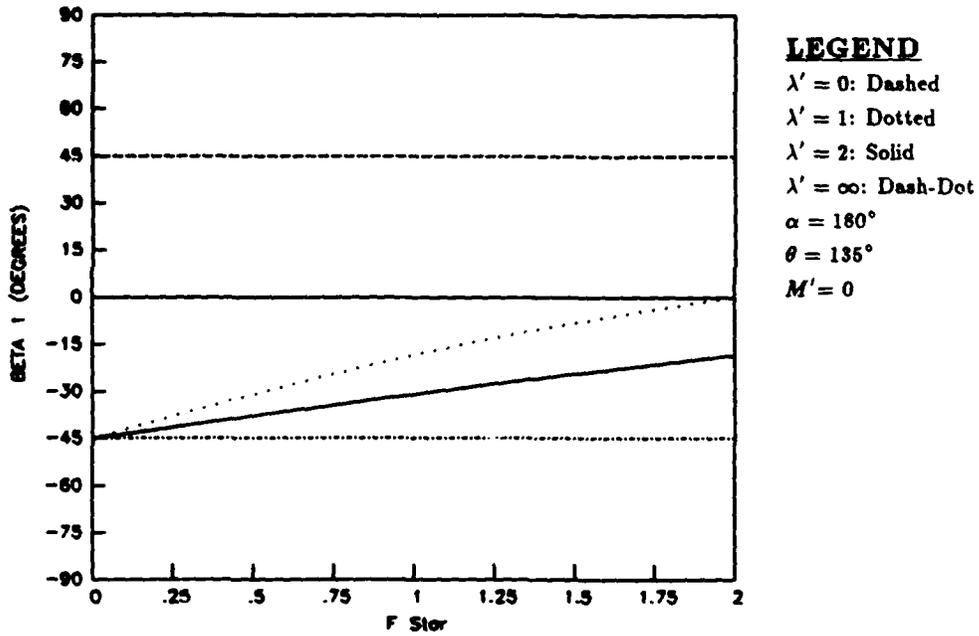
Figure 5.11.   Friction angle at fingertip 1 versus F^*, the ratio of the external force magnitude to the nominal external force magnitude
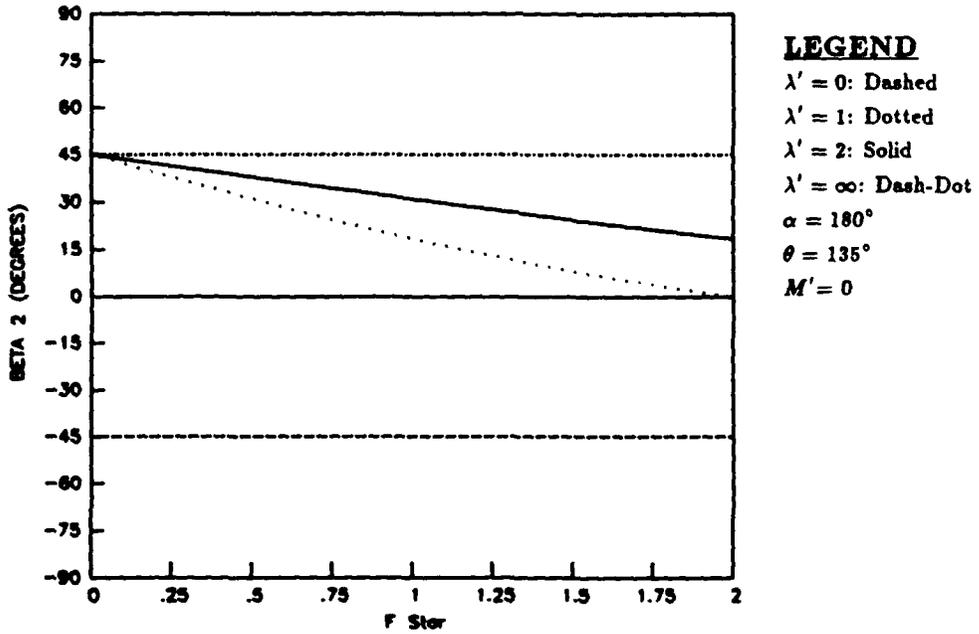

Figure 5.12.   Friction angle at fingertip 2 versus F^*, the ratio of the external force magnitude to the nominal external force magnitude

the object was stationary in a zero-gravity field or if it was in a gravity field and resting on some support external to the gripper.

When all non-zero values of λ' coincide at one point on these plots, it indicates that one could 'squeeze' the object as hard as one wanted without changing the friction angle required for an equilibrium grasp. For example, consider a cylindrical object resting on a pedestal support. If only the friction limit constraint is considered for the moment, Figures 5.11 and 5.12 indicate that the object can be grasped with $\theta = 135°$ and increase λ' to any desired value without upsetting the equilibrium or violating the friction limit constraint as long as $\mu_s > 1$. Such a condition allows one to preset λ' before lifting the object, thereby ensuring that a 'firm' grasp is maintained.

One could model the act of quasistatically lifting the object straight up from the support in a uniform downward-acting gravity field, as increasing F^* from an initial value of zero to some final nominal value, F_{ext}^{nom}, which might represent the weight of the object. Consequently, when the object was lifted completely off of the support, F^* would be equal to one. In Figures 5.11 and 5.12, increasing F^* for constant, finite, non-zero λ' results in a reduction of the required friction angle. However, recognize that this characteristic is unique to cradling grasps (i.e. θ between 90° and 180°.) with F^* less than 2. If the plot of β_1 was extended to include F^* greater than 2, the constant λ' lines would cross $\beta = 0°$ and asymptotically approach $\beta = -45°$ as F^* approaches infinity. Since the friction angle limits for this example are $\beta \in (-45° < \beta < 45°)$, for this grasp configuration, there are no finite restrictions on the range of F^* which can be tolerated by the grasp when the friction limit constraint is scrutinized.

The lines in the figures for $\lambda' = 0$ have specific physical meanings. When $\lambda' = 0$, the contact force vector, $\vec{C}$, consists entirely of the particular solution, $\vec{C}_p$. When $\alpha = 180°$ and $M' = 0$, the load is symmetric which means that $\vec{C}_{1p}$ and $\vec{C}_{2p}$ must be directed along the y_o-axis to oppose $\vec{F}_{ext}$ no matter what magnitude F_{ext} takes on. One can easily verify that if the contact forces are directed along the y_o-axis, that the friction angles must be 45° and -45° at fingertips one and two, respectively. This is consistent with the known directions of $\vec{C}_{1p}$ and $\vec{C}_{2p}$.

5-15

5.2.2 CRUSH LIMIT CONSTRAINT. To examine the effect of varying F_{ext} on the crush limit constraint, recall the expression for the normal contact forces as given by Eq (5.10)

$$C'_n = \frac{C_n}{F_{ext}^{nom}} = \lambda' \sin \theta - 0.5 F^* \cos \theta \tag{5.13}$$

Because the nominal load is symmetric, the normalized contact normal forces at fingertips 1 and 2 are equal so they are both referred to as C'_n. The requirement to prevent crushing the object is that C'_n must remain less than the $C'_{n_{max}}$ that was defined in Eq (4.15). Therefore, the following inequality constraint equation must be obeyed:

$$C'_n = \lambda' \sin \theta - 0.5 F^* \cos \theta \le C'_{n_{max}} \tag{5.14}$$

This can be rewritten as

$$- F^* \cos \theta \le 2(C'_{n_{max}} - \lambda' \sin \theta) \tag{5.15}$$

Since Eq (5.15) is linear in F^*, it can solved for the bounds on F_{ext}. Care must be taken to ensure that the proper sign of $\cos \theta$ is used when solving for F^* because the direction of the equality will change depending on the sign of $\cos \theta$ when dividing both sides by it.

When $\theta \in (0 \le \theta < 90°)$ it is a palming grasp[2] and the $\cos \theta$ will be positive so the crush limit constraint is

$$F^* \ge 2(\lambda' \tan \theta - C'_{n_{max}} \sec \theta) \qquad (0 \le \theta < 90°) \tag{5.16}$$

Eq (5.16) implies that there is a minimum value of F^* which corresponds to the crush limit for a palming grasp. Intuition tells one that, for a palming grasp, increasing F_{ext} will tend to pull the object from the grasp and cause the normal forces to decrease. Decreasing F_{ext}, on the other hand, will increase the magnitudes of the normal contact forces. Therefore, for a palming grasp there is a lower bound on F^* and there is no upper bound based on the crush limit. This behavior is accurately represented in Eq (5.16).

---

[2]See Section 3.2.1 for definition of palming grasp.

When $\theta \in (90° < \theta \leq 180°)$ there is a cradling grasp[3] and $\cos\theta$ will be negative so the crush limit constraint is

$$F^* \leq 2(\lambda' \tan\theta - C'_{n_{max}} \sec\theta) \qquad (90° < \theta \leq 180°) \qquad (5.17)$$

Eq (5.17) implies that there is a maximum value of F^* which corresponds to the crush limit in a cradling grasp. Intuition tells one in the case of a cradling grasp that increasing F_{ext} will tend to press the object into the fingers and cause the normal forces to increase. Decreasing F_{ext}, on the other hand, will decrease the magnitudes of the normal contact forces. Therefore, for a cradling grasp there is an upper bound on F^* and the lower bound is zero, based on the crush limit. Eq (5.17) accurately represents this type of behavior.

In the example grasp under analysis, $\theta = 135°$, $\lambda' = 1$, and $C'_{n_{max}} = 1.5$. Since $\theta = 135°$ is a cradling grasp, these values are substituted into Eq (5.17) and the bounding F^* is found to be

$$F^* \leq 2.243$$

This tells one that F_{ext} can more than double and the structural limits of the object will not be exceeded while trying to maintain an equilibrium grasp.

5.2.3 TORQUE LIMIT CONSTRAINT.
Evaluating the torque limit constraint tolerance of a grasp configuration subjected to changes in the magnitude of F_{ext} will be done in a fashion similar to the analysis of the crush limit constraint in the preceding section. Begin by recalling the expressions for the homogeneous and particular solutions of the finger joint torque vector from Eqs (3.142) and (3.143) in Section 3.7 which are repeated here for convenience:

$$\vec{\tau}_p = \frac{F_{ext}}{2} \left\{ \begin{array}{c} l_{11}\cos\zeta_1 + l_{12}\cos\zeta_{12} \\ l_{12}\cos\zeta_{12} \\ l_{21}\cos\zeta_4 + l_{22}\cos\zeta_{45} \\ l_{22}\cos\zeta_{45} \end{array} \right\} \qquad (5.18)$$

---

[3]See Section 3.2.1 for a definition of a cradling grasp.

$$\vec{\tau}_h = \lambda \left\{ \begin{array}{c} -l_{11} \sin \zeta_1 - l_{12} \sin \zeta_{12} \\[2mm] -l_{12} \sin \zeta_{12} \\[2mm] l_{21} \sin \zeta_4 + l_{22} \sin \zeta_{45} \\[2mm] l_{22} \sin \zeta_{45} \end{array} \right\} \tag{5.19}$$

where the ζ's are defined in Eqs (3.144) through (3.147).

To form the vector of dimensionless torque parameters as defined in Eq (4.22) and used in Eq (4.23), one must sum the expressions in Eqs (5.18) and (5.19) and divide the result by F_{ext}^{nom}. Doing so, and introducing the definition of F^* given by Eq (5.5), yields

$$\vec{\tau}' = \left\{ \begin{array}{c} -\lambda'\left(l_{11} \sin \zeta_1 + l_{12} \sin \zeta_{12}\right) + 0.5F^*\left(l_{11} \cos \zeta_1 + l_{12} \cos \zeta_{12}\right) \\[2mm] -\lambda'l_{12} \sin \zeta_{12} + 0.5F^*l_{12} \cos \zeta_{12} \\[2mm] \lambda'\left(l_{21} \sin \zeta_4 + l_{22} \sin \zeta_{45}\right) + 0.5F^*\left(l_{21} \cos \zeta_4 + l_{22} \cos \zeta_{45}\right) \\[2mm] \lambda'l_{22} \sin \zeta_{45} + 0.5F^*l_{22} \cos \zeta_{45} \end{array} \right\} \tag{5.20}$$

In order not to violate the torque limit constraint, one must satisfy the following inequalities:

$$\vec{\tau}' \le \vec{\tau}'_{max} = \left\{ \begin{array}{c} \tau'_{1max} \\[2mm] \tau'_{2max} \\[2mm] \tau'_{4max} \\[2mm] \tau'_{5max} \end{array} \right\} \tag{5.21}$$

where, in general, the torque limit of each finger joint may be different. If the bounding value of F^* for the ith joint is represented as F_i^*, then one can solve Eq (5.21) for the F_i^*. The bounding F^* for the grasp would be the most restrictive F_i^* that is found to be positive and simultaneously satisfies all of the inequalities in Eq (5.21). The requirement for F^* to be positive can be expressed as a fifth inequality relationship which must be simultaneously satisfied:

$$F^* \ge 0 \tag{5.22}$$

The inequalities in Eq (5.21) can be rewritten as

$$F_1^* \left(l_{11} \cos \zeta_1 + l_{12} \cos \zeta_{12}\right) \le 2\left[\tau'_{1max} + \lambda'\left(l_{11} \sin \zeta_1 + l_{12} \sin \zeta_{12}\right)\right] \tag{5.23}$$

$$F_2^* \left(l_{12} \cos \zeta_{12}\right) \le 2\left[\tau'_{2max} + \lambda'\left(l_{12} \sin \zeta_{12}\right)\right] \tag{5.24}$$

5-18

$$F_4^* \left(l_{21} \cos \zeta_4 + l_{22} \cos \zeta_{45} \right) \leq 2 \left[\tau'_{4max} + \lambda' \left(l_{21} \sin \zeta_4 + l_{22} \sin \zeta_{45} \right) \right] \qquad (5.25)$$

$$F_5^* \left(l_{22} \cos \zeta_{45} \right) \leq 2 \left[\tau'_{5max} + \lambda' \left(l_{22} \sin \zeta_{45} \right) \right] \qquad (5.26)$$

The signs of the parenthetical terms on the left hand sides of Eqs (5.23) through (5.26) are dependent on the configuration of the grasp. In solving for the F_i^*, the direction of the inequality must be reversed if the parenthetical quantity is negative for the ith joint. These parenthetical quantities are equal to the X_p-components of the position vectors pointing from the ith joint to the tip of the finger. Therefore, referring to Figure 3.10, whenever the fingertip is to the left of the ith joint, the parenthetical quantity will be negative and the direction of the inequality must be reversed when solving for F_i^*.

To determine the range of tolerable variations of F_{ext}, one must solve the four inequalities in Eqs (5.23) through (5.26) for the F_i^* and take the intersection of their solution spaces with the solution space of Eq (5.22).

For the example grasp problem under analysis, the inverse kinematic solution results in

$$\zeta_1 = 147.88°$$

$$\zeta_{12} = 6.59°$$

$$\zeta_4 = 32.12°$$

$$\zeta_{45} = 173.41°$$

Using these joint angles, $\lambda' = 1$, $l_{11} = l_{12} = l_{21} = l_{22} = 1$, and $\tau'_{max} = 1$ for all joints, yields

$$F_1^*(0.146) \leq 3.293$$

$$F_2^*(0.993) \leq 2.230$$

$$F_4^*(-0.146) \leq 3.293$$

$$F_5^*(-0.993) \leq 2.230$$

Solving these equations for their corresponding F^*'s results in

$$F_1^* \leq 22.485$$

$$F_2^* \leq 2.244$$

$$F_4^* \geq -22.485$$

$$F_5^* \geq -2.244$$

Simultaneous consideration of all F^* for this example indicates that, based on the torque limit constraint, the grasp can only tolerate variations in the magnitude of the external load wrench within the bounds defined by

$$F_{ext} \in (0 \leq F_{ext} \leq 2.244 F_{ext}^{nom})$$

while maintaining an equilibrium grasp.

5.3 CHANGES IN THE EXTERNAL LOAD MOMENT

Applying a nonzero moment to the object will cause a change in the equilibrium requirements for a grasp. In Chapter IV candidate values for θ and λ' were selected by analyzing the nominal load requirements of a grasp. In this section the tolerance of the grasp characterized by the candidate values of θ and λ' to the presence of a non-zero external load moment will be examined. The requirements of the grasp will be analyzed in terms of each of the three constraints individually.

The nominal external moment on the object was taken as zero for the analysis conducted in Chapter IV so introducing a non-zero M' constitutes a variation in the external load moment. To facilitate this exploration of the effect of variations in the external load moment on grasp equilibrium, a dimensionless parameter, M^*, is defined as

$$M^* \equiv \frac{M_{ext}}{r F_{ext}^{nom}} = \frac{M'}{r} \tag{5.27}$$

where r is the radius of the object. By defining this parameter some physical insight has been fabricated into its meaning. One can interpret M^* to be related to the moment arm of an equivalent force couple where the two forces have magnitudes equal to F_{ext}^{nom}. With this insight, M^* is equal to the moment arm of the force couple expressed as a fraction of the object radius. Therefore, an M^* of one could be thought of as corresponding to a couple consisting of two parallel, opposing forces, F_{ext}^{nom}, separated by a perpendicular distance equal to r.

5.3.1 FRICTION LIMIT CONSTRAINT.

Equation (3.39) gives the expression for the total contact force vector in its most general form. The normal and tangential components are repeated here for convenience.

$$\vec{C} = \frac{F_{ext}}{2r\sin\theta} \left\{ \begin{array}{c} 2r\lambda'\sin^2\theta + r\cos\alpha\,\sin\theta\,\cos\theta + r\sin\alpha - M'\cos\theta \\ 2r\lambda'\sin\theta\,\cos\theta - r\cos\alpha\,\sin^2\theta + M'\sin\theta \\ 2r\lambda'\sin^2\theta + r\cos\alpha\,\sin\theta\,\cos\theta - r\sin\alpha + M'\cos\theta \\ -2r\lambda'\sin\theta\,\cos\theta + r\cos\alpha\,\sin^2\theta + M'\sin\theta \end{array} \right\} \tag{5.28}$$

where

$$M' = \frac{M_{ext}}{F_{ext}^{nom}} \tag{5.29}$$

If M^* from Eq (5.27) and $\alpha = 180°$ are substituted into Eq (5.28), it reduces to

$$\vec{C} = \frac{F_{ext}}{2\sin\theta} \left\{ \begin{array}{c} 2\lambda'\sin^2\theta - \sin\theta\,\cos\theta - M^*\cos\theta \\ 2\lambda'\sin\theta\,\cos\theta + \sin^2\theta + M^*\sin\theta \\ 2\lambda'\sin^2\theta - \sin\theta\,\cos\theta + M^*\cos\theta \\ -2\lambda'\sin\theta\,\cos\theta - \sin^2\theta + M^*\sin\theta \end{array} \right\} \tag{5.30}$$

The expressions for the friction angles at fingertips one and two are formed by selecting the appropriate components from Eq (5.30). The result is

$$\beta_1 \equiv \frac{C_{1t}}{C_{1n}} = \frac{2\lambda'\sin\theta\,\cos\theta + \sin^2\theta + M^*\sin\theta}{2\lambda'\sin^2\theta - \sin\theta\,\cos\theta - M^*\cos\theta} \tag{5.31}$$

$$\beta_2 \equiv \frac{C_{2t}}{C_{2n}} = \frac{-2\lambda'\sin\theta\,\cos\theta - \sin^2\theta + M^*\sin\theta}{2\lambda'\sin^2\theta - \sin\theta\,\cos\theta + M^*\cos\theta} \tag{5.32}$$

One can plot Eq (5.31) and (5.32) for various values of λ' as functions of F^* to explore the equilibrium requirements of a grasp characterized by θ. The plot information is evaluated in the same way as the nominal friction limit constraint plots were evaluated. All M^* having a friction angle within the bounds of $\pm\beta_{max} = \pm\arctan\mu_s$ are tolerable external moment loads as far as the friction limit constraint is concerned.

If the data for the example grasp nominal conditions given in Section 4.4 are plotted, Figures 5.13 and 5.14 result.

One immediately notices the discontinuity in the plots for $\lambda' = 0$. As was seen in the analysis of the grasp for a nominal load, this discontinuity is due to a direction
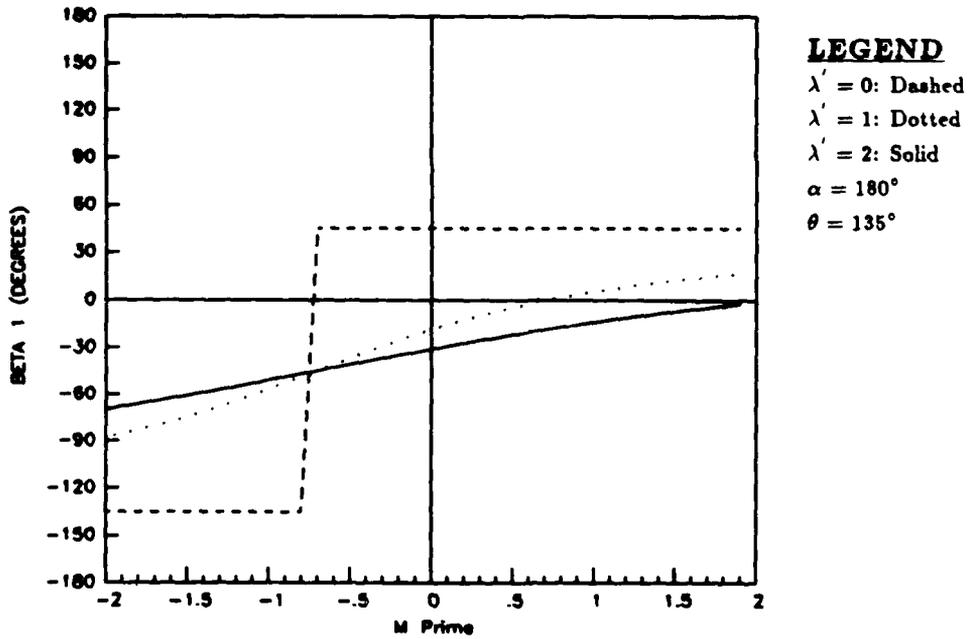
Figure 5.13. Friction angle at fingertip 1 versus M^*, the variation in the moment of the external load
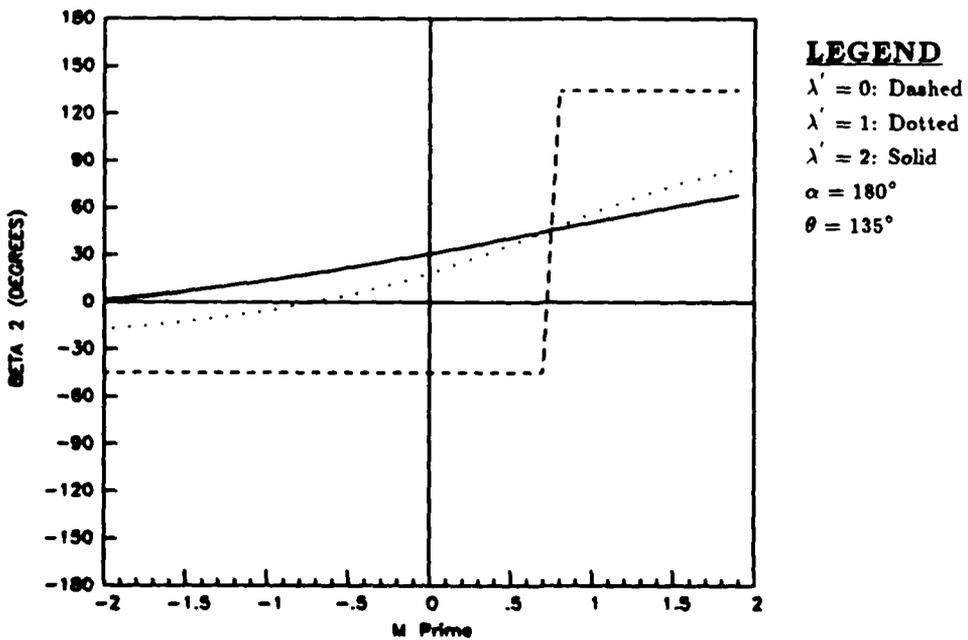

Figure 5.14. Friction angle at fingertip 2 versus M^*, the variation in the moment of the external load

change in the contact forces. In the case of this example, the discontinuity in β_1 occurs when $M^* = -0.707$ because that is when the tangential force required to equilibrate the moment is exactly equal and opposite to the tangential force of the nominal-load particular solution contact force for fingertip one. Therefore, the tangential contact force is zero at this value of M^*. In general, a geometric analysis reveals that the discontinuity of $\lambda' = 0$ will occur at $M^* = -\sin\theta$ for β_1 and at $M^* = \sin\theta$ for β_2.

The reason that the β are constant for $\lambda' = 0$ is that, when there can be no interaction force, the directions of the resultant contact forces at the fingertips cannot change unless the direction of F_{ext} changes. Since presently only changes in the external moment are to be considered, the direction of $\vec{F}_{ext}$ must remain at $\alpha = 180$ degrees. Thus, for equilibrium, the contact forces can have no components in the x_o-direction. It follows then, if the tangential force component changes magnitude to compensate for the external moment, then the normal force component must change proportionally as well. Hence, the friction angle remains constant until the two contact force components change sign simultaneously. This occurs at the point where the external moment requires a change in the tangential force that exactly cancels the tangential force of the grasp that was required at $M^* = 0$. At this point, the particular solution contact force vector at fingertip one, $\vec{C}_{1p}$, is equal to zero.

Figure 5.13 shows that this point is also a crossover point for all values of λ'. Since $\vec{C}_{1p}$ is equal to zero when $M^* = -0.707$, a non-zero λ' produces $\vec{C}_1 = \vec{C}_{1h}$ which must be directed along the x_o-axis. For such a force, β_1 must equal $-45°$ no matter what its magnitude, λ', may be. Consequently, all λ' curves pass through the point corresponding to $(M^*, \beta_1) = (-0.707, -45°)$.

Figure 5.14 shows trends in the data for fingertip 2 that are equivalent to those discussed for fingertip 1. However, the crossover point occurs at a value of M^* which is the negative of the value at which the crossover occurred for fingertip 1 (i.e. $M^* = 0.707$.)

Aside from the foregoing interpretation of the physical phenomenon associated with the features of Figures 5.13 and 5.14, one can also determine the limits of tolerable M^*. Since the allowable bounds on the friction angle for the example grasp are $\pm 45°$ one

can determine from consideration of both the β_1 and the β_2 plots that the friction limit constraint is satisfied for

$$M^* \in (-0.707 \le M^* \le 0.707)$$

This is true, of course, only if an internal grasp force having $\lambda' \ge 1$ is applied. The corresponding limits on the external load moment, M', are

$$M' \in (-0.354 \le M' \le 0.354)$$

5.3.2   CRUSH LIMIT CONSTRAINT. The crush limit constraint states that in order to keep from deforming the object structure, the normal contact forces must be kept below some maximum value given by Eq (4.15). This condition can be expressed as

$$\vec{C}'_n \le \vec{C}'_{n_{max}} \tag{5.33}$$

The vector notation is used to denote that there are actually two independent inequality constraints which must simultaneously be met in order for the crush limit constraint not to be violated. In general, the $C'_{n_{max}}$ can vary from point to point on the surface of the object, and it may in fact be a function of θ. One would have to perform a structural analysis or make conservative estimates to obtain $C'_{n_{max}}$ at the two contact points.

To obtain $\vec{C}'_n$ the first and third components are selected from the vector $\vec{C}$ given in Eq (5.30) and divided by F_{ext} to get

$$C'_{1n} = \lambda' \sin\theta - 0.5\cos\theta - 0.5M^* \cot\theta \tag{5.34}$$

$$C'_{2n} = \lambda' \sin\theta - 0.5\cos\theta + 0.5M^* \cot\theta \tag{5.35}$$

From the form of Eqs (5.34) and (5.35), it is clear that the relationships between the normal forces and M^* will be linear. Both functions will intersect the C'_n-axis at $C'_n = \lambda'\sin\theta - 0.5\cos\theta$. A plot of C'_{1n} versus M^* would have a slope equal to $(-0.5\cot\theta)$ while a plot of C'_{2n} would have a slope equal to $(0.5\cot\theta)$. From this information, one can solve these linear equations for the bounding values of M^*. Substituting Eqs (5.34) and (5.35) into Eq (5.33), yields the following inequality constraints:

$$\lambda' \sin\theta - 0.5\cos\theta - 0.5M^* \cot\theta \le C'_{n_{max}} \tag{5.36}$$

$$\lambda' \sin\theta - 0.5\cos\theta + 0.5M^* \cot\theta \le C'_{n_{max}} \tag{5.37}$$

If the terms with M^* are isolated on the left hand sides, Eqs (5.36) and (5.37) become

$$-0.5M^* \cot\theta \quad \le \quad C'_{n_{max}} - \lambda' \sin\theta + 0.5\cos\theta \tag{5.38}$$

$$0.5M^* \cot\theta \quad \le \quad C'_{n_{max}} - \lambda' \sin\theta + 0.5\cos\theta \tag{5.39}$$

which can be combined into a single inequality given by

$$|M^*| \le |2\tan\theta(C'_{n_{max}} - \lambda' \sin\theta) + \sin\theta| \tag{5.40}$$

From Eq (5.40) it is clear that the upper and lower bounds on M^* are equal in magnitude and opposite in direction for the crush limit constraint. This is primarily due to the fact that $M' = 0$ for the nominal condition. In this case then, only a single number need be calculated when defining the range of M^* which are tolerable for a grasp.

For the example grasp, the maximum C'_n was given as 1.5 and the grasp configuration (as determined by a nominal load analysis) had $\theta = 135°$ and $\lambda' = 1$. When these values are inserted into Eq (5.40), the results show that the grasp can tolerate M^* given by

$$|M^*| \le 0.879$$

without violating the crush limit constraint. The corresponding limits on the external load moment, M', are

$$M' \in (-0.439 \le M' \le 0.439)$$

5.3.3 TORQUE LIMIT CONSTRAINT.

The torques required in the finger joints will vary as the external moment on the object varies. Since the finger joint actuators have physical limitations as to their maximum outputs, one must examine the torque requirements for varying M^* in light of the torque limit constraint.

The global hand Jacobian matrix that was derived in Section 3.5 for a gripper with two, three-link fingers can be reduced to apply for a gripper with two, two-link fingers by assigning zero to lengths of the most distal links and eliminating the resulting zero rows and columns to yield a 2x2 matrix. If this is done to the expression given in Eq (3.131)

for the transpose of the global hand Jacobian matrix, the result is

$$\mathcal{J}^T = \begin{bmatrix} j_{111} & j_{121} & 0 & 0 \\ j_{112} & j_{122} & 0 & 0 \\ 0 & 0 & j_{211} & j_{221} \\ 0 & 0 & j_{212} & j_{222} \end{bmatrix} \tag{5.41}$$

where

$$j_{111} = -(l_{11} \sin \phi_1 + l_{12} \sin \phi_{12}) \sin (\theta + \psi) -$$
$$(l_{11} \cos \phi_1 + l_{12} \cos \phi_{12}) \cos (\theta + \psi) \tag{5.42}$$

$$j_{112} = -l_{12} \sin \phi_{12} \, \sin (\theta + \psi) - l_{12} \cos \phi_{12} \, \cos (\theta + \psi) \tag{5.43}$$

$$j_{121} = -(l_{11} \sin \phi_1 + l_{12} \sin \phi_{12}) \cos (\theta + \psi) +$$
$$(l_{11} \cos \phi_1 + l_{12} \cos \phi_{12}) \sin (\theta + \psi) \tag{5.44}$$

$$j_{122} = -l_{12} \sin \phi_{12} \, \cos (\theta + \psi) + l_{12} \cos \phi_{12} \, \sin (\theta + \psi) \tag{5.45}$$

$$j_{211} = (l_{21} \sin \phi_4 + l_{22} \sin \phi_{45}) \sin (\theta - \psi) -$$
$$(l_{21} \cos \phi_4 + l_{22} \cos \phi_{45}) \cos (\theta - \psi) \tag{5.46}$$

$$j_{212} = l_{22} \sin \phi_{45} \, \sin (\theta - \psi) - l_{22} \cos \phi_{45} \, \cos (\theta - \psi) \tag{5.47}$$

$$j_{221} = -(l_{21} \sin \phi_4 + l_{22} \sin \phi_{45}) \cos (\theta - \psi) -$$
$$(l_{21} \cos \phi_4 + l_{22} \cos \phi_{45}) \sin (\theta - \psi) \tag{5.48}$$

$$j_{222} = -l_{22} \sin \phi_{45} \, \cos (\theta - \psi) - l_{22} \cos \phi_{45} \, \sin (\theta - \psi) \tag{5.49}$$

To compute the joint torque vector, substitute the contact force vector given by Eq (5.30) and the transpose of the global hand Jacobian given by Eq (5.41) into

$$\vec{\tau} = \mathcal{J}^T \, \vec{C} \tag{5.50}$$

In order to compute $\mathcal{J}^T$ one must use the same inverse kinematic solution as was given in Section 3.7 to produce the finger joint angles. In keeping with the previous analysis, a vector of normalized joint torques is defined by

$$\tau_i' \equiv \frac{\tau_i}{aF_{ext}} \tag{5.51}$$

5-26

In light of Eq (5.51), Eq (5.50) can be modified to give

$$\vec{\tau}' = \frac{1}{a}\mathcal{J}^T \vec{C}' \qquad (5.52)$$

where $\vec{C}'$ is defined as $(1/F_{ext})\vec{C}$.

Since the contact force vector given by Eq (5.30) is an explicit function of M^*, one can easily calculate the vector of contact forces for a given M^* and substitute it into Eq (5.52) to get the vector of joint torques for varying values of M^*. One could symbolically derive the explicit expressions for the joint torques as functions of M^* using a symbolic mathematical manipulation programming tool such as MACSYMA [VAX85], however, such a derivation was beyond the schedule of this thesis.

The torque limit constraint can be written as the following vector relationship which is essentially a set of four inequality constraints:

$$\vec{\tau}' \le \vec{\tau}'_{max} \qquad (5.53)$$

If one had symbolic expressions for the joint torques as functions of M^*, one could symbolically manipulate them to isolate M^*, thereby yielding explicit expressions for the range of tolerable M^* for each finger joint. The solution space for the grasp limits of tolerable M^* would be the intersection of the four solution spaces given in Eq (5.53).

Instead of solving the equations symbolically, one could numerically calculate the joint torque vector for the grasp and load configuration of interest and plot the joint torques as functions of M^*. One could then identify the limits of M^* which do not violate the torque limit constraint from the plots. Those limits would be given by the range of M^* for which all of the joint torques simultaneously remain below their corresponding maximum joint torques, τ'_{max}.

The data for the example grasp under study have been plotted in Figures 5.15 through 5.18 for M^* ranging from -2 to 2. The figures indicate that the finger joint torques vary linearly with M^*. If the symbolic solution was computed as outlined above, the results would be expressions that clearly showed a linear relationship. This notion can be reinforced by examining the linearity in Eqs (5.30) and (5.52). The contact force vector can be thought of as the sum of a constant portion and a portion dependent on M^*. The

Figure 5.15.   Dimensionless torque of joint 1 versus M^*, the variation in the moment of the external load
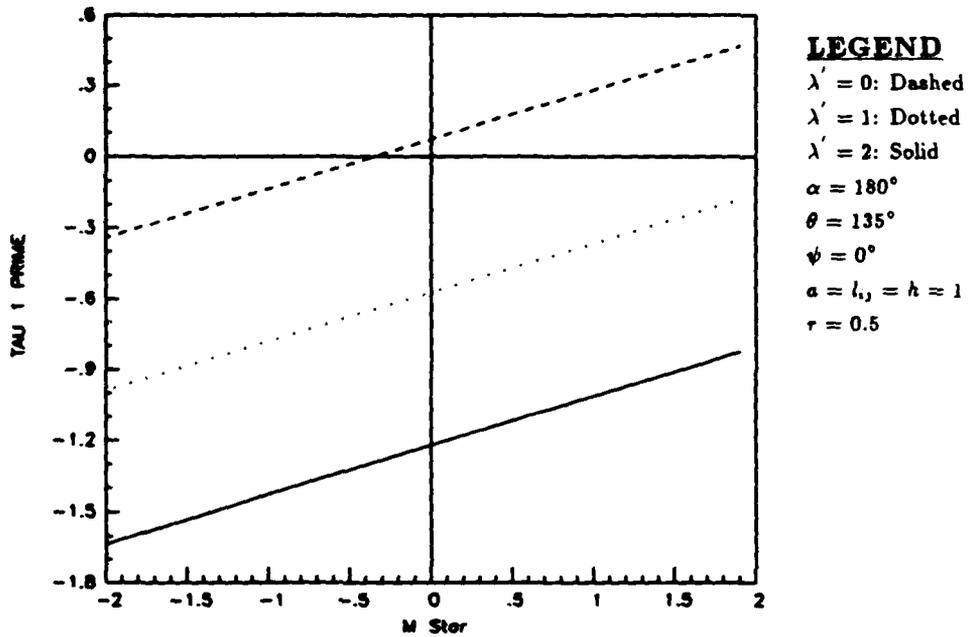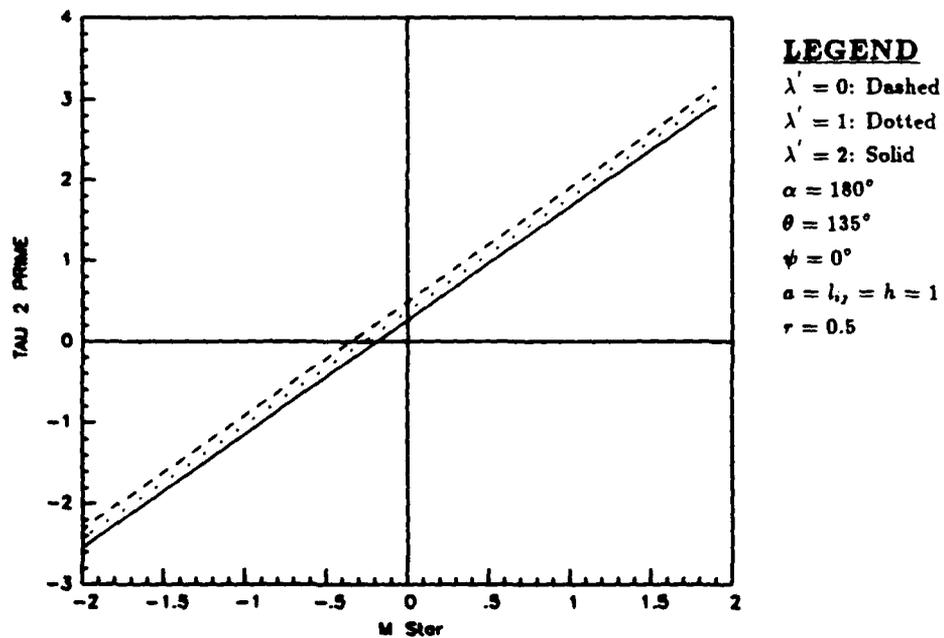

Figure 5.16.   Dimensionless torque of joint 2 versus M^*, the variation in the moment of the external load
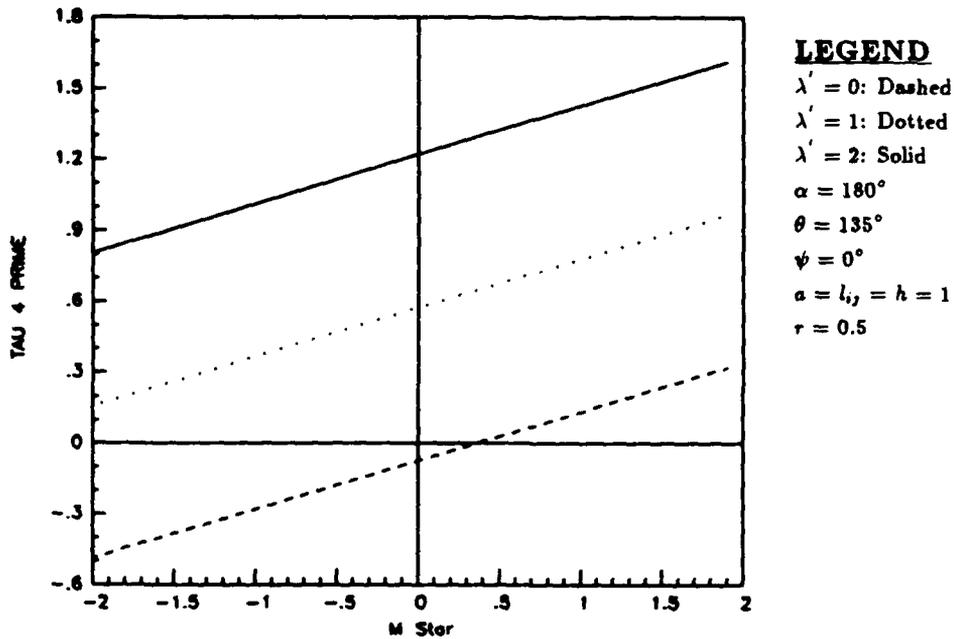
Figure 5.17. Dimensionless torque of joint 4 versus M^+, the variation in the moment of the external load
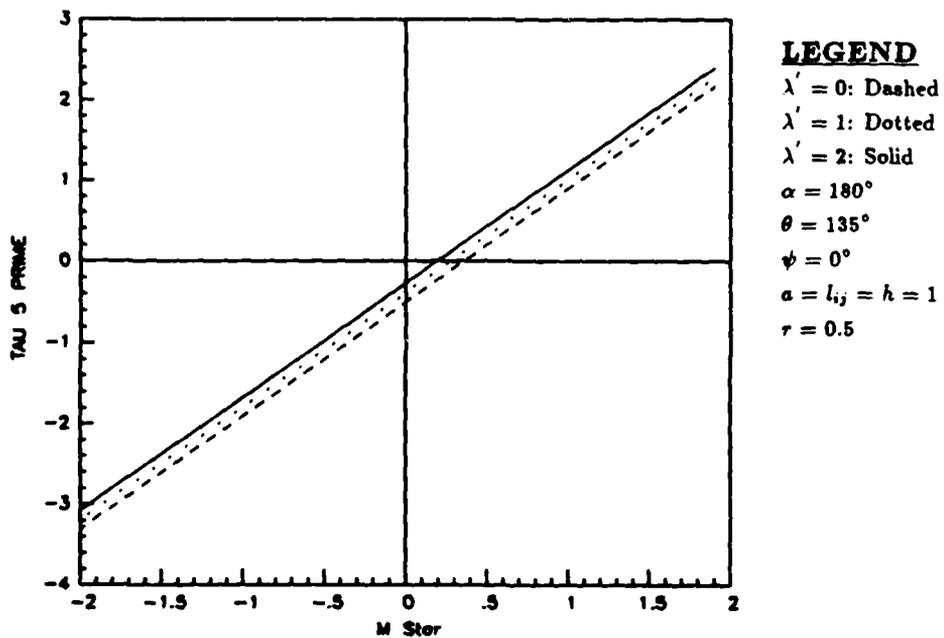

Figure 5.18. Dimensionless torque of joint 5 versus M^+, the variation in the moment of the external load

constant portion of the contact force vector will result in a constant torque offset for each joint at $M^* = 0$. The variable part of the contact force will give joint torques which are linear with M^*, therefore, the total torque at each joint will vary linearly with M^*.

The data plotted in Figure 5.15 for $\lambda' = 1$ indicates that, if $\tau'_{max} = 1$, joint 1 can tolerate variations in M^* within the bounds

$$M^* \in (-2 \leq M^* \leq 2+)$$

where, 2+ means some number greater than 2 that is not within our range of concern. From the data in Figure 5.16 the bounds on the tolerable variations are

$$M^* \in (-0.984 \leq M^* \leq 0.440)$$

for joint 2. Figure 5.17 gives bounds for joint 4 as

$$M^* \in (-(-2) \leq M^* \leq 2)$$

where, $-(-2)$ means some number less than -2 that is not within our range of concern. Finally, Figure 5.18 gives the bounds for joint 5 as

$$M^* \in (-0.440 \leq M^* \leq 0.984)$$

Therefore, the composite range of tolerable variation in M^* for the grasp is

$$|M^*| \leq 0.440$$

which corresponds to a range of M' given by

$$|M'| \leq 0.220$$

In this case, the bounds on M^* are symmetric with respect to the nominal load condition because the grasp angle, ψ, is zero. If the grasp was asymmetric[4] the bounds on M^* based on the torque limits would not be symmetric with respect to the nominal load condition.

If one now considers all of the constraints simultaneously for the example grasping problem, we conclude that the range of M^* which we can tolerate without loosing equilibrium is

$$|M^*| \leq 0.440$$

---

[4]An asymmetric grasp is characterised by $\psi \neq 0$ which is not to be confused with an asymmetric load that is characterised by $\alpha = 180°$.

which corresponds to a range on the value of M' defined by

$$|M'| \leq 0.220$$

The most restrictive constraint is the torque limit constraint in this case.

One may have noticed that the range of allowable M^* was symmetric with respect to the nominal M^* for all of the constraints for this example grasp problem. By way of explanation, one should recall that both the grasp and the load were symmetric for the example. In general, when $\alpha \neq 180°$ and/or $\psi \neq 0°$ the composite bounds on the range of tolerable M^* will not be symmetric with respect to $M^* = 0$.

5.4 CHAPTER SUMMARY

In this chapter analytic expressions which can be used to examine a grasp's ability to tolerate variations in the characteristics of the external load wrench were presented. Three types of variations were addressed: magnitude variation, direction variation, and moment variation from the nominal wrench. A method of using the expressions to evaluate the robustness of a grasp was illustrated by an example. One distinct limitation of the illustrated method is that it only considered the three possible modes of variation individually. The method did not look at the cumulative effect of simultaneous variations. Therefore, although the method could be used to determine if the grasp could tolerate some $\Delta \alpha$ or some ΔF_{ext}, or some M', it cannot determine if the grasp can tolerate some $\Delta \alpha$ and some ΔF_{ext}, and some M'. Using such a method, the best that one might be able to do is to generate a pessimistic estimate of whether the grasp would remain in equilibrium by summing the effects of the three individual variations and examining the equilibrium.

To quantify the effects of varying the load direction on the equilibrium requirements of a grasp, data plots similar to those for the nominal load analysis were constructed. In this case, however, α was the independent parameter instead of θ. Consequently, one could say that this method evaluates a candidate grasp described by candidate values for θ and λ'. The candidate values are taken from the nominal load analysis.

In the course of examining the trends in the data plots for <u>direction variations</u> of the external load, the following trends were noted:

5-31

- At external load angles given by $\alpha = (180° - \theta)$ or $\alpha = (360° - \theta)$ the friction angle at fingertip 1 is single-valued for all λ' except zero.

- At external load angles given by $\alpha = \theta$ or $\alpha = (180° + \theta)$ the friction angle at fingertip 2 is single-valued for all λ' except zero.

- The contact normal force magnitude corresponding to a constant λ' varies sinusoidally with α.

- For a constant λ' the magnitude of the contact normal force at fingertip 1 for some α is equal to that of fingertip 2 for $-\alpha$. This implies that the plot of C_{1n} versus α is the mirror image of C_{2n} versus α when it is reflected about $\alpha = 0$.

- The joint torques corresponding to a constant λ' vary sinusoidally with α.

- For a symmetric grasp[5] the joint torque plots for joints 1 and 4 are closely related. The sinusoidal joint torque plots for joints 1 and 4 both have the same peak-to-peak amplitude variations and periods, but have equal and opposite constant offsets from zero torque. A similar relationship holds true for joints 2 and 5.

To quantify the effects of varying the load magnitude on the equilibrium requirements of a grasp, data plots were constructed for the friction limit constraint that were similar to those for the nominal load analysis and the plots for the crush limit and torque limit constraints were bypassed in favor of simple linear expressions. Since an understanding of the influence of variations in F_{ext} was desired, F_{ext} was assigned as the independent variable and λ' was maintained as a parameter. In order to generalize the variation of F_{ext}, a new variable called F^* was defined as the ratio of F_{ext} to its nominal value, F_{ext}^{nom}. The inequality constraint equations were derived as functions of the new free variable, F^*. The crush limit and torque limit inequality constraint equations turned out to be explicitly linear functions of F^* so the bounds on F^* were determined symbolically instead of using data plots.

While examining the data plots and equations for <u>magnitude variations</u> in the external load, the following points were found to be true:

---

[5]A symmetric grasp is characterised by $\psi = 0°$.

- The friction angles at fingertips 1 and 2 remained equal and opposite while the external force magnitude, F_{ext}, varied.

- When $\lambda' = 0$ or $\lambda' = \infty$, the friction angle is a constant for all F^*.

- For non-zero, finite λ' and θ less than 90°, increasing F^* from zero to 2 increases the friction angle required for grasp equilibrium.

- For non-zero, finite λ' and θ greater than 90°, increasing F^* from zero to 2 reduces the friction angle required for grasp equilibrium.

- For F^* between 0 and 2, the friction angles corresponding to minimum internal grasp force ($\lambda' = 0$) are

$$\beta_{1min} = (180° - \theta) = -\beta_{2min}$$

while the friction angles corresponding to maximum internal grasp force ($\lambda' = \infty$) are

$$\beta_{1max} = (90° - \theta) = -\beta_{2max}$$

Thus, there is a 90 degree band of β for both fingertips which contains all possible λ'.

- For $F^* = 0$, all positive λ' require the same friction angle as given in the previous bullet for $\lambda' = \infty$. Therefore, prior to picking up an object resting on a support, friction will allow one to preset λ' to any value without disturbing the object, as long as that common friction angle is within the friction limit constraint.

- The bounding values of F^* for the crush limit constraint were found to be linear functions of the grasp angle, θ, the selected internal grasp force magnitude, λ', and the maximum normalized normal contact force, $C'_{n_{max}}$.

- For θ between 0 and 90 degrees, there is a minimum F^* corresponding to the crush limit constraint, while for θ between 90 and 180 degrees, the bounding F^* is a maximum. The bounding values are given in Eqs (5.16) and (5.17), respectively.

- Based on the torque limit constraint, the range of tolerable F^* is given by the intersection of the solution spaces of five inequality equations given in Eqs (5.22) through (5.26). In general, there is one more inequality equation than there are finger joints because the additional constraint that F^* must be positive is imposed.

- The torque limit constraint inequalities are linear in F^* and can be solved explicitly for the bounding values of F^*. There will be a single bounding value for each joint which may be an upper bound or a lower bound.

- For a symmetric grasp, the upper bounding value of joint 1 will be the negative of the lower bounding value of joint 4. Also, the upper bounding value for joint 2 will be the negative of the lower bounding value of joint 5.

To quantify the effects of varying the load moment from its nominal value of zero, data plots were constructed for the friction limit and torque limit constraints that were similar to those constructed for the nominal load analysis. However, plots for the crush limit constraint were bypassed because the crush limit was found to be an explicitly linear function of M'. To gain an understanding of the influence of variations in M', M' was assigned as the independent variable and λ' was maintained as a parameter. In order to generalize the variation of M', a new variable called M^* was defined as the ratio of M' to the object radius, r. The constraint equations were derived as functions of the new free variable, M^*.

While evaluating the susceptibility of grasp equilibrium to variations in M^*, the following points were found to be true:

- For $\lambda' = 0$, the friction angle at fingertip one has a discontinuity at $M^* = -\sin\theta$ while the friction angle at fingertip two has a discontinuity at $M^* = \sin\theta$. These values of M^* correspond to a zero contact force at the respective fingertips.

- For $\lambda' > 0$, the friction angle plots are single-valued at the same values of M^* which cause discontinuities when $\lambda' = 0$. This is because $\vec{C}_p = 0$ and therefore, $\vec{C} = \vec{C}_h$. Since the direction of $\vec{C}_h$ does not change with varying λ', the friction angle does not change either.

- The range of tolerable variations in M^* can be expressed as a single inequality equation given by Eq (5.40). Since the nominal external load moment was taken as zero, the crush limit constraint is symmetric with respect to $M^* = 0$. Therefore, the grasp can tolerate as much external moment in one direction as it can in the other.

- The bounds on M^* for the joint torque limit constraint could be expressed as a set of linear inequality equations if one were to perform an extensive amount of algebra and trigonometry. One could delegate that task to a symbolic mathematical manipulation program such as MACSYMA [VAX85]. Instead of deriving the explicit symbolic expressions for the joint torques as linear functions of M^*, one could numerically generate data for plotting. The numerical approach was used for this thesis.

- The torque data were, in fact, found to be linear with joints 1 and 4 having equal slopes and joints 2 and 5 having equal slopes for the example grasp.

VI. RESULTS, CONCLUSIONS, AND RECOMMENDATIONS

6.1 RESULTS

In Chapter IV analytic expressions were given which model the equilibrium require-
ments for grasping cylindrical objects confined to planar motion. The expressions represent
the equilibrium requirements in terms of inequality constraints on the allowable frictional
forces, normal contact forces, and the finger joint torques.

The constraining equations for the frictional forces at fingertips 1 and 2 are given
by Eqs (4.8) and (4.9), respectively, which are equal and opposite in sign. In order to
maintain equilibrium between the hand and the object, the static coefficient of friction
must be sufficiently large to support the friction angles given by Eqs (4.8) and (4.9). In
general, the static coefficient of friction may be different for the two fingertip contacts.
By plotting Eqs (4.8) and (4.9) as functions of the grasp angle, θ, and parameterized by
the internal grasp force, λ', one can examine trends in the required friction angles for all
possible grasp configurations of a nominally-loaded object. The friction angle was found
to be linearly related to the grasp angle for a given λ'. A symbolic expression explicitly
revealing the linearity of the friction angle relationship was not derived because of the
transcendental nature of the expression. However, several sets of numerical data were
linearly fit with perfect correlations.

The constraining equation for the crush limit is given by Eq (4.14) for a nominally-
loaded object. Since the normal contact force components are equal when there is a nominal
external load, only one constraint equation is required. One can examine trends in the
required normal contact force component for all possible grasp configurations by plotting
Eq (4.14) as a function of θ and parameterized by λ'. In order to maintain equilibrium
without crushing the object, the normalized contact normal force given by Eq (4.14) must .
be less than the upper bound on the allowable normal force given by Eq (4.15). In general,
the upper bound may be different at each of the two fingertip locations. In fact, the
upper bound may be given as a function of θ. Some applications may not require one
to consider the object crush limit constraint. For example, if the structure of the object
corresponds to normal contact forces which are far beyond the capability of the gripper,

then there is no point in monitoring the crush limit constraint because the finger joint torque limit constraint will always be more dominant. Since one cannot universally exclude the possibility of crushing the object, Eq (4.15) was derived so that it could be used to check the equilibrium normal contact force component magnitudes against an object crush limit value.

The constraining equations for the finger joint torque limits are given by the sum of Eqs (4.24) and (4.25). In order to solve these torque limit equations, one must first use Eqs (4.16) through (4.21) to solve for the finger joint angles. This is due to the configuration dependence of the global hand Jacobian matrix which is part of the relationship between the contact force vector and the vector of finger joint torques. In addition to the grasp variables in Table 4.1 that must be specified to solve for the finger joint torques, one must also specify 'knuckle-in' or 'knuckle-out' because there are two solutions to the inverse kinematic equations. The 'knuckle-out' configuration is favored because it reduces the possibility of finger/object interferences although it does not exclude the possibility.

One can examine trends in the finger joint torque requirements by plotting the sum of Eqs (4.24) and (4.25) as a function of θ and parameterized by λ'. Among other things, such plots reveal the finger joint actuator demands caused by increasing the internal grasp force.

Chapter V examines the consequences of varying the characteristics of the external load from the conditions of a nominal load. The analysis presumes that the object has been grasped and θ is known. In addition, the value of λ' is to remain fixed as the grasp attempts to maintain equilibrium with the object under the influence of the load variations. Constraint equations on allowable friction forces, normal contact forces, and finger joint torques are derived and examined for each variation in the external load. Variations in the magnitude, direction, and moment of the external load are considered. The variations are only considered individually; not cumulatively.

The first external load variation considered was a change in the nominal load direction which is characterized by α taking on values other than 180 degrees. A range of allowable α was found by simultaneous consideration of the three different grasp constraints. Once

6-2

again, however, one may not find it necessary to include all three of the constraints under special circumstances. The equilibrium requirements were found to vary in a sinusoidal fashion as α was varied from $0°$ to $360°$.

A situation where the external load may vary in direction is when an object in a uniform gravity field is picked up and then accelerated horizontally. The horizontal acceleration introduces an inertial force component which, when added to the gravity force, results in the external load varying in direction. The direction of the external load as defined for the analysis would also vary if the orientation of the hand was changed while the external load was constant with respect to an inertial coordinate frame. In either case, the external load would no longer act through the center of the palm of the gripper and the analytic expressions given contain the information necessary to determine the range of variation in external load direction which could be tolerated without the grasp losing equilibrium.

The second external load variation that is considered is a change in the magnitude. The nominal magnitude of the external load is designated by F_{ext}^{nom}. Using F^+ to represent the ratio of the varied magnitude to the nominal magnitude, equations were derived which express the equilibrium constraint requirements as functions of F^+. In keeping with the nominal analysis, the equations were parameterized by λ'. A range of allowable F^+ was found by simultaneous consideration of the three different grasp constraints. The crush limit and finger joint torque limit constraints were found to be explicitly linear with respect to F^+. This linearity allows fast and accurate symbolic solution for the maximum and minimum values of F^+ which can be tolerated by a grasp. The friction angle constraint expression was not found to be linear with respect to F^+ so the equation must be plotted to analyze trends in the data.

A physical situation which corresponds to a variation in the external load magnitude is when an object is picked up off of a spring platform. Before the gripper contacts the object, the magnitude of F^+ can be taken as zero. As the gripper contacts the object and then lifts it using position control, F^+ can be made to slowly (quasistatically) increase. If the nominal value of F_{ext} was taken as the weight of the object, then, when the object was suspended above the spring platform, F^+ would be equal to one. Therefore, by examining

6-3

the equilibrium requirements of a given grasp configuration for F^* between zero and one using the analytic expressions derived in Section 5.2, one can determine if it is possible to lift the given object from the spring platform without losing equilibrium.

The third external load variation which was considered in Chapter V was a change in the moment of the external load. By considering moment variations, one can analyze cylindrical objects whose centers of mass are not coincident with their geometric centers. In this case the moment variation is due to the moment arm of the gravity force about the object center. An additional benefit of considering moment variations is that one adds to the repertoire of the analysis a whole class of problems which includes determining the equilibrium requirements for turning a bolt in a threaded hole. In this case the moment variation is due to the frictional torque caused by the interface of the bolt and the threaded hole. In order to generalize the analysis as much as possible, a dimensionless variable, M^*, was introduced and defined in Eq (5.27). The objective then was to determine the range of M^* which could be tolerated without violating any of the three grasp constraints. Eqs (5.31) and (5.32) are the expressions for β_1 and β_2, respectively, as functions of M^* and represent the friction limit constraint. Because these equations are not explicitly linear in M^*, they were plotted to reveal any possible trends and identify the range of tolerable M^*. On the other hand, the object crush limit constraint equations did turn out to be explicitly linear in M^*, thereby enabling explicit symbolic solution for the bounds on tolerable M^*. The single inequality equation which gives the bounds on M^* for the object crush limit constraint is given in Eq (5.40). The upper and lower bounding M^* based on the crush limit constraint were found to be symmetric with respect to $M^* = 0$. This means that the grasp can maintain equilibrium for the same range of external load moment in both directions about the z-axis.

Symbolic analytic expressions for the finger joint torques as explicit functions of M^* were not derived because the complexity of the expressions became unmanageable by hand. The algebra is not particularly difficult, but it is tedious and prone to error. This is a perfect application for a symbolic mathematical solver as was mentioned in Chapter V. In order to expedite results, the choice was made to solve for the finger joint torques numerically. In this case, numerically means evaluating intermediate values and

then substituting them into subsequent equations rather than carrying large symbolic substitutions. The numerical application here in no way implies an approximation or iteration. When the expressions were evaluated and plotted, they revealed that the finger joint torques are all linear functions of M^*. This realization enables one to compute just two points and then interpolate between them rather than continue to plod through a long numerical algorithm. For application to a real-time algorithm this is important.

6.2 CONCLUSIONS

Analytic expressions which model the equilibrium requirements of grasping cylindrical objects in planar motion with two, two-link robotic fingers have been developed. These expressions include consideration of constraints on the allowable frictional forces, contact normal forces, and finger joint torques. Expressions were derived for grasping an object subjected to a nominal external load wrench and for modeling variations in the magnitude, direction, and moment of the external load from the nominal external load configuration.

6.3 FUTURE WORK

There are many follow-on research areas which might prove fruitful. The most important next step is to generate an index which represents the quality of a grasp and use that index to determine the 'optimal' grasp for a given cylinder/load configuration in a real-time algorithm. If one could develop such an algorithm for the specific conditions under which the derivations of this thesis were conducted, then it would be relatively simple to generalize the method in a step-by-step fashion.

Possibly the first generalizing step would be to generalize the gripper. Initially one should consider grippers having three links per finger rather than two. This would require some refinements in the inverse kinematic solution to resolve the nonuniqueness of the joint angle solution. It would also allow one to choose a configuration which might be best suited to the grasp. In addition, one might want to consider methods for checking the inverse kinematic solution to account for interferences between the object and the fingers as they try to reach for a particular grasp angle.

Another generalization of the gripper might be to add a third contact point between the gripper and the object. The third contact could be an extra fingertip contact or contact between the object and the gripper palm. In either case, one would like to know if there are ranges of the grasp angle for which adding the third contact might degrade the grasp equilibrium. There may also be ranges of the grasp angle for which adding the third contact would enhance the grasp equilibrium. The regions of possible force closure grasps would also be an area of interest if a third contact point was included.

Generalizing the object would constitute another major effort of future research. One could consider elliptical object shapes before proceeding to examine further deviations in object shape. A method of determining whether the object is too large for the gripper to secure an equilibrium grasp would also be an important contribution.

After the hand and the object have been generalized to the extent possible, one should investigate spatial motion rather than planar motion. The extension to spatial motion should be relatively straight-forward because of the inherent power of the linear algebra method of analyzing grasp equilibrium. This step could be taken prior to any or all of the other proposed research steps.

Other issues which remain to be addressed include consideration of multiple contacts between each finger and the object, consideration of various fingertip contact types, and examination of the dynamics encountered when capturing the object.

Although the many topics just mentioned remain to be explored, the techniques presented in this thesis constitute significant steps towards developing real-time algorithms for grasping cylindrical objects. In the course of extending this thesis as outlined above, one should be able to begin demonstrating simplified real-time algorithms which automate the process of grasping. One day we will see versatile, dexterous robotic hands which are as autonomous as our own. It is only a matter of time- tick...tick...tick.

.

Appendix A.

DETAILS OF FORMING TWISTS AND WRENCHES

This appendix presents a detailed geometric description of how to form a twist or a wrench from a given velocity or force state, respectively. It is intended as a layman's interpretation of the material presented by Hunt [Hun78: 47].

A.1 TWIST FORMATION

Any displacement of a body can be described as a screw displacement along a unique screw axis. In the case when the displacement is infinitesimally small, there is an instantaneously defined unique screw axis called an infinitesimal twist about which the body is rotating and along which the body is moving. For gross motion, this infinitesimal twist changes from one instant to another as the body displacement is described by a succession of infinitesimal displacements.

The twist axis in three-space motion is the equivalent of an instantaneous center in planar motion. From planar motion kinematics, we know that if the extent of the body of interest includes the instant center, the point on the body which coincides with the instant center has no translation at that instant in time – it only rotates. In effect, it is the temporary hinge point for the body to rotate about. Similarly, if there is a point on a body in three space that lies on the twist axis, then its motion in the plane perpendicular to the axis is purely rotational at that instant in time. Note, however, that it can translate along the twist axis.

To form an infinitesimal twist, start with a rigid body undergoing an infinitesimal displacement. If we choose an arbitrary point **A** as the origin of our coordinate system, then the infinitesimal displacement can be expressed as an angular displacement, $\delta\vec{\theta}$, about some axis which passes through point **A** and a linear displacement, $\delta\vec{x}$, of a point on the body at the origin. In general, the vectors $\delta\vec{\theta}$ and $\delta\vec{x}$ will not be parallel. However, $\delta\vec{x}$ can be resolved into two components; $\delta\vec{x}^{\perp}$ perpendicular to $\delta\vec{\theta}$ and $\delta\vec{X}$ parallel as shown in Figure A.1. Now, $\delta\vec{\theta}$ can be shifted by some perpendicular directed distance $\vec{r}$ to a line l which is both parallel to $\delta\vec{\theta}$ and in the plane perpendicular to $\delta\vec{x}^{\perp}$ as shown in Figure A.2.
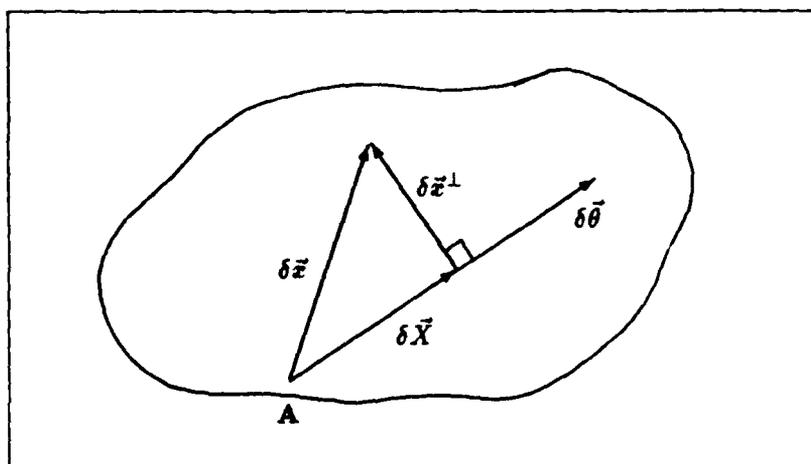
Figure A.1. Resolving $\delta\vec{x}$ into components perpendicular and parallel to $\delta\vec{\theta}$

The shifted angular displacement vector is now called $\delta\vec{\Theta}$ and the vector $\vec{r}$ is chosen so that the displacement $\vec{\Theta} \times \vec{r} = -\delta\vec{x}^{\perp}$ and ,therefore, $\delta\vec{x}^{\perp}$ is canceled. The vector $\delta\vec{\Theta}$ has the same magnitude and direction as $\delta\vec{\theta}$. When $\delta\vec{\Theta}$ is along the line l, the resultant linear displacement, $\delta\vec{X}$, is also parallel to l.

Thus, we have attained a representation which is equivalent to the original displacement and whose vectors, $\delta\vec{\Theta}$ and $\delta\vec{X}$ are parallel.

This representation of the motion is termed an *infinitesimal twist* and it can be denoted in terms of twist coordinates as

$$\mathcal{T} = (t_1, t_2, t_3, t_4, t_5, t_6) \qquad (A.1)$$

where the first three components (t_1, t_2, t_3) constitute the angular displacement, $\vec{\Omega}$, of the body while the last three components (t_4, t_5, t_6) constitute the linear displacement, $\vec{V}$, of a point on the body at the origin of the coordinate system.

A.2 WRENCH FORMATION

Consider a single rigid body in any arbitrary external force and moment state as shown in Figure A.3. Let the forces on the body be called $\mathbf{F}_i$ where $i = 1, 2, \ldots, n$ and the moments be called $\mathbf{M}_j$ where $j = 1, 2, \ldots, m$. Choose an arbitrary point, $\mathbf{A}$, on the body and shift all of the externally applied forces to act through that point. According
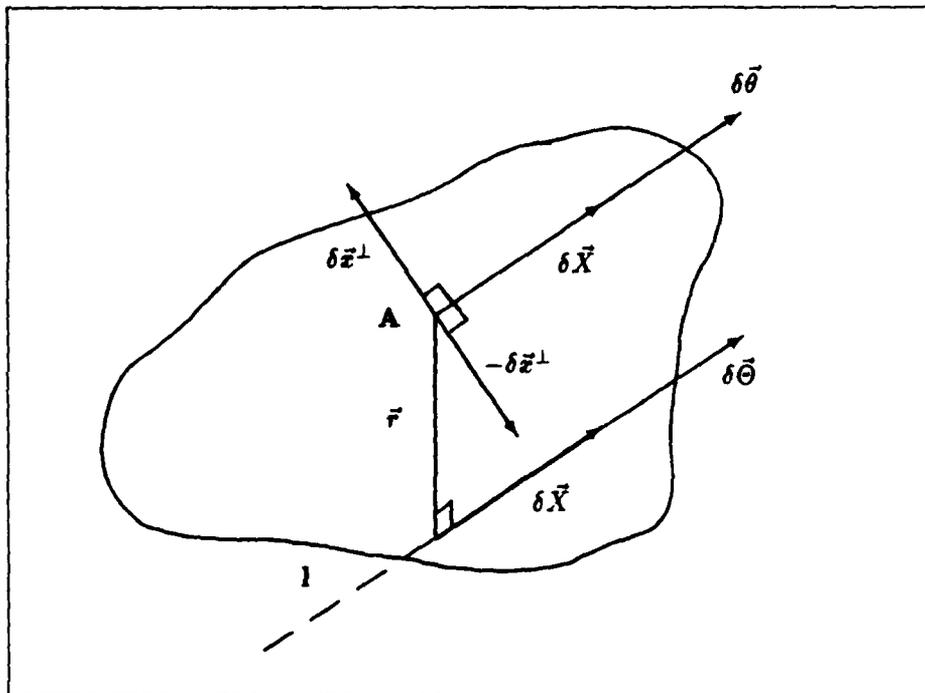
Figure A.2. Shifting $\delta\vec{\theta}$ so as to cancel $\delta\vec{x}^{\perp}$
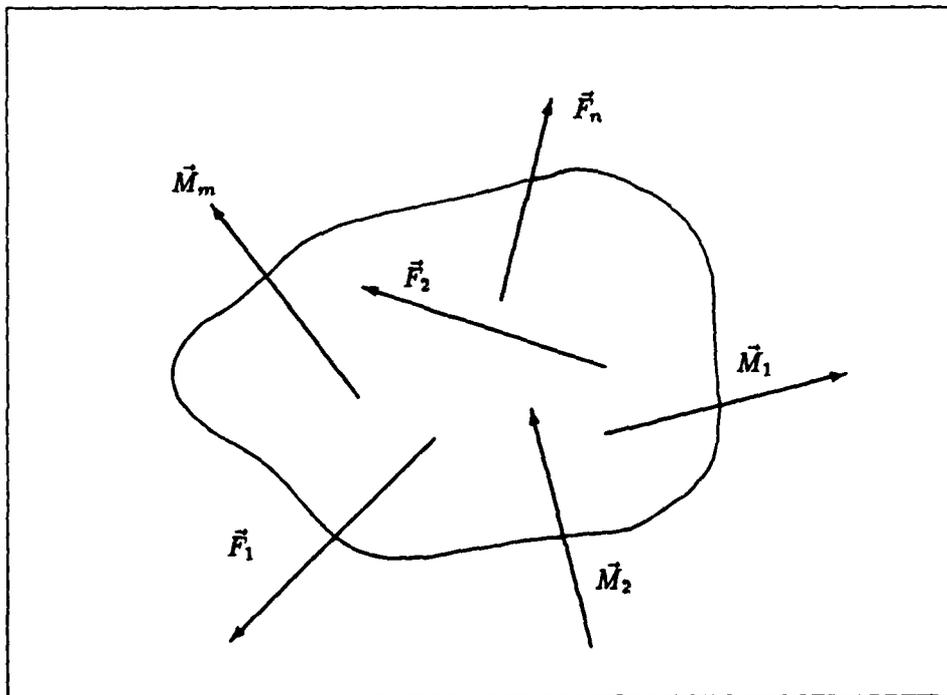

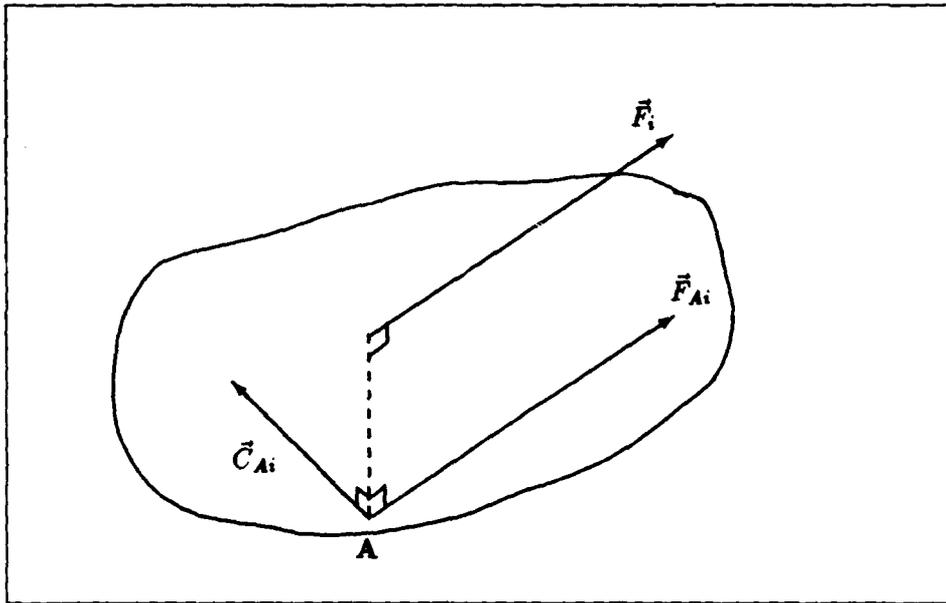Figure A.3. Rigid body in an arbitrary external force and moment state

Figure A.4.   Additional moments are required to compensate for shifting
              forces to act through point A

to elementary statics, in order to preserve the original force and moment state when the
forces are shifted to act through point **A**, additional moments must be applied to the body
to compensate for new moment arms of the new forces $\mathbf{F}_{Ai}$ as shown in Figure A.4. Call
the vector sum of these additional moments $\mathbf{C}_A$, and let $\mathbf{F}_A$ be the vector sum of all $\mathbf{F}_{Ai}$.

If the induced moment $\mathbf{C}_A$ and all of the externally applied moments $\mathbf{M}_i$ are summed,
the result is a net moment vector, $\mathbf{M}_A$, through point **A** as shown in Figure A.5. In
general, $\mathbf{F}_A$ and $\mathbf{M}_A$ are not parallel. However, $\mathbf{M}_A$ can be resolved into two components;
M parallel to $\mathbf{F}_A$, and $\mathbf{M}_r$ perpendicular as shown in Figure A.6. Now, $\mathbf{F}_A$ is shifted by
some perpendicular distance r to a line $\mathbf{w}$ which is both parallel to $\mathbf{F}_A$ and in the plane
perpendicular to $\mathbf{M}_r$ as shown in Figure A.7. The distance r is chosen so that the couple
$\mathbf{F}_A \times r = -\mathbf{M}_r$. This shifted force vector is now called $\mathbf{F}$ and has the same magnitude
and direction as $\mathbf{F}_A$. When $\mathbf{F}$ is along the line $\mathbf{w}$, the resultant couple $\mathbf{M}$ is parallel to $\mathbf{w}$
also.

Thus, we have attained a resultant force and moment representation which is equiva-
lent to the original force and moment state and whose vectors, $\mathbf{F}$ and $\mathbf{M}$ are parallel. We
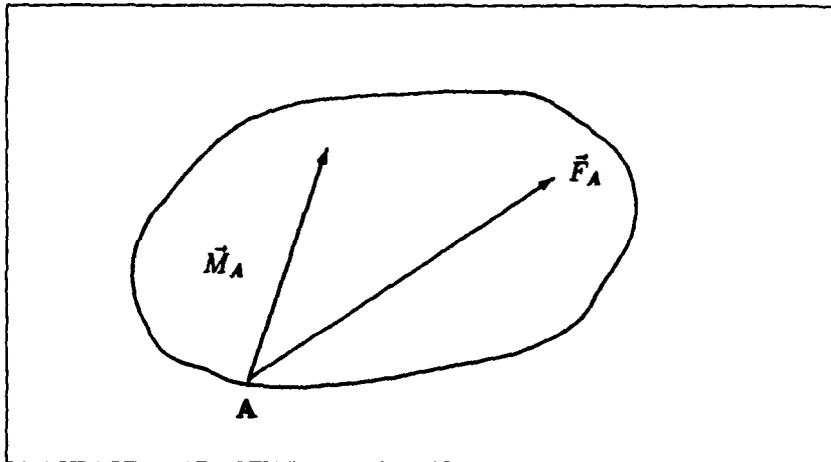
Figure A.5. Induced moments and external moment are summed to get net moment, M_A
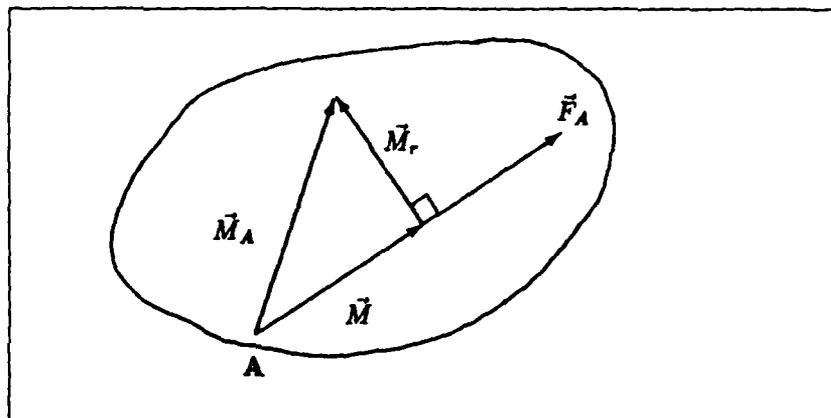

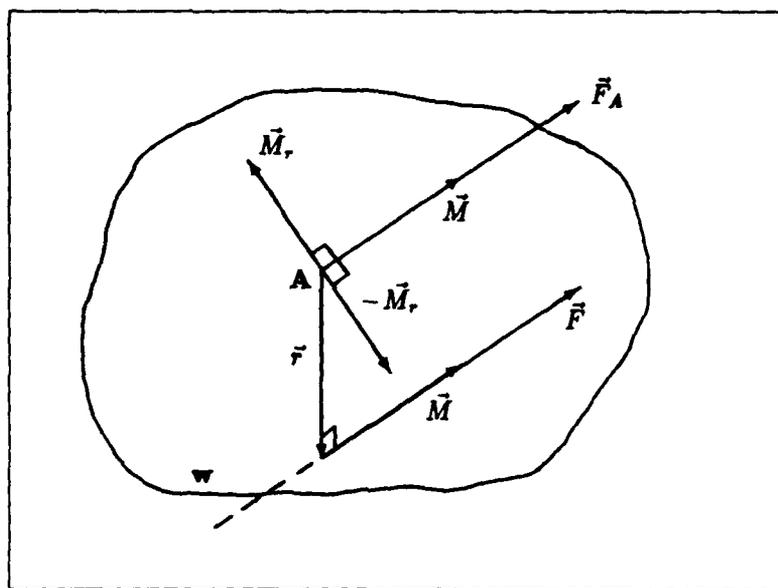Figure A.6. Resolving M_A into components parallel and perpendicular to F_A

A-5

Figure A.7. Shifting $\vec{F}_A$ so as to create a moment which cancels M_r.

call this representation a *wrench* and denote it as

$$\mathcal{W} = (\mathbf{F}, \mathbf{M}) \tag{A.2}$$

where $\mathbf{F}$ is the net force exerted on the body and $\mathbf{M}$ is the net moment about the origin of the reference frame. The line $\mathbf{w}$ is known as the *wrench axis*.

If I now specify that $\mathbf{F}$ has components (w_1, w_2, w_3) and that $\mathbf{M}$ has components (w_4, w_5, w_6), I can identify the *wrench coordinates* as

$$\mathcal{W} = (w_1, w_2, w_3, w_4, w_5, w_6) \tag{A.3}$$

Regardless of what point A one chooses to use when deriving the wrench (on or off of the physical body), the same wrench axis, $\mathbf{w}$, will result. Thus, there is a unique wrench representation for any particular external force and moment state.

Appendix B.
GEOMETRIC DERIVATION OF
CONTACT FRICTION ANGLE EQUATIONS

The derivations presented in this chapter are for a two-fingered grasp on a cylindrical object. The object is assumed to be made of a homogenous material so that its center-of-gravity (CG) is located at its center. The fingers are assumed to be rigid members and contact the object only at their fingertips. The contacts between the fingertips and the object are taken as point contacts with friction. Since planar motion is also assumed, each contact can only apply forces normal and tangential to the surface of the object [MS85: 19].

In general, the object is subjected to a load external to that imposed by the grasping hand. This external load consists of external forces on the object due to contact with something other than the gripper, $\vec{F}_{applied}$, and body forces. The body forces are due to gravity and/or centripetal acceleration acting on the object mass, m. The sum of all of these external forces is denoted by $\vec{F}_{ext}$ which is assumed to act through the center of the object:

$$\vec{F}_{ext} = m(\vec{a} + \vec{g}) + \vec{F}_{applied} \qquad (B.1)$$

Since the resultant external force, $\vec{F}_{ext}$, acts through the object center, it produces no external moment on the object. For this analysis no externally applied moment is allowed. Thus, the external load is a wrench with zero-pitch and an intensity equal to F_{ext}. In general, $\vec{F}_{ext}$ may act in any direction through the CG of the object creating an asymmetric load configuration. To begin the analysis, however, $\vec{F}_{ext}$ will be assumed to act perpendicular to the line connecting the contact points so that a symmetric load configuration results.

The two-fingered grasp is overconstrained [KR86b: 1362] because there are four contact force components (C_{1n}, C_{1t}, C_{2n}, C_{2t}) and only three degrees of freedom in planar motion (translation along x- and y-axes and rotation about z-axis). Overconstraint implies that there are more unknown contact force components than there are equations of motion and, therefore, solution is indeterminate. For an overconstrained grasp, the contact force

vectors can be separated into two orthogonal components; the particular solution, $\vec{C}_p$, and the homogeneous solution, $\vec{C}_h$. They are related to the total solution by

$$\vec{C} = \vec{C}_p + \vec{C}_h \qquad (B.2)$$

Besides the four unknown contact force components, there are three additional unknowns that will appear in the equations; θ, α, and $\vec{F}_{ext}$. This will make a total of seven unknowns with only three static equilibrium equations available. To alleviate this problem, instead of solving for the four individual contact force components, two new variables will be defined as the ratios of the normal and tangential contact force components at each contact point. The two new variables, β_1 and β_2, are related to the active friction angle at each contact point.

Defining β_1 and β_2 reduces the number of unknowns from seven to five, but still requires three parameters to be specified before the set of three simultaneous equations can be solved. For this thesis θ and α are two of the three parameters which will be arbitrarily specified because they define the geometry of the grasp and can be measured. The third arbitrary variable must then be related to F_{ext} without introducing additional unknowns. With this as the only constraint, many different variables could be chosen as the third arbitrary parameter. For this thesis, however, only one possibility was investigated which was a dimensionless parameter involving the internal grasp force and F_{ext}. Both the symmetric and the asymmetric load configurations will be investigated using this set of variables.

B.1 SYMMETRIC LOAD CONFIGURATION

The internal grasp force is defined as the indeterminate contact force vector which will result in no net force on the object [KR86b: 1363]. As shown in Eq (B.2), the internal grasp force vector is represented by $\vec{C}_h$ and has a magnitude of λ.

Figure B.1 shows the configuration of the contact forces at fingertip 1 for a symmetric load configuration. The internal grasp force, C_h, for a two-fingered grasp will always act along the line connecting the contact points of the two fingers which, for the coordinate system defined here, is equivalent to acting along the x-axis. In addition, for a symmetric
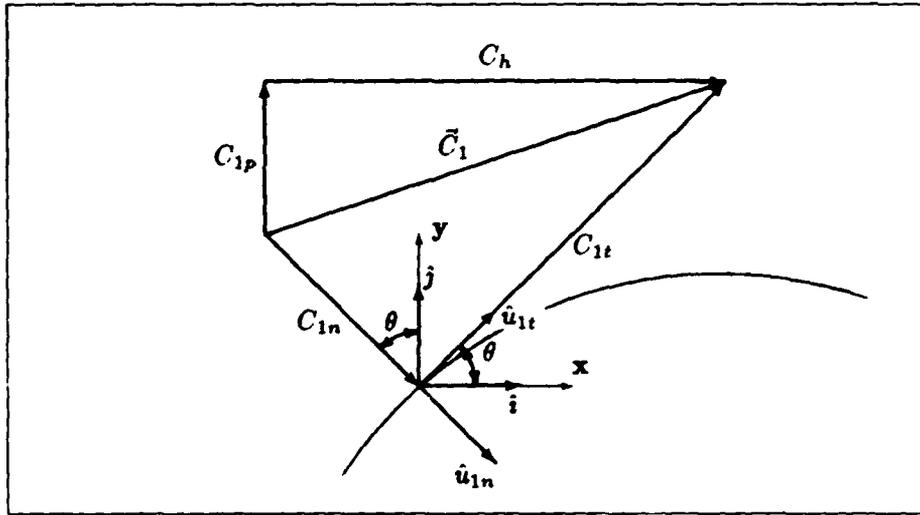
B-2

Figure B.1. Vector diagram of the contact force components and coordinate system for the contact of fingertip 1 with the object under a symmetric load.

load configuration, $\vec{C}_p$ will always be along the y-axis and the magnitude C_{1p} will be equal to C_{2p}. Thus, C_p and C_h are orthogonal.

The component of $\vec{C}_1$ which is internal to the grasp will be equal in magnitude to the component of $\vec{C}_2$ which is internal. Therefore, there is no need to separately consider C_{1h} and C_{2h}.

The origin of the coordinate system is taken to be at the center of the cylinder and the positive y-axis is directed upward through the centroid of the two contact points. As a consequence of this coordinate system, C_h is along the x-axis.

From Figure B.1 one can see that

$$\vec{C}_1 = \lambda \hat{i} + C_{1p} \hat{j} \qquad (B.3)$$

$$\vec{C}_1 = C_{1n} \hat{u}_{1n} + C_{1t} \hat{u}_{1t} \qquad (B.4)$$

where $\hat{i}$ is the unit vector along the x-axis, $\hat{j}$ is the unit vector along the y-axis, $\hat{u}_{1n}$ is the inward unit normal vector at contact 1, $\hat{u}_{1t}$ is the unit tangential vector at contact 1 which is oriented positive as shown in Figure B.1. Since this derivation is for the symmetric case, the results for the friction angle at contact one, β_1, will be equal and opposite in sign to

B-3

that at contact two, β_2. Consequently, the derivation which follows for β_1 also applies for the derivation of β_2. From Figure B.1, the following unit vector relations can be derived:

$$\hat{i} = \sin\theta\,\hat{u}_{1n} + \cos\theta\,\hat{u}_{1t} \tag{B.5}$$

$$\hat{j} = -\cos\theta\,\hat{u}_{1n} + \sin\theta\,\hat{u}_{1t} \tag{B.6}$$

Substituting Eqs (B.5) and (B.6) into Eq (B.3) results in

$$\vec{C}_1 = \lambda\left(\sin\theta\,\hat{u}_{1n} + \cos\theta\,\hat{u}_{1t}\right) + C_{1p}\left(-\cos\theta\,\hat{u}_{1n} + \sin\theta\,\hat{u}_{1t}\right) \tag{B.7}$$

Now rearrange Eq (B.7) to get

$$\vec{C}_1 = \left(\lambda\sin\theta - C_{1p}\cos\theta\right)\hat{u}_{1n} + \left(\lambda\cos\theta + C_{1p}\sin\theta\right)\hat{u}_{1t} \tag{B.8}$$

By definition, the friction angle, β_1, is equal to the arctangent of the magnitude of the tangential contact force component divided by the magnitude of the normal contact force component:

$$\beta_1 \equiv \arctan\left(\frac{\left|\vec{C}_{1t}\right|}{\left|\vec{C}_{1n}\right|}\right) \tag{B.9}$$

The magnitude of the tangential contact force component can be found from the dot product of the contact force, $\vec{C}_1$, with the unit tangential vector, $\hat{u}_{1t}$:

$$\left|\vec{C}_{1t}\right| = \vec{C}_1 \bullet \hat{u}_{1t} = \lambda\cos\theta + C_{1p}\sin\theta \tag{B.10}$$

Similarly, the magnitude of the normal contact force component can be found from the dot product of the contact force, $\vec{C}_1$, with the unit normal vector, $\hat{u}_{1n}$:

$$\left|\vec{C}_{1n}\right| = \vec{C}_1 \bullet \hat{u}_{1n} = \lambda\sin\theta - C_{1p}\cos\theta \tag{B.11}$$

Substituting Eqs (B.10) and (B.11) into Eq (B.9) results in

$$\beta_1 = \arctan\left(\frac{\lambda\cos\theta + C_{1p}\sin\theta}{\lambda\sin\theta - C_{1p}\cos\theta}\right) \tag{B.12}$$

Equation (B.12) represents the solution for β_1 in terms of the homogeneous and particular solutions for the contact forces. Since the magnitude of the homogeneous solution,

λ, is arbitrary it will be left in the equation as a parameter. However, the particular solution, C_{1p}, is a determinate quantity which can be found using the linear algebra method presented by Kerr and Roth (see Section 3.4). When that method is used the result is

$$C_{1p} = C_{2p} = \frac{F_{ext}}{2} \tag{B.13}$$

Using Eq (B.13) to substitute for C_{1p} in Eq (B.12) yields

$$\beta_1 = \arctan\left(\frac{\lambda\cos\theta + (F_{ext}/2)\sin\theta}{\lambda\sin\theta - (F_{ext}/2)\cos\theta}\right) \tag{B.14}$$

which can be rearranged to give

$$\beta_1 = \arctan\left(\frac{(2\lambda/F_{ext})\cos\theta + \sin\theta}{(2\lambda/F_{ext})\sin\theta - \cos\theta}\right) \tag{B.15}$$

For convenience, the internal grasp force is divided by F_{ext} to form a dimensionless parameter, λ', defined as

$$\lambda' \equiv \frac{\lambda}{F_{ext}} \tag{B.16}$$

When Eq (B.16) is substituted into Eq (B.15) it results in the following:

$$\beta_1 = \arctan\left(\frac{2\lambda'\cos\theta + \sin\theta}{2\lambda'\sin\theta - \cos\theta}\right) \tag{B.17}$$

Equation (B.17) is the desired result which gives β_1 as a function of θ and parameterized by the internal grasp force magnitude, λ'.

Recalling that β_2 is equal and opposite to β_1 we find that the friction angle at contact point 2 is given by

$$\beta_2 = -\arctan\left(\frac{2\lambda'\cos\theta + \sin\theta}{2\lambda'\sin\theta - \cos\theta}\right) \tag{B.18}$$

The expressions in Eqs (B.17) and (B.18) are identical with the expressions for β_1 and β_2 in Eqs (4.8) and (4.9) that were derived in Chapter IV.

B.2 ASYMMETRIC LOAD CONFIGURATION

For a two-fingered grasp on an asymmetrically loaded circular cylinder the internal grasp force will be along the line connecting the two contact points. Using the same coordinate system defined in Figure 3.1, this means that $\vec{C}_h'$ will act parallel to the x-axis
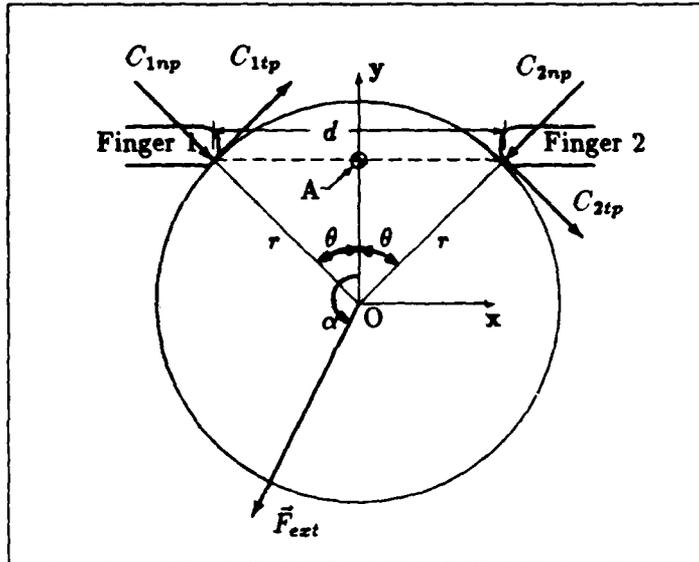
Figure B.2.   Force configuration and coordinate system for the particular
solution contact forces of a grasp on an asymmetrically loaded
object

as it did for the symmetric load configuration. However, the particular solution component
of the total contact force vector, $\vec{C}_p$, will not be constrained to act along the y-axis as it was
for the symmetric load configuration. In fact, its direction is dependent on the direction
of $\vec{F}_{ext}$ as one would expect.

The approach used for this derivation is to solve for the particular and homogeneous
solutions independently and then substitute them into Eq (B.2) to get the total contact
force solutions. The total solutions will then be resolved in the normal and tangential
directions and, finally, the friction angles will be computed.

B.2.1 FINDING THE PARTICULAR SOLUTION. To determine the particular
solution, we begin by redrawing the free body diagram with only the particular solution
components shown. The nomenclature used to symbolize this is C_{ixp} to represent the par-
ticular solution component of the ith contact force in the x-direction. Similarly, C_{iyp}, C_{inp},
and C_{itp} represent the particular solution component of the ith contact force in the y-,
normal-, and tangential-directions, respectively. Figure B.2 illustrates the nomenclature
of the particular solution forces equilibrating $\vec{F}_{ext}$. From Figure B.2, the three equations

for static equilibrium are

$$\sum \vec{F}_x = 0$$
$$= C_{1np} \sin\theta + C_{1tp} \cos\theta - C_{2np} \sin\theta + C_{2tp} \cos\theta - F_{ext} \sin\alpha \quad (B.19)$$

$$\sum \vec{F}_y = 0$$
$$= -C_{1np} \cos\theta + C_{1tp} \sin\theta - C_{2np} \cos\theta - C_{2tp} \sin\theta + F_{ext} \cos\alpha \quad (B.20)$$

$$\sum \vec{M}_o = 0 = -rC_{1tp} - rC_{2tp} \quad (B.21)$$

One additional equation is required to solve for the particular solution component of $\vec{C}$. The additional equation must express the orthogonality of the particular and homogeneous solutions while simultaneously isolating the particular solution, $\vec{C}_p$ from the homogeneous solution. To do this we note that the internal grasp force must be zero and apply Kumar and Waldron's *zero force interaction principle* [KW87: 253] which is mathematically expressed as:

$$\left(\vec{C}_{1p} - \vec{C}_{2p}\right) \bullet \left(\vec{P}_1 - \vec{P}_2\right) = 0 \quad (B.22)$$

where $\vec{P}_i$ is the position vector from the origin of the coordinate system to the ith contact point. In words, Eq (B.22) says that the vector difference between the two contact forces, $\vec{C}_{1p}$ and $\vec{C}_{2p}$ should have no component along the line connecting the two contact points. This is in keeping with the definition of zero internal grasp force thereby leaving only the particular solution.

For the coordinate system in Figure B.2, Eq (B.22) reduces to the constraint that the component of $\vec{C}_{1p}$ in the x-direction must be equal to the component of $\vec{C}_{2p}$ in the x-direction:

$$\vec{C}_{1xp} - \vec{C}_{2xp} = 0 \quad (B.23)$$

Figure B.3 shows the vector relationships among the particular solution components for the contact of finger 1 while Figure B.4 shows the relationships for the contact of finger 2 with the object. From Figures B.3 and B.4, the following magnitude relationships can
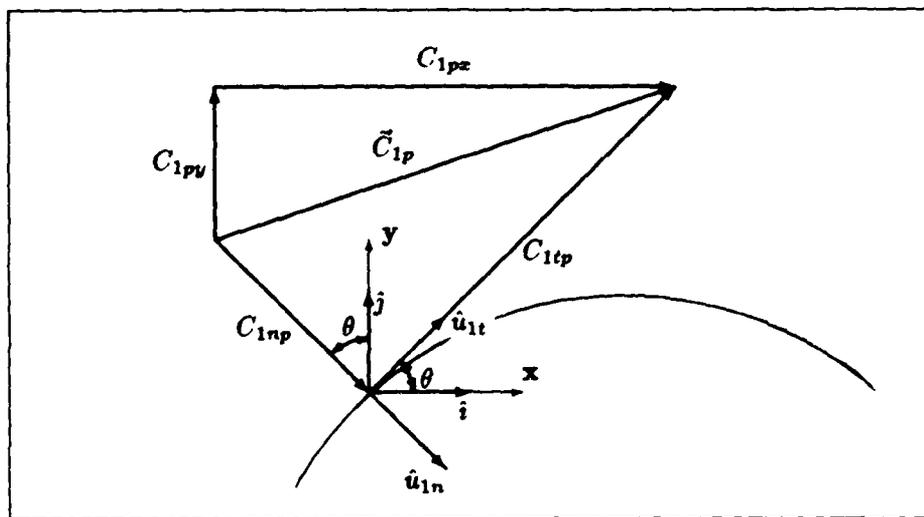
Figure B.3. Vector diagram of the particular solution contact force components and coordinate system for the contact of fingertip 1 with an asymmetrically loaded object
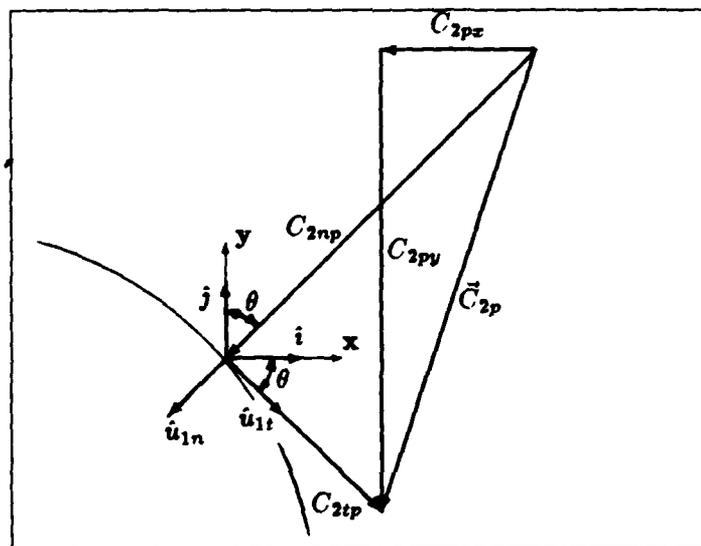

Figure B.4. Vector diagram of the particular solution contact force components and coordinate system for the contact of fingertip 2 with an asymmetrically loaded object.

be derived:

$$C_{1px} = C_{1np} \sin \theta + C_{1tp} \cos \theta \tag{B.24}$$

$$C_{2px} = -C_{2np} \sin \theta + C_{2tp} \cos \theta \tag{B.25}$$

When Eqs (B.24) and (B.25) are substituted into Eq (B.23), the result is

$$C_{1np} \sin \theta + C_{1tp} \cos \theta + C_{2np} \sin \theta - C_{2tp} \cos \theta = 0 \tag{B.26}$$

The sum of the moments in Eq (B.21) implies that

$$C_{1tp} = -C_{2tp} \tag{B.27}$$

which can be substituted into Eq (B.26) to get

$$(C_{1np} + C_{2np}) \sin \theta + 2C_{1tp} \cos \theta = 0 \tag{B.28}$$

When Eq (B.27) is substituted into Eqs (B.19) and (B.20), we get

$$(C_{1np} - C_{2np}) \sin \theta = F_{ext} \sin \alpha \tag{B.29}$$

and

$$-(C_{1np} + C_{2np}) \cos \theta + 2C_{1tp} \sin \theta = -F_{ext} \cos \alpha \tag{B.30}$$

If Eqs (B.28), (B.29), and (B.30) are put into the matrix form of $\mathbf{Ax=b}$, we get

$$
\begin{bmatrix}
\sin \theta & \sin \theta & 2\cos \theta \\
\sin \theta & -\sin \theta & 0 \\
-\cos \theta & -\cos \theta & 2\sin \theta
\end{bmatrix}
\begin{Bmatrix}
C_{1np} \\
C_{2np} \\
C_{1tp}
\end{Bmatrix}
=
\begin{Bmatrix}
0 \\
F_{ext} \sin \alpha \\
-F_{ext} \cos \alpha
\end{Bmatrix}
\tag{B.31}
$$

Equation (B.31) can be solved by using one of several methods including Cramer's method [Kre83: 319]. Using Cramer's method requires one to find the determinant of the coefficient matrix, $\mathbf{A}$. The determinant of the coefficient matrix in Eq (B.31) is found to be $-4 \sin \theta$. Applying Cramer's method to solve for C_{1np} then yields

$$C_{1np} = \frac{F_{ext}}{2} \left(\cos \theta \cos \alpha + \frac{\sin \alpha}{\sin \theta} \right) \tag{B.32}$$

Similarly, the solution for C_{2np} gives

$$C_{2np} = \frac{F_{ext}}{2} \left(\cos\theta \cos\alpha - \frac{\sin\alpha}{\sin\theta} \right) \tag{B.33}$$

while solving for C_{1tp} results in

$$C_{1tp} = \frac{-F_{ext}}{2} \cos\alpha \sin\theta \tag{B.34}$$

Substituting Eq (B.34) into Eq (B.27) we find that

$$C_{2tp} = \frac{F_{ext}}{2} \cos\alpha \sin\theta \tag{B.35}$$

So the particular solutions for the contact forces of fingers 1 and 2 can be written as

$$\vec{C}_{1p} = \frac{F_{ext}}{2} \left[\left(\cos\theta \cos\alpha + \frac{\sin\alpha}{\sin\theta} \right) \hat{u}_{1n} - (\cos\alpha \sin\theta) \hat{u}_{1t} \right] \tag{B.36}$$

and

$$\vec{C}_{2p} = \frac{F_{ext}}{2} \left[\left(\cos\theta \cos\alpha - \frac{\sin\alpha}{\sin\theta} \right) \hat{u}_{2n} + (\cos\alpha \sin\theta) \hat{u}_{2t} \right] \tag{B.37}$$

Equations (B.36) and (B.37) represent the portions of the contact forces at the fingertips of fingers 1 and 2, respectively, which maintain static equilibrium with $\vec{F}_{ext}$ under the constraint of the zero force interaction principle.

B.2.2 FINDING THE HOMOGENEOUS SOLUTION.
To determine the homogeneous solution, we first note that a positive internal grasp force will be a compressive force along the line connecting contact point 1 with contact point 2. In addition, since the homogeneous solution must not impart any net force on the object, we note that the magnitude of the homogeneous component of $\vec{C}_1$ must be equal to that of $\vec{C}_2$. This common magnitude will be represented by λ. Figure B.5 illustrates the nomenclature used for the homogeneous solution in the form of a vector diagram of the homogeneous components of the contact forces for fingertips 1 and 2. Note that the tangential contact force at fingertip 2, C_{2ht}, is shown in the negative direction. From Figure B.5 we can say

$$C_{1nh} = \lambda \sin\theta \tag{B.38}$$

$$C_{1th} = \lambda \cos\theta \tag{B.39}$$

$$C_{2nh} = \lambda \sin\theta \tag{B.40}$$

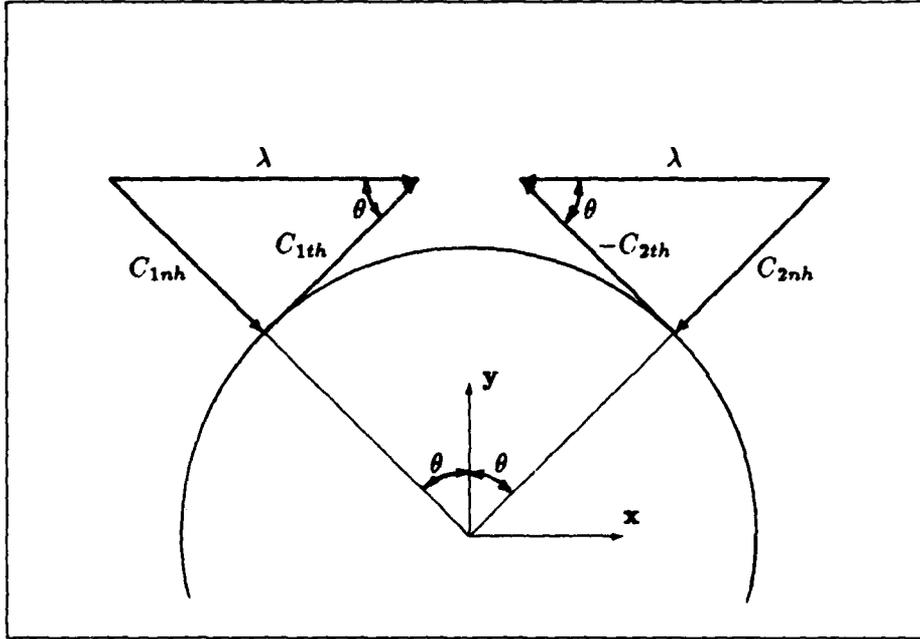$$C_{2th} = -\lambda \cos\theta \tag{B.41}$$

Figure B.5.   Vector diagram of the homogeneous solution contact force
components for the grasp of an asymmetrically loaded object

So the homogeneous solutions for the contact forces of fingers 1 and 2 can be written as

$$\vec{C}_{1h} = \lambda \sin\theta \; \hat{u}_{1n} + \lambda \cos\theta \; \hat{u}_{1t} \tag{B.42}$$

and

$$\vec{C}_{2h} = \lambda \sin\theta \; \hat{u}_{2n} - \lambda \cos\theta \; \hat{u}_{2t} \tag{B.43}$$

Equations (B.36) and (B.42) can be substituted into Eq (B.2) to yield the total solution for the contact force between fingertip 1 and the object:

$$
\begin{aligned}
\vec{C}_1 &= \vec{C}_{1p} + \vec{C}_h \\
&= \frac{F_{ext}}{2}\left(\cos\theta\cos\alpha + \frac{\sin\alpha}{\sin\theta} + \frac{2\lambda}{F_{ext}}\sin\theta\right)\hat{u}_{1n} \\
&\quad + \frac{F_{ext}}{2}\left(-\cos\alpha\sin\theta + \frac{2\lambda}{F_{ext}}\cos\theta\right)\hat{u}_{1t}
\end{aligned}
\tag{B.44}
$$

Similarly, Eqs (B.37) and (B.43) can be substituted into Eq (B.2) to yield the total solution for the contact force between fingertip 2 and the object:

$$
\begin{aligned}
\vec{C}_2 &= \vec{C}_{2p} + \vec{C}_h \\
&= \frac{F_{ext}}{2}\left(\cos\theta\cos\alpha - \frac{\sin\alpha}{\sin\theta} + \frac{2\lambda}{F_{ext}}\sin\theta\right)\hat{u}_{2n}
\end{aligned}
$$

B-11

$$+\frac{F_{ext}}{2}\left(-\cos\alpha\sin\theta+\frac{2\lambda}{F_{ext}}\cos\theta\right)\hat{u}_{2t} \tag{B.45}$$

When the normal and tangential components of $\vec{C}_1$ are substituted into the definition of β_1 given by Eq (B.9) the resulting expression for β_1 is

$$\beta_1 = \arctan\left[\frac{2\lambda\cos\theta - F_{ext}\cos\alpha\sin\theta}{F_{ext}\cos\theta\cos\alpha + F_{ext}\frac{\sin\alpha}{\sin\theta} + 2\lambda\sin\theta}\right] \tag{B.46}$$

If the dimensionless parameter, λ', defined in Eq (B.16) is substituted, Eq (B.46) can be rewritten as

$$\beta_1 = \arctan\left[\frac{2\lambda'\cos\theta - \cos\alpha\sin\theta}{\cos\theta\cos\alpha + \frac{\sin\alpha}{\sin\theta} + 2\lambda'\sin\theta}\right] \tag{B.47}$$

With a couple of trigonometric substitutions and some algebraic rearrangement, Eq (B.47) becomes

$$\beta_1 = \arctan\left[\frac{2\lambda'\sin 2\theta - \cos\alpha\left(1 - \cos 2\theta\right)}{2\lambda'\left(1 - \cos 2\theta\right) + \cos\alpha\sin 2\theta + 2\sin\alpha}\right] \tag{B.48}$$

Similarly, β_2 can be found to be given by

$$\beta_2 = \arctan\left[\frac{2\lambda'\sin 2\theta - \cos\alpha\left(1 - \cos 2\theta\right)}{2\lambda'\left(1 - \cos 2\theta\right) + \cos\alpha\sin 2\theta - 2\sin\alpha}\right] \tag{B.49}$$

When $\alpha = 180$ degrees is substituted into Eqs (B.48) and (B.49), they reduce to Eqs (B.17) and (B.18), respectively.

Bibliography

AHM85. Jacob M. Abel, W. Holzmann, and J. Michael McCarthy. On Grasping Planar Objects With Two Articulated Fingers. *IEEE Journal of Robotics and Automation*, RA-1(4):211–214, December 1985.

Bal00. R. S. Ball. *A Treatise on the Theory of Screws*. Cambridge University Press, Cambridge, 1900.

BG74. A. Ben-Israel and T. N. E. Greville. *Generalized Inverses: Theory and Applications*. Wiley & Sons, New York, 1974.

BTG86. J. C. Becker, N. V. Thakor, and K. G. Gruben. A Study of Human Hand Tendon Kinematics With Applications to Robotic Hand Design. In *IEEE 1986 International Conference on Robotics and Automation*, pages 1540–1545, IEEE Computer Society Press, 1986. Volume 3.

CS84. M. Caporali and M. Shahinpoor. Design and Construction of a Five-Fingered Robotic Hand. *Robotics Age*, 6(2):14–20, February 1984.

CW86. Mark R. Cutkosky and Paul K. Wright. Modeling Manufacturing Grips and Correlations With the Design of Robotic Hands. In *IEEE Proceedings of the 6th International Conference on Robotics and Automation*, pages 1533–1539, IEEE Computer Society Press, 1986. Volume 3.

DH81. John J. D'Azzo and Constantine H. Houpis. *Linear Control Systems Analysis and Design: Conventional and Modern*. McGraw-Hill, New York, 2nd edition, 1981.

Fea86. Ronald S. Fearing. Simplified Grasping and Manipulation With Dexterous Robot Hands. *IEEE Journal of Robotics and Automation*, RA-2(4):188–195, December 1986.

HM85. W. Holzmann and J. Michael McCarthy. Computing the Friction Forces Associated With a Three-Fingered Grasp. *IEEE Journal of Robotics and Automation*, RA-1(4):206–210, December 1985.

Hun78. Kenneth H. Hunt. *Kinematic Geometry of Mechanisms*. Clarendon Press, Oxford, 1978.

Ibe87. T. Iberall. The Nature of Human Prehension: Three Dexterous Hands In One. In *Proceedings of the 1987 IEEE International Conference on Robotics and Automation*, page 396, IEEE Computer Society Press, 1987. Volume 1.

JIKJ86. S. C. Jacobsen, E. K. Iversen, D. F. Knutti, R. T. Johnson, and K. B. Biggers. Design of the Utah/MIT Dexterous Hand. In *Proceedings of IEEE International Conference on Robotics and Automation*, pages 1520–1532, IEEE Computer Society Press, March 1986. Volume 2.

Ker84. Jeffrey R. Kerr. *An Analysis of Multi-Fingered Hands*. Ph.D. dissertation, Stanford University, December 1984. Department of Mechanical Engineering.

KR86a. Jeffrey Kerr and Bernard Roth. Analysis of Multifingered Hands. *The International Journal of Robotics Research*, 4(4):3–17, 1986. Winter.

KR86b. Jeffrey Kerr and Bernard Roth. Special Grasping Configurations With Dexterous Hands. In *IEEE Proceedings of the 6th International Conference on Robotics and Automation*, pages 1361–1367, IEEE Computer Society Press, 1986. Volume 3.

Kre83. Erwin Kreyszig. *Advanced Engineering Mathematics*. Wiley & Sons, New York, 5th edition, 1983.

KW87. Vijay Kumar and Kenneth J. Waldron. Sub-Optimal Algorithms for Force Distribution In Multifingered Grippers. In *IEEE Proceedings of the 7th International Conference on Robotics and Automation*, pages 252–257, IEEE Computer Society Press, 1987. Volume 3.

Lak78. K. Lakshminarayana. Mechanics of Form Closure. ASME preprint 78-DET-32, 1978. pages 1-8.

Mas82. Matthew T. Mason. *Manipulator Grasping and Pushing Operations*. Ph.D. dissertation, Massachusetts Institute of Technology, 1982. Department of Computer Science.

MS85. Matthew T. Mason and J. Kenneth Salisbury. *Robot Hands and the Mechanics of Manipulation*. MIT Press, 1985.

Ngu86. Van-Duc Nguyen. Constructing Force-Closure Grasps. In *IEEE Proceedings of the 6th International Conference on Robotics and Automation*, pages 1368–1373, IEEE Computer Society Press, 1986. Volume 2.

NHF84. Dr. Yoshiyuki Nakano, Yuji Hosada, and Masakatsu Fujie. Hitachi's Robot Hand. *Robotics Age*, 6(7):18–20, July 1984.

Ohw80. Morgan S. Ohwovoriole. *An Extension of Screw Theory and Its Application to the Automation of Industrial Assemblies*. Ph.D. dissertation, Stanford University, April 1980. Department of Mechanical Engineering.

Sal82. J. Kenneth Salisbury. *Kinematic and Force Analysis of Articulated Hands*. Ph.D. dissertation, Stanford University, May 1982. Department of Mechanical Engineering.

SR83. J. Kenneth Salisbury and Bernard Roth. Kinematic and Force Analysis of Articulated Mechanical Hands. In *Transactions of the ASME, Journal of Mechanisms, Transmissions and Automation in Design*, pages 35–41, March 1983. Volume 105.

TAP87. Jeffrey C. Trinkle, Jacob M. Abel, and Richard P. Paul. Enveloping, Frictionless, Planar Grasping. In *IEEE Proceedings of the 7th International Conference on Robotics and Automation*, pages 246–251, IEEE Computer Society Press, 1987. Volume 3.

TBK87. Rajko Tomovic, George A. Bekey, and Walter J. Karplus. A Strategy for Grasp Synthesis With Multifingered Robot Hands. In *IEEE Proceedings of the 7th International Conference on Robotics and Automation*, pages 83–89, IEEE Computer Society Press, 1987. Volume 3.

VAX85.   *VAX UNIX MACSYMA Reference Manual.* Symbolics, Inc., Cambridge, Mass., October 1985.

Wal86.   Kenneth J. Waldron. Force and Motion Management In Legged Locomotion. In *IEEE Proceedings of the 6th International Conference on Robotics and Automation*, pages 214–220, IEEE Computer Society Press, 1986.

Vita

Captain Paul V. Whalen was born on ███████████████████████ In 1980 he graduated from ███████████ High School ██████████ In that same year he entered Purdue University's School of Engineering in West Lafayette, Indiana on a four-year Air Force ROTC scholarship. While attending Purdue, he was initiated into the mechanical engineering honorary fraternity, Pi Tau Sigma. He received the degree of Bachelor of Science in Mechanical Engineering from Purdue in May 1984. Upon graduation he received a Regular Air Force commission and was designated a distinguished ROTC graduate. In July 1984 he reported for duty as a Conventional Munitions R&D Test Engineer at Eglin AFB, Florida. While serving at Eglin he was awarded the AF Commendation Medal and the AF Achievement Medal for outstanding service. He entered the School of Engineering, Air Force Institute of Technology, in July 1987. Upon completion of his master's degree in aeronautical engineering Captain Whalen will continue to study towards a doctoral degree in engineering at the Air Force Institute of Technology under the sponsorship of the Armstrong Aerospace Medical Research Laboratory.

REPORT DOCUMENTATION PAGE

1a. REPORT SECURITY CLASSIFICATION	1b. RESTRICTIVE MARKINGS
UNCLASSIFIED	N/A

2a. SECURITY CLASSIFICATION AUTHORITY	3. DISTRIBUTION / AVAILABILITY OF REPORT
	Approved for public release; distribution unlimited.
2b. DECLASSIFICATION / DOWNGRADING SCHEDULE	

4. PERFORMING ORGANIZATION REPORT NUMBER(S)	5. MONITORING ORGANIZATION REPORT NUMBER(S)
AFIT/GAE/AA/88D-39	

6a. NAME OF PERFORMING ORGANIZATION	6b. OFFICE SYMBOL (If applicable)	7a. NAME OF MONITORING ORGANIZATION
School of Engineering	AFIT/ENY	

6c. ADDRESS (City, State, and ZIP Code)	7b. ADDRESS (City, State, and ZIP Code)
Air Force Institute of Technology (AU) Wright-Patterson AFB, OH 45433-6583	

8a. NAME OF FUNDING / SPONSORING ORGANIZATION	8b. OFFICE SYMBOL (If applicable)	9. PROCUREMENT INSTRUMENT IDENTIFICATION NUMBER
Armstrong Aerospc Med Resrch Lb	AAMRL/BBA	

8c. ADDRESS (City, State, and ZIP Code)	10. SOURCE OF FUNDING NUMBERS			
Wright-Patterson AFB, OH 45433-6583	PROGRAM ELEMENT NO.	PROJECT NO.	TASK NO	WORK UNIT ACCESSION NO.

11. TITLE (Include Security Classification)

Two-Fingered Grasp of Cylindrical Objects in Planar Motion (Unclassified)

12. PERSONAL AUTHOR(S)
Captain Paul V. Whalen

13a. TYPE OF REPORT	13b. TIME COVERED	14. DATE OF REPORT (Year, Month, Day)	15. PAGE COUNT
MS Thesis	FROM _____ TO _____	88 Dec	

16. SUPPLEMENTARY NOTATION

17. COSATI CODES			18. SUBJECT TERMS (Continue on reverse if necessary and identify by block number)
FIELD	GROUP	SUB-GROUP	Robotic, Grippers, Grasping, Force Closure, Form Closure, Load Variations, Screw Theory
12	09		

19. ABSTRACT (Continue on reverse if necessary and identify by block number)

THESIS ADVISOR: Dr. Curtis H. Spenny, Professor
Department of Aeronautics and Astronautics

ABSTRACT ON REVERSE SIDE

12 Jan 1989

20. DISTRIBUTION / AVAILABILITY OF ABSTRACT	21. ABSTRACT SECURITY CLASSIFICATION
☒ UNCLASSIFIED/UNLIMITED ☐ SAME AS RPT. ☐ DTIC USERS	Unclassified

22a. NAME OF RESPONSIBLE INDIVIDUAL	22b. TELEPHONE (Include Area Code)	22c. OFFICE SYMBOL
Dr. Curtis H. Spenny	(513) 255-3517	AFIT/ENY

DD Form 1473, JUN 86   *Previous editions are obsolete.*

19. ABSTRACT:

One goal of this thesis is to develop analytic expressions which model the
equilibrium requirements of a grasp by two robotic fingers on a nominally-
loaded cylindrical object confined to planar motion. Another goal is to
derive analytic expressions which can be used to evaluate the ability of a
grasp to tolerate changes in the external load magnitude, direction, and
moment without loss of equilibrium. The gripper fingers are each assumed
to be two-link serial mechanisms with revolute joints. The contact of
each finger on the object is taken as a point contact with friction. The
resulting analytic expressions are based on the static equilibrium require-
ments and include consideration of constraints on: Coulomb friction forces,
unisense normal forces, object crush limits, and finger joint torque limits.
Plotting the expressions yields new graphical insight into the consequences
of employing various fingertip spacings and "squeeze" force levels when
grasping cylindrical objects in planar motion. In addition, the analytic
equations indicate the range of variation in external load configuration
which can be tolerated by a selected grasp without violating any of the
aforementioned grasp constraints. Variations in the magnitude, direction,
and moment of the external load configuration are considered. The derived
analytic expressions can be used as the foundation for developing simplified
grasping algorithms under the stated conditions.